Lehrstuhl für Ernährungsmedizin

Bioenergetic characterization of white adipocytes in obesity

Britta Wessels

Vollständiger Abdruck der von der Fakultät Wissenschaftszentrum Weihenstephan für Ernährung, Landnutzung und Umwelt der Technischen Universität München zur Erlangung des akademischen Grades eines

Doktors der Naturwissenschaften

genehmigten Dissertation.

Vorsitzende: Prof. Dr. Hannelore Daniel

Prüfer der Dissertation:

1. Prof. Dr. Johann J. Hauner

2. Prof. Dr. Martin Klingenspor

Die Dissertation wurde am 11.09.2017 bei der Technischen Universität München eingereicht und durch die Fakultät Wissenschaftszentrum Weihenstephan für Ernährung, Landnutzung und Umwelt am 11.12.2017 angenommen.

TABLE OF CONTENTS

SUMMARY

Obesity is not only accompanied by the expansion of adipose tissue, but also by adipocyte dysregulation. This dysregulation is considered to promote metabolic disorders such as type 2 diabetes mellitus (T2DM). Within the last years, it has been recognized that obesity is also associated with an impairment of mitochondrial function within adipocytes, and that this might be involved in the progression of adipocyte dysregulation. Furthermore, particularly obese subjects suffering from T2DM were suggested to exhibit disturbances within their adipocyte mitochondrial function.

Therefore, the objective of the present work was to gain further knowledge about mitochondrial function in adipocytes in relation to body mass index (BMI) and the relevance of the diabetic status. Moreover, mechanisms underlying an impaired mitochondrial function in adipocytes of obese subjects were investigated as well as implications of impaired mitochondrial function on adipocyte energy metabolism. In addition, comparisons of results between subcutaneous and visceral adipocytes were performed.

Oxygen uptake measurements of isolated adipocytes as well as in isolated mitochondria of the subcutaneous, but not within the visceral depot, showed impairments within the respiratory capacity with increasing BMI of the donors. Focusing on T2DM, the current study did not reveal any association between impaired mitochondrial respiration in adipocytes and deteriorations of glucose homeostasis. Furthermore, the diabetic status was not found to be influencing the association between donor's BMI and mitochondrial oxygen uptake. Additionally, in subcutaneous adipocytes, mitochondrial content was inversely associated with donor's BMI. Therefore, the study clearly points to disturbances in subcutaneous adipocyte mitochondrial function in obesity independent from the diabetic status.

Protein expression analysis of the present study suggests that especially impairments of the electron transport chain complex IV might be responsible for the BMI dependent decline in mitochondrial respiratory capacity, although this was not yet confirmed by an enzymatic activity assay.

The study revealed that the inhibition of mitochondrial ATP production is leading to a doubling in lactate release in adipocytes of both investigated depots. Moreover, lactate levels were found to be elevated with increasing BMI in both depots. Therefore, it can be concluded that

glycolysis is compensating for impairments of mitochondrial function in obesity. However, the present work was not able to show a significant link between mitochondrial respiratory capacity and the release of lactate in a smaller subsample. Furthermore, it could be suggested that adipocytes do not meet their ATP demands primarily by mitochondrial respiration, but rather by glycolysis. Therefore, the study is emphasizing the importance of glycolytic ATP production in contrast to mitochondrial ATP production in adipocytes. In line with this, adipocyte ATP levels were neither in visceral nor in subcutaneous adipocytes reduced with increasing BMI.

Another objective of the study was to determine differences of adipocytes derived from the visceral and the subcutaneous depot. Hereby, it was evident that distinctions between the depots are BMI dependent. Investigating mitochondrial respiration, subcutaneous adipocytes showed a trend towards higher oxygen consumption rates compared with visceral adipocytes in subjects with BMI values below 30 kg/m². Whereas in obese individuals the reverse finding was detected. Subjects with BMI values above or equal to 30 kg/m² showed significantly lower oxygen uptake rates in visceral adipocytes. Investigating lactate release, it was shown that subcutaneous adipocytes released significantly higher amounts of lactate, whereas after dividing the cohort according to their BMI, this finding only remained to be statistically significant in the group including obese individuals. Basal ATP levels were significantly higher only in subcutaneous adipocytes of subjects with BMI values below 30 kg/m².

In conclusion, obesity is accompanied by decreased subcutaneous adipocyte mitochondrial respiratory capacity which is not linked to the diabetic status. Therefore, the investigation suggests that adipocyte mitochondrial dysfunction is not relevant for the progression of T2DM. Overall, it still needs to be confirmed that impairments within adipocyte mitochondrial function is contributing to adipocyte dysfunction as seen in obesity and, therefore influencing the health status of obese subjects.

ZUSAMMENFASSUNG

Adipositas ist neben der Zunahme von Fettmasse auch durch eine gesteigerte Fehlregulation der Adipozyten gekennzeichnet. Die Entwicklung Adipositas-abhängiger metabolischer Störungen, zu denen unter anderem der Typ 2 Diabetes mellitus gehört (T2DM), ist hiermit assoziiert. Welche Faktoren ursächlich für diese Fehlregulation sind ist jedoch noch nicht vollständig geklärt. In den vergangenen Jahren deuten Studien vermehrt darauf hin, dass Adipositas mit einer Beeinträchtigung der Mitochondrien-Funktion in Adipozyten einhergeht und diese zu einer Fehlregulation von Adipozyten bei Adipositas beitragen könnte. Zudem gibt es Hinweise, dass hiervon insbesondere adipöse Patienten betroffen sind, die gleichzeitig an T2DM erkrankt sind.

Ziel der vorliegenden Arbeit war es daher, die Mitochondrien-Funktion in Adipozyten in Abhängigkeit des Body-Mass-Index (BMI) zu bestimmen und darüber hinaus die Bedeutung des Diabetesstatus zu untersuchen. Ferner sollten Erkenntnisse gewonnen werden, welche Mechanismen einer gestörten Mitochondrien-Funktion bei Adipositas zu Grunde liegen und inwiefern hierdurch der Energiestatus der Fettzelle beeinträchtigt ist. Zusätzlich wurde eine Gegenüberstellung von Ergebnissen subkutaner und viszeraler Adipozyten vorgenommen.

In permeabilisierten isolierten Adipozyten sowie in isolierten Mitochondrien konnte gezeigt werden, dass die Atmungskapazität humaner subkutaner Mitochondrien mit zunehmendem BMI vermindert ist. Bei isolierten Adipozyten viszeralen Ursprungs konnte dieser Zusammenhang hingegen nicht gezeigt werden. Überdies deutete die Quantifizierung mitochondrialer Marker auf eine Reduktion der Anzahl an Mitochondrien in subkutanen Adipozyten mit zunehmendem BMI hin. Die mitochondriale Atmung von Adipozyten beider Fettdepots wiesen keinen Unterschied zwischen adipösen Probanden mit und ohne beeinträchtigter Glukosehomöostase auf. Ferner hatte der Diabetesstatus keinen Einfluss auf den Zusammenhang zwischen der mitochondrialen Respiration und dem BMI. Die vorliegende Arbeit konnte somit deutlich zeigen, dass Adipositas unabhängig vom Diabetesstatus mit einer beeinträchtigten Mitochondrien-Funktion in subkutanen Adipozyten einhergeht.

Ergebnisse von Proteinexpressionanalysen deuteten darauf hin, dass insbesondere eine Beeinträchtigung des Atmungskettenkomplexes IV zu einer BMI-abhängigen Abnahme der mitochondrialen Atmungskapazität beiträgt. Diese Beobachtung konnte jedoch durch eine

Komplex IV-Aktivitätsanalyse noch nicht bestätigt werden.

Die Hemmung der oxidativen ATP Produktion resultierte in subkutanen und viszeralen Adipozyten in einer Verdopplung der Laktatfreisetzung. Mit zunehmendem BMI konnte außerdem ein Anstieg der Laktatausscheidung von Adipozyten beider Depots gezeigt werden. Folglich kann eine Kompensation der beeinträchtigten Mitochondrien-Funktion mit zunehmendem Übergewicht durch eine gesteigerte Glykolyse angenommen werden. Einen Zusammenhang zwischen der mitochondrialen Atmung sowie den Laktatkonzentrationen konnte hingegen nicht beobachtet werden. Ferner deuten die Ergebnisse der vorliegenden Arbeit daraufhin, dass Adipozyten ihren ATP-Bedarf überwiegend über den glykolytischen Weg und nicht durch die mitochondriale oxidative Phorsphorylierung decken. Dementsprechend konnte weder in viszeralen noch in subkutanen Adipozyten ein Abfall der zellulären ATP Spiegel mit zunehmendem BMI beobachtet werden.

Gegenstand der vorliegenden Arbeit war außerdem die Untersuchung der Unterschiede zwischen subkutanen und viszeralen Adipozyten. Hierbei konnte allgemein gezeigt werden, dass diese maßgeblich vom BMI der Probanden abhängig sind. Probanden mit einem BMI kleiner 30 kg/m² zeigten in subkutanen Adipozyten im Vergleich zu viszeralen tendenziell höhere Atmungsraten. In adipösen Probanden hingegen konnten signifikant niedrigere Sauerstoffverbrauchsraten von subkutanen verglichen mit viszeralen Adipozyten beobachtet werden. Die Freisetzung von Laktat zeigte ebenfalls BMI-abhängige Unterschiede. Bei Probanden mit einem BMI kleiner als 30 kg/m² unterschied sich die Laktatfreisetzung zwischen Fettzellen der beiden Depots nicht. In der Gruppe, die nur adipöse Probanden einschloss, zeigten sich hingegen signifikant höhere Laktatwerte bei subkutanen Adipozyten im Vergleich zu denen von viszeralen. Überdies konnten nur in Probanden mit einem BMI kleiner 30 kg/m² in subkutanen Adipozyten verglichen mit viszeralen signifikant höhere basale ATP Konzentrationen ermittelt werden. Bei einem Vergleich der basalen ATP Konzentrationen von adipösen Probanden zeigte sich hingegen kein Unterschied zwischen den beiden Depots.

Insgesamt konnte die vorliegende Arbeit zeigen, dass eine Zunahme des BMI mit einer verminderten mitochondrialen Atmungskapazität in subkutanen Adipozyten einhergeht welche jedoch vom Diabetesstatus unabhängig ist. Demzufolge scheint eine eingeschränkte Mitochondrien-Funktion in subkutanen Fettzellen keinen Beitrag zur Entwicklung eines T2DM zu leisten. Eine abschließende Aussage, ob die Beeinträchtigung der Mitochondrien-Funktion

in subkutanen Adipozyten ungünstige Auswirkungen auf die Fettzelle selbst und somit auf den Gesundheitszustand adipöser Personen hat, kann basierend auf den vorliegenden Daten noch nicht getroffen werden.

ABBREVIATIONS

ADP	adenosine diphosphate
AMP	adenosine monophosphate
AMPK	5' adenosine monophosphate-activated protein kinase
ATP	adenosine triphosphate
AU	arbitrary units
BMI	body mass index (english) / Body-Mass-Index (deutsch)
BSA	bovine serum albumin
CS	citrate synthase
CSV	comma-separated values
2-deoxy-D-glc	2-deoxy-D-glucose
DiGH	disturbances in the glucose homeostasis
DMEM/F12	Dulbecco's Modified Eagle Medium: Nutrient Mixture F-12
DNA	deoxyribonucleic acid
dsDNA	double-stranded DNA
ETS	electron transfer system
faf	fatty acid free
FCCP	carbonyl cyanide 4-(trifluoromethoxy)phenylhydrazone
FI	fraction I
FIV	fraction IV
GAPDH	glyceraldehyde-3-phosphate dehydrogenase
GLUT4	glucose transporter type 4
HbA_{1c}	glycated hemoglobin A1c
HIF-1	hypoxia-inducible-factor 1
HOMA	homeostatic model assessment

IL-6	interleukin 6
IQR	inter quartile range
IRS-1	insulin receptor substrate 1
LDH	lactate dehydrogenase
LQ	lower quartile
mtDNA	mitochondrial DNA
NAD^+/NADH	nicotinamide adenine dinucleotide
ND	no recognized disturbances within the glucose homeostasis
OXPHOS	oxidative phosphorylation
Pen-Strep	Penicillin-Streptomycin
PI3K	phosphoinositide 3-kinase
pO_2	partial pressure of oxygen
ROS	reactive oxygen species
RT	room temperature
sc	subcutaneous
SD	standard deviation
SGBS	Simpson-Golabi-Behmel syndrome
rpm	rounds per Minuit
TCA	tricarboxylic acid cycle
TFAM	mitochondrial transcription factor A
TNF-α	tumor necrosis factor alpha
UQ	upper quartile
UV	ultraviolet
vc	visceral
vs	versus

WAT	white adipose tissue
WHO	World Health Organization

1 INTRODUCTION

1.1 Obesity, a worldwide challenge

According to the World Health Organization (WHO), the worldwide prevalence of obesity has more than doubled since 1980. In the year 2014 from 1.9 billion overweight adults, 600 million were actually obese (World Health Organization, 2015). In Germany, the prevalence for overweight reached 58 % between 2007 and 2008, whereas 21 % of these persons were classified as obese (Max Rubner-Institut, 2008). Due to its simplicity and availability the body mass index (BMI; kg/m²) is usually applied for assessing overweight and obesity, although misclassification e.g. of athletics is possible (Khosla and Lowe, 1967; World Health Organization, 2000). The classification in accordance to the WHO (shown in Table 1) is based primarily on the link between BMI and mortality (World Health Organization, 2000). As obesity is accompanied by several health issues, and it is also linked to economic costs, obesity is considered a world health problem with increasing relevance (World Health Organization, 2000). Therefore, research in this field is of increasing importance.

Table 1: The WHO Classification of adult underweight, overweight and obesity according to the BMI

Classification	BMI (kg/m²)
Underweight	**< 18.50**
Normal range	**18.5 - 24.99**
Overweight	**≥ 25.00**
Pre-obese	25.00 - 29.99
Obese	**≥ 30.00**
Obese class I	30.00 - 34.99
Obese class II	35.00 - 39.99
Obese class III	≥ 40.00

Adapted from WHO (World Health Organization, 2000).

1.2 Adipocyte biology in obesity

In general, obesity is characterized by an increase in fat mass. While lean male adults show 15-20 % adipose tissue of total body composition, in obesity the fat mass composition can actually exceed 40 % (Schuster, 2009; Trayhurn, 2013).

Adipose tissue is an organ incorporating blood vessels and nerves as well as connective tissue. It is constituted of different cell types. The predominant fraction is mature adipocytes, but there is also the stromal-vascular fraction, which includes precursor cells of adipocytes, preadipocytes but also macrophages, mast cells, lymphocytes, or fibroblasts (Cryer and Van, 1985).

The main function of white adipose tissue is the storage of energy in a compact manner (Wang et al., 2008). Whereas fat pad formation starts between the 14th and 23rd week of gestation (Poissonnet et al., 1983), the number of adipocytes are defined during childhood and adolescence (Spalding et al., 2008). In obese subjects, an increase in fat mass is mostly developed by hypertrophy (increase of adipocyte size) (Spalding et al., 2008). But it is also indicated that hyperplasia might take place in obese subjects during a higher age (Björntorp and Sjöström, 1971; Hirsch and Batchelor, 1976). Nevertheless, during weight loss the number of adipocytes does not decrease (Spalding et al., 2008). Independent of weight gain or reduction, 10 % of adipocytes are replaced annually (Spalding et al., 2008). However, the exclusive role of adipose tissue as an organ to store energy has shifted towards an organ with secretory functions. Besides the secretion of free fatty acids (FFAs) during fasting, proteins are also secreted from adipose tissue (Wang et al., 2008). One milestone occurred in 1994 with the discovery of the adipokine leptin which highlighted the role played by adipose tissue as a secretory organ (Zhang et al., 1994). With the enlargement of adipose tissue, the secretion of many inflammatory cytokines is increased, and therefore, contributes considerably to an inflammatory status in obesity (Hauner, 2005). In comparison, the secretion of the adipokine adiponectin, is inversely related to the amount of adipose tissue (Cnop et al., 2003) and the BMI (Arita et al., 1999). Moreover, serum levels of adiponectin are higher in insulin sensitive subjects (Kern et al., 2003). In turn, the release of pro-inflammatory cytokines is increased with hypertrophy of adipocytes (Blüher et al., 2004; Skurk et al., 2007a). Besides the increase in fat mass and adipocyte hypertrophy also fat distribution contributes to the inflammatory phenotype commonly seen in obesity. In comparison to the subcutaneous depot, the pattern of secreted factors of the visceral depot is more pronounced as pro-inflammatory (Fried et al., 1998; Bruun et al., 2005; Harman-Boehm et al., 2007). Also the secretion of leptin is distinct between the subcutaneous and the visceral depot. However, a higher secretion of leptin occurs in the subcutaneous depot. As the secretion of leptin correlates to fat cell size and adipocytes are larger in the subcutaneous depot (Goldrick and McLoughlin, 1970), a reduced

secretion of leptin, seen in the visceral depot, could be due to the size of adipocytes (van Harmelen et al., 1998). Moreover, it has been shown that the adiponectin secretion also differs within the subcutaneous and the visceral depots. The visceral depot shows higher secretion rates of adiponectin and is, furthermore, influenced by the treatment with insulin or rosiglitazone, whereas the subcutaneous secretion is unaffected. Therefore, it had been suggested that the visceral depot is responsible for declining adipokine levels, observed with an increasing BMI (Motoshima et al., 2002).

A proposed mechanism for adipose tissue dysfunction associated with increasing adiposity is adipose tissue hypoxia. If an increase of fat mass and adipocyte size in obesity is not followed by an adequate vascularization, this is increasing the distance for oxygen diffusion and could therefore trigger adipose tissue hypoxia (Trayhurn, 2013). Evidence from animal models indicates that obesity is accompanied by adipose tissue hypoxia (Hosogai et al., 2007; Ye et al., 2007; Rausch et al., 2008). Furthermore, human adipose tissue of obese compared with lean subjects was also found to be hypoxic (Blaak et al., 1995; Pasarica et al., 2009). But the situation is not as clear as in animal models; in contrast, there are studies which failed to show a metabolic signature of hypoxia in adipose tissue in obese subjects (Hodson et al., 2013), and even hyperoxia had been reported (Goossens et al., 2011). Nevertheless, hypoxia had been repeatedly described to contribute to the switch towards an inflammatory profile of adipose tissue as seen in obesity (Wang et al., 2007; Ye et al., 2007; Wood et al., 2011; Goossens et al., 2011). A hypoxic state has also been connected to an increase in the release of lactate which is a product of glycolysis (Priyanka et al., 2014). Beside the oxidative phosphorylation (OXPHOS) process, glycolysis is another source for adenosine triphosphate (ATP) (Alberts et al., 1994). In adipocyte cell models an increase in lactate production had been observed after a decrease in oxygen tension (Pérez de Heredia et al., 2010; Wood et al., 2011). Findings from the human Simpson-Golabi-Behmel Syndrome (SGBS) preadipocyte cell strain even suggest that adipocytes only switch to mitochondrial ATP production, when glycolysis cannot fulfill the actual need for ATP (Keuper et al., 2014). Circulating levels of lactate were found to be higher in obese, compared to lean subjects (DiGirolamo et al., 1989). Furthermore, *in vivo* measurements of lactate release from subcutaneous adipose tissue showed proportionality between the fat mass and the release of lactate and was therefore found to be higher in obese compared to lean subjects (Jansson et al., 1994). Studies with rats showed a higher basal lactate release from the mesenteric depot (Newby et al., 1988; Newby et al., 1990; King and

DiGirolamo, 1998). However, this was not the case anymore in the response to insulin (King and DiGirolamo, 1998). Microarray analysis revealed that genes encoding key glycolysis enzymes are differentially expressed in adipose tissue of obese and lean subjects and therefore suggest that not only fat mass accounts for differences in lactate production between lean and obese subjects (Baranova et al., 2005).

1.3 Adipose tissue and impaired glucose homeostasis

Type 2 diabetes mellitus (T2DM) is an obesity associated comorbidity. With the progression of T2DM, chronic hyperglycemia, can have severe long-term effects on different organs; especially the heart, blood vessels, kidneys, nerves, and eyes (American Diabetes Association, 2013; World Health Organization, 2016). Between 1980 and 2014, the worldwide prevalence for diabetes among adults rose from 4.7 % to 8.8 % and has, therefore, nearly doubled. The majority of diabetic patients are suffering from T2DM (World Health Organization, 2016). In contrast to Type 1 diabetes, where auto-immune destruction of pancreatic ß-cells leads to an insufficient insulin production, resulting in the total absence of insulin, the pathogenesis of T2DM is started with insulin resistance (American Diabetes Association, 2013). As T2DM progresses, β cell failure occurs which leads to an impaired insulin secretion. This failure of β cells is partially caused by the attempt to compensate for insulin resistance (Prentki and Nolan, 2006). Early stages of T2DM and insulin resistance are often undiagnosed, as the disease is not severe enough for the patients to be recognized in the initial phase (American Diabetes Association, 2013). Individuals with impaired fasting glucose and/or impaired glucose tolerance, but not yet diagnosed as diabetic patients, are referred to as pre-diabetic (American Diabetes Association, 2013).

Insulin resistance is characterized by an impaired signal cascade of the insulin receptor substrate 1 (IRS-1)/ phosphoinositide 3-kinase (PI3K)/Akt signal pathway, followed by an insufficient glucose transporter type 4 (GLUT4) translocation, and thus, an impaired transport of glucose into muscle cells (Choi and Kim, 2010).

Dysregulated adipose tissue is thought to be acting as a contributor to the onset of T2DM. A decrease in storage capacity of adipose tissue leads to an increase in the release of FFAs (Lionetti et al., 2009). Increased levels of circulating FFAs in turn have been linked to insulin resistance and T2DM (Boden and Chen, 1995; Paolisso et al., 1995; Roden et al., 1996). Glucose uptake is inhibited by FFAs (Roden et al., 1996) through the inhibition of the IRS-1

tyrosine phosphorylation (Griffin et al., 1999; Yu et al., 2002) and IRS-1 associated PI3K activity, which is responsible for the transport of glucose into muscle cells (Dresner et al., 1999; Griffin et al., 1999; Yu et al., 2002). Furthermore, the switch towards a pro-inflammatory secretory profile is promoting insulin resistance. Thereby, adiponectin, which is considered as anti-inflammatory (Ouchi and Walsh, 2007), has been proposed to function as an anti-diabetic adipokine. In obese subjects, levels are higher in healthy compared to diabetic patients (Hotta et al., 2000; Klöting et al., 2010). Moreover, circulating adiponectin levels are inversely correlated to glucose levels as well as fasting plasma insulin (Hotta et al., 2000; Weyer et al., 2001). Studies with rodents imply that the antidiabetic action of adiponectin is mediated by the suppression of the hepatic glucose production. Therefore, basal glucose levels are decreasing (Berg et al., 2001) as well as the muscle and liver triglycerides content due to an increased skeletal muscle fatty-acid combustion and dissipation of energy (Yamauchi et al., 2001).

The anti-inflammatory adipokine adiponectin is negatively associated to disturbances in glucose metabolism, whereas the number of macrophages in adipose tissue is increasing with insulin resistance (Harman-Boehm et al., 2007; Klöting et al., 2010). Hereby, the release of pro-inflammatory cytokines like tumor necrosis factor alpha (TNF-α) and interleukin 6 (IL-6) by macrophages, are thought to play a key role in the genesis of T2DM (Harford et al., 2011). During the treatment of T2DM, the improvement of the subject's glucose homeostasis goes along with a reduction of systemic inflammation markers (Larsen et al., 2007).

The mentioned aspects are further supported by an unfavorable distribution of adipose tissue in favor of an increase in the visceral fat, as the infiltration of adipose tissue with macrophages is higher in omental adipose tissue compared to the subcutaneous depot (Cancello et al., 2006). Moreover, the surgically removal of intra-abdominal fat has beneficial effects on the subject's glucose metabolism in comparison to the subcutaneous depot (Thörne et al., 2002; Klein et al., 2004; Dillard et al., 2013). In addition, there are associations between an impaired glucose homeostasis and the amount of visceral adipose tissue mass (Basat et al., 2006). On the contrary, it has also been shown that there is a strong correlation between the subcutaneous abdominal depot and insulin resistance after adjusting for the visceral depot. However, this correlation was not seen any more for visceral fat mass after adjustment for the subcutaneous fat mass (Goodpaster et al., 1997). Taken additionally into account that subcutaneous adipose tissue represents 80 % of the total body fat (Spalding et al., 2008), the

investigation of subcutaneous adipose tissue is a crucial part in the research of obesity and T2DM.

Besides adipose tissue distribution, also adipoyte hypertrophy has been linked to the development of T2DM, as the release of pro-inflammatory cytokines is increased with the size of adipocytes (Blüher et al., 2004; Skurk et al., 2007a). Furthermore, it has been reported, that there is an association between fat cell size and T2DM (Weyer et al., 2000; Dubois et al., 2006), and that a favorable glucose homeostasis is linked to adipose tissue hyperplasia rather than to hypertrophy (Hoffstedt et al., 2010). It even has been proposed an adipocyte size threshold, which increases the risk for T2DM (Cotillard et al., 2014).

The degree of which hypoxic adipose tissue in obesity is contributing to T2DM is controversially discussed, as there are studies with contrary findings (Klöting et al., 2010; Lecoultre et al., 2013). The cellular adaptive response to hypoxia is regulated by the hypoxia-inducible-factor 1 (HIF1), consisting of the oxygen labile subunit HIF-1α and the constitutively expressed subunit HIF-1β. Under normoxia the alpha subunit is degraded (Giaccia et al., 2004; Semenza, 2011). The knockout of HIF-1β in adipose tissue retains high fat fed mice from the development of obesity and glucose intolerance, accompanied by small adipocytes and reduced visceral fat mass (Lee et al., 2011). Analogously, the overexpression of HIF-1α is followed by an increase in adipose tissue inflammation and a decrease in glucose tolerance (Halberg et al., 2009). Nevertheless, a chronic exposure of mice to hypoxia showed beneficial effects on body weight, adipocyte size and adiponectin expression (van den Borst et al., 2013). Moreover, the exposure of humans to hypoxia during night was followed by a decrease in the partial pressure of oxygen (pO_2) and an increase in insulin sensitivity (Lecoultre et al., 2013). However, also human studies suggest that low adipose tissue pO_2 drives inflammation (Pasarica et al., 2009) and that there might be a link between the hypoxia signal cascade and insulin resistance (Regazzetti et al., 2009; Klöting et al., 2010). Moreover, an inverse association between circulating lactate levels and the degree of insulin sensitivity has been observed (Lovejoy et al., 1992). As mentioned before, in adipocyte cell models, a decrease in oxygen tension was found to result into an increase in lactate production (Pérez de Heredia et al., 2010; Wood et al., 2011).

1.4 Cellular mitochondrial function

Mitochondria are cellular organelles with their own double-stranded circular deoxyribonucleic acid (dsDNA). They are composed of an outer membrane, surrounding the mitochondrion, an intermembrane space between outer and inner membrane and the mitochondrial matrix embraced by the inner mitochondrial membrane. The surface of the inner mitochondrial membrane, which incorporates the respiratory chain complexes, is increased by the formation of cristae structures (Alberts et al., 1994; Scheffler, 2001; McBride et al., 2006). According to the endosymbiotic theory, mitochondria descend from bacteria, which where endocytosed about two billion years ago, presumably, after oxygen entered the atmosphere (Alberts et al., 1994; Archibald, 2015). Although mitochondria are often depicted as static organelles, it is widely accepted that mitochondria are highly flexible organelles which constantly undergo fusion and fission and can built complex networks (Wiesner et al., 1992; Bereiter-Hahn and Vöth, 1994). The main function of mitochondria is recognized as the “powerhouse of the cell”, as energy is produced through the oxidative phosphorylation process, where electrons are passed along the electron transport chain. The mitochondrial generated ATP meets, under normal conditions, 80 % of the cellular energy demand. Electrons are transferred via the different complexes to its final acceptor oxygen at complex IV (or cytochrome c oxidase). Hereby, a proton gradient across the membrane is built. Electrons from nicotinamide adenine dinucleotide (NADH), originated from the oxidation of nutrients, enter the electron transport chain via complex I (or NADH-ubiquinone oxidoreductase). Thereby, NADH is oxidized to NAD^+, protons are pumped into the intermembrane space, and electrons are transferred to ubiquinone. Complex II (or succinate-ubiquinone reductase) which is a part of the tricarboxylic acid cycle (TCA), passes electrons from succinate to the ubiquinone pool, but without pumping protons across the inner mitochondrial membrane. By complex III (or ubiquinone-cytochrome c oxidoreductase), electrons are transferred from ubiquinol to cytochrome c, and protons are transported via the inner membrane. Complex IV in turn, is using cytochrome c as a substrate. Cytochrome c is oxidized and the final electron acceptor oxygen is reduced into two H_2O molecules and again, protons are pumped across the membrane. The production of ATP from adenosine diphosphate (ADP) and phosphate through complex V (or ATP-synthase) is driven by the proton motive force through the flow of protons from the intermembrane space back to the mitochondrial matrix (see Figure 1) (Saraste, 1999; Papa et al., 2012).

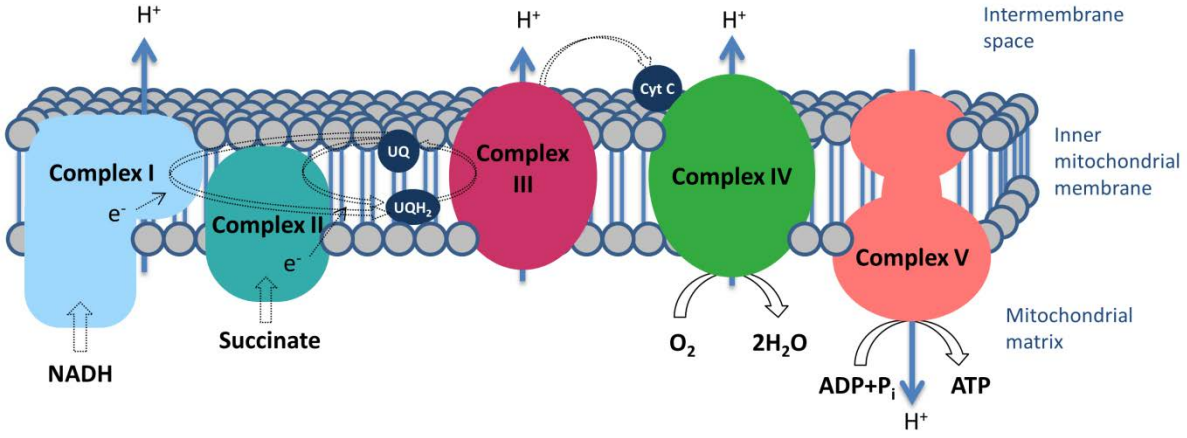

Figure 1: Illustration of the oxidative phosphorylation at the inner mitochondrial membrane

Electrons are transferred via the complexes to its final acceptor oxygen at complex IV. Thereby protons are pumped across the inner mitochondrial membrane by complex I, III and IV. Using the built proton motive force, ATP is synthesized by complex V through the return of protons to the mitochondrial matrix (adapted from Saraste, 1999 and Kanehisa et al., 2016).

Beside the OXPHOS process, there are further functions which can be attributed to mitochondria. As brought up before, also the TCA is localized in the mitochondrion; so the matrix comprises enzymes involved in the TCA (Alberts et al., 1994; Scheffler, 2008). Furthermore, the final degradation of fatty acids to acetyl-CoA within the beta-oxidation takes place within the mitochondrion and is than fed into the TCA (Houten and Wanders, 2010). Additionally, mitochondria are involved in the cellular calcium regulation (Dupont, 2014), the synthesis of heme and Fe-S-clusters, the degradation of amino acids by the urea cycle (Scheffler, 2008), and in the intrinsic apoptotic pathway – the process of programmed cell death (Elmore, 2007; Li and Dewson, 2015).

Even though mitochondria have their own DNA, consisting of 16,569 base pairs; the majority of mitochondrial proteins are encoded by the nuclear DNA. Only 13 of the 37 mitochondrial genes encode for proteins of the OXPHOS system: seven subunits of complex I, one of complex III, three of complex IV, and two of complex V (Anderson et al., 1981). The copy numbers of mitochondrial DNA (mtDNA) per mitochondrion are thought to be almost constant in different mammalian cell types, but the number of mitochondria differs (Robin and Wong, 1988; D'Erchia et al., 2015). It is assumed that mtDNA is equally distributed over mitochondria within one cell, as mitochondrial fusion allows complementation of mtDNA between different mitochondria (Hayashi et al., 1994; Chan, 2006).

1.5 Mitochondria in adipocytes of white adipose tissue

Compared with beige and brown adipocytes, white adipocytes show fewer numbers of mitochondria (Park et al., 2014). Furthermore, mitochondria in beige and brown adipocytes differ in their function as they dissipate energy by non-shivering thermogenesis. Thereby, protons are translocated from the intermembrane space back into the mitochondrial matrix via uncoupling proteins (UCP), heat is produced and ATP-synthase is eluded (Peirce et al., 2014). Furthermore, human white adipose tissue revealed an average of mtDNA copy number of 350 to 2,000 per adipocyte (Gahan et al., 2001; Bogacka et al., 2005; Kaaman et al., 2007; Lindinger et al., 2010). Therefore, mtDNA content in human white adipose tissue is in the lower third compared to mtDNA content in other human tissues (D'Erchia et al., 2015).

Due to the formation of glycerol 3-phosphate and the activation of FFAs mitochondria are thought to be important for lipogenesis in adipocytes. This is further supported by a strong association between the mtDNA copy number and adipocyte lipogenesis in cell models (Kaaman et al., 2007; Pauw et al., 2009). Moreover, lipolysis can be linked to mitochondria in adipocytes, as the oxidation of fatty acids by β-oxidation takes place in the mitochondrial matrix, and lipolysis is inhibited by a decrease in ATP levels and the activation of the 5' adenosine monophosphate-activated protein kinase (AMPK) (Pauw et al., 2009). In addition to lipogenesis and lipolysis, specifically in adipocytes, mitochondria are suggested to play an important role in adipocyte differentiation (Lu et al., 2010; Kajimoto et al., 2005). Concerning adipokine secretion, cell culture models suggest that mitochondrial function in adipocytes is essential for adiponectin synthesis (Chevillotte et al., 2007; Koh et al., 2007).

1.6 Mitochondria in white adipose tissue adipocytes of obese subject

Evidence of impaired adipocyte mitochondria in the context of obesity was revealed from mice models first. It was shown that genes encoding for mitochondrial proteins are downregulated in obese mice (Wilson-Fritch et al., 2004). The attempt to ascertain gene expression in human adipocytes in dependency on obesity led to controversial results. Whereas upon the FinnTwin16 study, where obese and lean co-twins were compared, a downregulation of genes involved in the electron transport chain in the abdominal subcutaneous adipose tissue (Mustelin et al., 2008) as well as diminished mitochondrial oxidative pathways in the obese twins were found (Heinonen et al., 2015), other groups

couldn't find a difference in the visceral or the subcutaneous depot between obese and non-obese subjects (Dahlman et al., 2006; Kaaman et al., 2007; Yehuda-Shnaidman et al., 2010). Even more controversial data were presented investigating the mtDNA copy number in adipocytes of obese and lean subjects. There are results showing a decreased mtDNA content in subcutaneous adipocytes of obese subjects (Kaaman et al., 2007; Heinonen et al., 2015), but no influence due to weight loss (Kaaman et al., 2007), whereas Yin et al. (2014) only found a trend towards a lesser mtDNA copy number in adipocytes of obese subjects, but no statistically significant difference between lean and obese subjects in visceral or subcutaneous adipocytes (Yin et al., 2014). Lindinger and colleagues even observed an increased mtDNA copy number in omental adipocytes with an increase in BMI values (Lindinger et al., 2010).

Aside from results regarding gene expression and mtDNA content, there is also literature presenting data of functional mitochondrial measurements in human adipocytes. Already in 1989 the observation was made that basal oxygen consumption of subcutaneous and omental adipose tissue is negatively related to the donor's degree of obesity (Hallgren et al., 1989). Differentiated subcutaneous preadipocytes showed no differences in their basal oxygen consumption rates with regard to the donor's BMI, but after the induction with isoproterenol, oxygen consumption rates were found to be lower in adipocytes from obese subjects (Yehuda-Shnaidman et al., 2010). In contrast to that, another study revealed that oxygen consumption rates of isolated mitochondria from omental and abdominal subcutaneous mature adipocytes differed between obese and lean subjects. Additional findings of the same study population were that mitochondria from small and large adipocytes do not differ in their oxygen uptakes, and that there is no difference in mitochondrial respiration between the subcutaneous and the visceral depot within the same subject (Yin et al., 2014). This result is not supported by measurements of whole visceral adipose tissue samples derived from obese subjects, which showed higher oxygen consumption per mtDNA compared with the subcutaneous depot (Kraunsøe et al., 2010). Looking at the activity of complex I and II measured in isolated mitochondria from omental adipose tissue, no link to obesity could be drawn. Only the activity as well as protein levels of the mitochondrial key enzyme citrate synthase (CS) had been found to be reduced in mitochondria from omental adipose tissue of obese subjects (Christe et al., 2013).

1.7 Mitochondria in white adipose tissue adipocytes of subjects with impaired glucose homeostasis

Hansen and colleagues (2015) found lower mtDNA copy numbers in subcutaneous adipocytes of subjects with T2DM compared with only obese subjects. Upon respiratory measurements of whole adipose tissue pieces, the calculated respiratory rates per adipocytes were lower in the group of diabetic subjects. But there was no difference between the two groups when the respiratory rates were expressed per adipose tissue mass or per mtDNA (Hansen et al., 2015).

Independent of the obese state, Dahlman and group (2006) found a downregulation of electron transport chain genes in visceral and subcutaneous adipose tissue of women suffering from T2DM (Dahlman et al., 2006).

Regarding mtDNA content, lower amounts were found in subcutaneous adipose tissue of T2DM compared to control subjects (Bogacka et al., 2005), and also in visceral adipose tissue a trend towards a lower mtDNA content in women with T2DM was reported (Lindinger et al., 2010). Additionally, the treatment with the antidiabetic drug pioglitazone led to an increase in mtDNA copy number as well as factors involved in mitochondrial biogenesis in subcutaneous adipose tissue (Bogacka et al., 2005). Further evidence for a link between T2DM and a reduced mtDNA content in adipose tissue was found in a study published by Heinonen et al. (2015), where the amount of mtDNA in subcutaneous adipose tissue was inversely related to the homeostatic model assessment (HOMA), an index for insulin resistance (Heinonen et al., 2015).

2 AIM OF THE WORK

Frequently, an increase in obesity goes along with a progression in adipocyte dysregulation. Furthermore, in many cases this is followed by metabolic consequences such as T2DM. Although several responsible aspects in this context had been revealed, the overall reason for a dysregulated adipose tissue in obese subjects is not fully understood yet. Different aspects, including macrophage infiltration, adipocyte hypertrophy, hypoxia and other factors, had been referred to a progression in adipose tissue impairment. As there had also been found indications for dysfunctional adipocyte mitochondria within obesity, this is investigated in the present thesis, with the attempt to gain further knowledge of adipose tissue biology in the context of obesity.

Therefore, the main mitochondrial function, the oxidative phosphorylation process, in dependency on the subjects BMI, was investigated within two different models. Furthermore, the role of the mitochondria's fat depot origin (subcutaneous, visceral) as well as the occurrence of a diagnosed T2DM or a pre-diabetic state had been taken into account. In order to reveal differences within the single complexes of the mitochondrial electron transport chain, protein expression analysis had been performed. Moreover, the consequences of an impaired mitochondrial respiration regarding ATP levels had been determined, as well as a possible compensatory role of glycolysis in this context.

3 MATERIAL AND METHODS

3.1 Subjects

Adipose tissue was obtained from patients who underwent either elective abdominal or visceral surgery. All patients were free of infectious diseases or malignancy. Written informed consent was provided by each subject. The study protocol had been approved by the ethical committee of the Technical University of Munich (project number: 5716/13).

Subjects who underwent visceral abdominal surgery were grouped according to their glucose homeostasis as follows: Subjects without any disturbances in their glucose metabolism where referred to as “no recognized disturbances within the glucose homeostasis” (ND). As C-peptide is reflecting endogenous insulin secretion and therefore, increasing with an over secretion of insulin (Saisho, 2016) and recently also C-peptide is now also taken into account when the state of impaired glucose homeostasis is estimated (Lee et al., 2017; Zachariah et al., 2016), the prerequisites for the ND group were: fasting plasma glucose levels < 110 mg/dl, glycated hemoglobin A_{1c} (HbA_{1c}) < 5.7 % and C-peptide < 4.4 ng/ml. Subjects with diagnosed diabetes were referred to as diabetic. Subjects with no diagnosed T2DM, but HbA_{1c} values above 5.7 % (American Diabetes Association, 2013), or a recognized insulin resistance by HOMA-Index, where referred to as pre-diabetic. The diagnosis of diabetes, as well as the determination of the HbA_{1c} values, plasma glucose, C-peptide and insulin resistance was measured by the attending physician.

3.1.1 Plastic surgery

Subcutaneous adipose tissue was obtained from healthy female patients who underwent abdominoplasty or abdominal liposuction. The tissue was transported in a sterile container with Dulbecco’s Modified Eagle medium: Nutrient Mixture F12 (DMEM/F12; Gibco® ThermoFisher Scientific, USA) containing 1 % Penicillin-Streptomycin (Pen-Strep; Sigma-Aldrich, USA) to the laboratory. Adipocytes had been isolated within the same day.

3.1.2 Visceral abdominal surgery

Small amounts of subcutaneous and visceral adipose tissue (approx. 1 to 10 g) were obtained from subjects who underwent visceral abdominal laparoscopic surgery (e.g. sleeve gastrectomy, fundoplication, appendectomy). Therefore, the surgeon removed visceral

adipose tissue in the proximity of the angel of His. The subcutaneous adipose tissue was taken from beneath the skin, after the trocar has been taken out and before suturing the incision. The tissue was transferred to sterile 50 ml tubes containing DMEM/F12 with 1 % Pen-Strep and transported to the laboratory. There it was immediately transferred to a T25 cell culture flask (TPP, Switzerland) with DMEM/F12 1 % Pen-Strep and stored in an incubator (5 % CO_2 atmosphere; 37 °C) over night.

All available data of the patients concerning anthropometric data, laboratory tests, comorbidities, medication, and smoking habits were collected from the medical file.

3.2 Adipocyte culture

3.2.1 Adipocyte isolation

Human primary adipocytes were isolated like previously described (Skurk et al., 2007b). In short, blood vessels and connective tissue was removed from the adipose tissue. Subsequently the tissue was minced with scissors in a 50 ml tube and 5 ml of Krebs-Ringer phosphate buffer (KRP) + 4 % bovine serum albumin (BSA, Sigma-Aldrich) containing 0.2 units collagenase (Biochrom, Germany) per g adipose tissue was added. The 50 ml tubes with adipose tissue and collagenase solution was incubated for one hour (h) under agitation in a water bath at 37 °C. After collagenase digestion the sample were initially filtered through a nylon mesh (VWR, USA) with a pore size of 2,000 µM. Thereafter, adipocytes were filtered together with KRP buffer + 0.1 % BSA through nylon mesh (VWR) pores with the size of 200 µm. The filtering steps were followed by washing steps with KRP + 0.1 % BSA until the supernatant appeared to be clear. Between the washing steps, the adipocytes floated for five minutes (min), to avoid washing away small adipocytes. Subsequently, adipocytes were depending on the received amount transferred into cell culture flasks (TPP) or cell culture plates (TPP) with DMEM F12 + 1 % Pen-Strep in the dilution 1:4 (see also Figure 2).

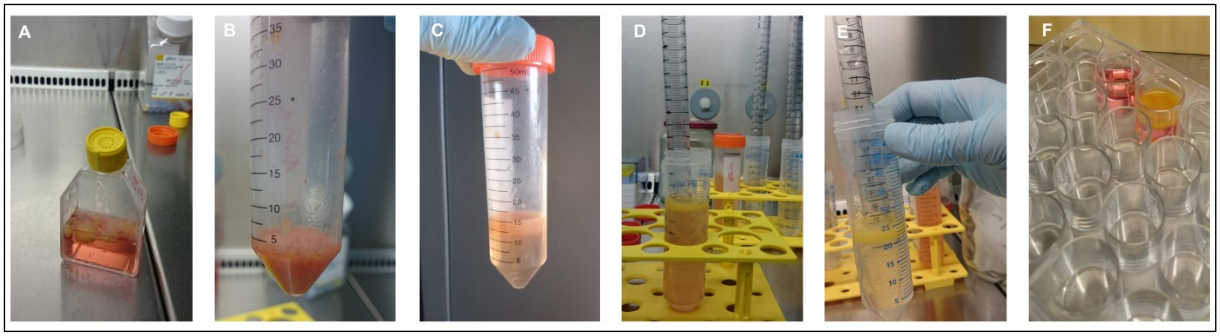

Figure 2: Isolation of adipocytes from visceral abdominal surgery

(A) Adipose tissue specimen in a T25 cell culture flask with DMEM/F12 + 1 % Pen-Strep. (B) Minced adipose tissue. (C) Minced adipose tissue with KRP + 4 % BSA containing 0.2 units collagenase. (D) Adipocytes after filtering steps. (E) Washed adipocytes with clear supernatant. (F) 12-well culture plate with adipocytes in DMEM/F12 + 1 % Pen-Strep.

KRP buffer

(12.35 mM KCl, 4.9 mM $CaCl_2$, 1.25 mM $MgSO_4x7\ H_2O$, 1.23 mM $NaH_2PO_4xH_2O$; pH 7.4)

3.2.2 Size determination

For cell size determination, 10 µl adipocytes were transferred on an object slide with KRP + 0.1 % BSA (see also Figure 3). The diameter of 100 adipocytes was determined under a light microscope (Leica, Germany) with included scale. Adipocyte volume was calculated by:

$$Volume = \frac{4}{3} * \pi * r^3$$

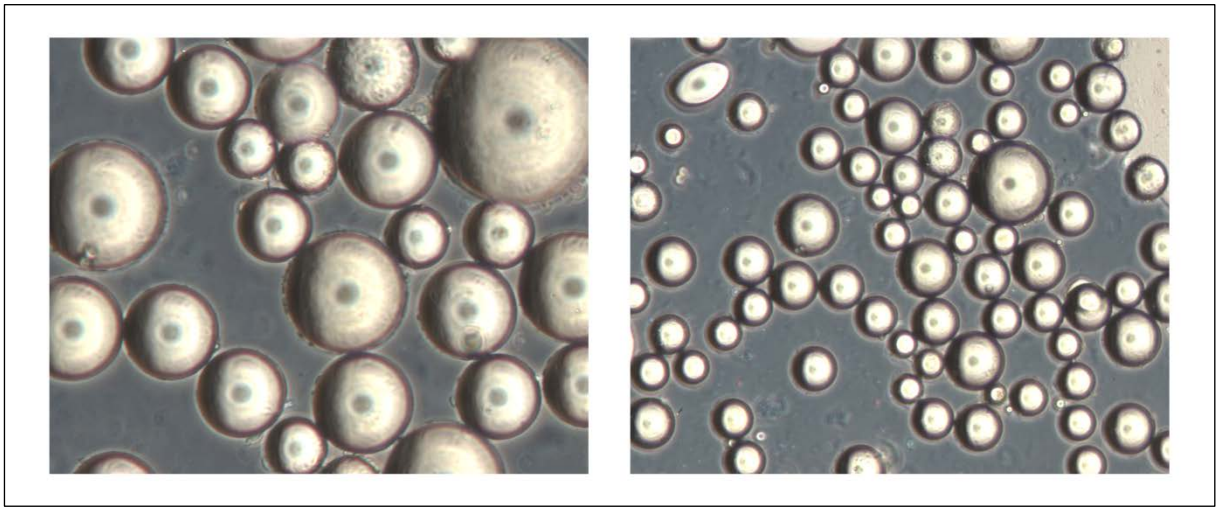

Figure 3: Exemplary microscope images of isolated adipocytes

Adipocytes were isolated from adipose tissue and transferred to an object slide for cell size determination. Two images of visceral adipocytes and varying magnification are shown exemplary.

3.2.3 Fractionation

Isolated adipocytes from lean and obese subcutaneous abdominal tissue (n = 5) were separated into very small cells (fraction I; FI) and very large cells (fraction IV; FIV) based on their buoyancy in a 100 ml separating funnel. Therefore, 10 to 20 ml of a total cell suspension and 50 ml of KRP + 0.1 % BSA buffer were gently mixed. After cells were allowed to float for 45 seconds (sec), 30 ml of cell suspension was collected to obtain FI (small cells). Intermediate-sized cells were collected and discarded after floating for 15 sec. Cells that remained in the funnel were defined as FIV. To determine cell size of each fraction, size was determined in accordance to 3.2.2. Experiments on fractionated adipocytes were conducted with the cooperation of Christina Schempp.

3.2.4 LDH activity

The enzyme lactate dehydrogenase (LDH), which is located in the cytoplasm of cells, was used as a marker for cellular stress. As also experiments were performed were adipocytes were permeabilized, hereby measurements of LDH activity levels can give additional information about the degree of permeabilization (Smolen et al., 1986; Boon and Zammit, 1988). LDH is converting pyruvate to L-lactate with NADH as a cofactor, whereby NAHD is oxidized to NAD^+. NADH is absorbing ultraviolet (UV) light at 339 nm. Therefore, the activity of LDH can be determined indirectly by a plate-reader (Infinite® 200 PRO, Tecan, Switzerland) measuring the absorbance at 339 nm photometrically over a time period of 10 min. Supernatants from adipocytes before and after permeabilization were taken and stored for maximal 24 h at 4 °C. After pipetting NADH (156 µl; Sigma-Aldrich) diluted in Tris/NaCl (0.24 mM NADH) in each well, a sample (6 µl) was added in duplicates. 31 µl of pyruvate (9.72 mM) diluted in Tris/NaCl was automatically added by the Tecan injector.

To reveal if cellular stress as well as the degree of permeabilization is associated to donor's BMI values and might therefore biasing the findings of the study, adipocyte LDH activity before and after permeabilization was correlated to BMI values. Both analyses showed no association between LDH activity before and after permeabilization and donor's BMI values (Appendix: Table 27). Furthermore, LDH activity of subjects with and without disturbances of glucose homeostasis was compared. This comparison also did not exhibit any statistically significant differences between the two groups (Appendix: Table 28).

Tris/NaCl (81.22 mM Tris, 200 mM NaCl, pH 7.2)

3.3 Respiration measurements

3.3.1 Isolated mitochondria

For the isolation of mitochondria, adipocytes were disrupted mechanically by a glass-Teflon Potter homogenizer in the presence of STE buffer + 4 % BSA (fatty acid free; faf; ROTH, Germany) at 4 °C. The homogenate was transferred to a 50 ml tube and was centrifuged (800 x *g*, 10 min, 4 °C) to separate the mitochondria-suspension from fat and to pellet the cell debris. Subsequently, the supernatant with mitochondria was ultracentrifuged (10,000 x *g*, 10 min, 4 °C). The supernatant was discarded and the pellet containing mitochondria was washed with KHE buffer. After another centrifugation step (10,000 x *g*, 10 min, 4 °C) and discarding the supernatant, the pellet was carefully resuspended with the help of a brush and in a small volume of KHE buffer and was subsequently transferred to a 1.5 ml reaction tube. Resuspended mitochondria were stored on ice for the following measurements.

Before respiratory analyses were performed, mitochondrial protein was measured using a BCA Protein Assay Kit (ThermoFisher Scientific), which is based on the biuret reaction and measures the absorbance of the formed bicinchoninic acid copper(I)-complex at 562 nm.

Oxygen consumption of isolated mitochondria was determined within a Clark-type oxygen electrode (Digital Model 10; Rank Brothers, UK). The Clark electrode is constituted of a platinum cathode and a silver anode which are in contact by a 3 M potassium chloride solution. The electrodes are separated from the measuring chamber by an oxygen permeable Teflon membrane. Therefore, oxygen diffuses from the incubation chamber towards the cathode through the membrane, its partial pressure respectively. The incubation chamber is separated from atmosphere with a plunger that only has a small hole for injections. The content in the incubation chamber has to be continuously stirred to ensure that partial pressure of O_2 is equilibrated in the complete test medium, thus a stable signal can be measured. To ensure a constant temperature of 37 °C the incubation chamber is surrounded by a warming-water outlet. As a polarization voltage of -0.6 V is applied to the platinum cathode, oxygen is reduced to a hydroxide ion with the aid of water. For every reduction reaction, an oxidation at the silver anode takes place. Hereby, silver and chloride become

oxidized. In total, the following electrochemical process occurs:

$$4Ag + O_2 + 2H_2O + 4Cl^- \rightarrow 4AgCl + 4OH^-$$

The resulting current between the two electrodes is proportional to the oxygen partial pressure within the incubation chamber (Rank Brothers Ltd, 2002). By the Lab-Chart 6 software (ADInstruments, New Zealand) the measured voltage is simultaneously displayed as percentage saturation per second.

$$\frac{Oxygen\ consumption\ [nmol\ O]}{min\ *\ mg\ protein} = \frac{\%/\ min\ *\ nmol\ O/ml\ buffer}{100 * mg\ protein/ml}$$

KHE +0.4 % BSA (faf) + 2 mM $MgCl_2$ (1 ml, air saturated) had been used as respiration buffer. To assess oxygen consumption rates, mitochondria (300 µg) were added to the respiration buffer and stirred during analysis at 550 rounds per minute (rpm). To prevent reverse electron transfer and therefore reactive oxygen species (ROS) production, rotenone (6 µM) as a complex I inhibitor was added at the beginning of respiration measurements (Hinkle et al., 1967). Succinate (4 mM) was injected as a substrate for complex II, ADP (300 µM) for initiating ATP production, and oligomycin (1 µg/ml) to inhibit ATP-synthase (all from Sigma-Aldrich). The complex II substrate succinate was used to obtain higher oxygen consumption rates than with NADH-based substrates to unravel even small differences in respiration. Respiratory measurements of isolated mitochondria were in part conducted with the cooperation of Christina Schempp.

STE buffer

(250 mM sucrose, 5 mM Tris, 2 mM EGTA, pH 7.4)

KHE buffer

(120 mM KCl, 5 mM KH_2PO_4 3 mM Hepes, 1 mM EGTA, pH 7.2)

3.3.2 Isolated adipocytes

Oxygen uptake of isolated adipocytes was measured by high-resolution respirometry (Oxygraph-2k, OROBOROS® INSTRUMENTS, Austria). Hereby, oxygen concentration is measured in two glass chambers by a Clark type polarographic oxygen sensor. The sensor consists of a gold cathode (2 mm), a silver/silverchloride anode and a KCl electrolyte reservoir,

separated from the sample by a 25 µm O_2 permeable membrane. Sensor calibration is performed by a two-point calibration using air-saturated media and sodium dithionite for zero oxygen concentration. As the sensitivity of polarographic oxygen sensors is a function of cathode area and the drift at zero oxygen decreases and the signal to noise ratio increases with cathode diameter, the relatively large cathode in the Oxygraph-2k, is increasing respirometric sensitivity (Gnaiger and Forstner, 1983). Furthermore, oxygen-tight materials, Petlier-temperature control, and a continuous background-correction of oxygen flux are determining for high-resolution respirometry (Gnaiger, 2008). Before adipocytes were transferred to the Oxygraph-2k glass chamber, mitochondrial respiration medium 05 (MIR05; oxygen solubility factor = 0.92) (Gnaiger et al.) was added and equilibrated with air. Thereafter 200 µl of packed adipocytes were transferred to the glass chamber and fully closed with the stopper. The adipocyte-buffer suspension was stirred during analysis at 750 rpm. Adipocytes were permeabilized by adding digitonin (2 µM, Sigma-Aldrich). To apply physiological conditions for measuring oxygen consumption rates during maximal oxidative phosphorylation (OXPHOS) capacity in permeabilized adipocytes, a convergent supply of complex I (pyruvate + malate) and II substrates (succinate) was chosen (Gnaiger, 2009). Therefore, malate (5 mM; Sigma-Aldrich) and pyruvate (5 mM; Sigma-Aldrich) were added, followed by ADP (5 mM) and succinate (5 mM). To examine leak respiration (also referred to as state4o), oligomycin (1 µg/ml) was added as an ATP-synthase inhibitor. Uncoupled respiration was determined by the titration of the ionophore Carbonyl cyanide 4-(trifluoromethoxy)phenylhydrazone (FCCP; 0.5 µM steps; Sigma-Aldrich). The complex III inhibitor antimycin A (2.5 µM, Sigma-Aldrich) was added to assess non mitochondrial respiration, which was then subtracted from all other respiratory states (see representative respiration measurement Figure 4). Subsequently, the cell suspension was transferred to a reaction tube and frozen at -80°C until DNA isolation.

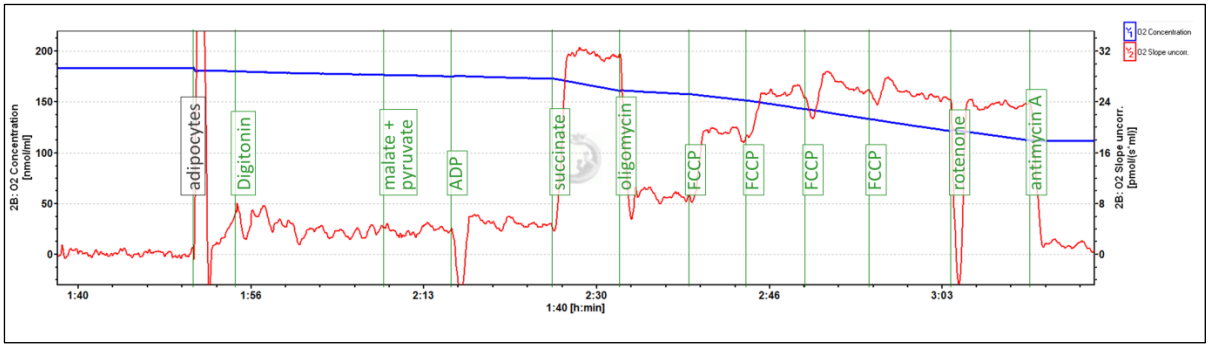

Figure 4: Representative oxygen consumption measurement in isolated adipocytes with Oxygraph-2k

Oxygen concentration (nmol/ml) is represented by the blue line, oxygen flux (pmol/s*ml) by the red line. Vertical green lines, shown on the x axes [h:min], indicate events where cells or chemicals were added to the glass chamber. Short interruptions or overshoots of the oxygen flux after injection of chemicals are due to different oxygen solubility's of the chemicals in comparison to the applied respiration medium MIR05.

MIR05

(110 mM sucrose, 60 mM potassium lactobionate, 0.5 mM EGTA, 3 mM $MgCl_2$*$6H_2O$, 20 mM taurine, 10 mM KH_2PO_4, 20 mM HEPES, 1 g/l BSA (faf), pH 7.2)

3.4 Protein expression

Protein expression was determined by Western blot analysis. Therefore, adipocytes were stored in radioimmunoprecipitation assay buffer (RIPA with phosphatase (phosSTOP; Roche, Basel, Switzerland) and protease inhibitors (cOmplete; Roche)) at -80 °C until protein extraction. Samples were thaw on ice and homogenized with zirconium/glass-Beads® (ø 0.5 mm; ROTH) in a high-speed benchtop homogenizer (max. speed, 5x 25 s; FastPrep®-24 Instrument, MP Biomedicals, USA). After centrifugation (20,000 x *g*, 4°C, 15 min), the fatty supernatant was removed, and protein concentrations were determined using a BCA Protein Assay Kit (ThermoFisher Scientific). Following, 15 µg of protein was diluted in Laemmli buffer (5x), heated (55°C, 5 min) and subsequently loaded onto a 15 % acrylamide gel. In addition to the protein samples 3 µl of a dual colored protein standard (BIO-RAD, Germany) was loaded as a reference. After SDS-PAGE with running buffer, proteins were transferred to a nitrocellulose membrane (Whatman, GE Healthcare, UK) via wet blot for 2 h (150 mA) in transfer buffer. Odyssey blocking buffer (LI-COR, USA) diluted in phosphate buffered saline (PBS; 1:2) was used for blocking the membrane. Antibodies were diluted in blocking buffer with 0.15 % Tween® 20 (Sigma-Aldrich) and 0.015 % SDS (AppliChem, Germany) (see also Table 2). The membrane was incubated with primary antibodies directed against CS (Abcam,

UK), glyceraldehyde-3-phosphate dehydrogenase (GAPDH; Ambion, ThermoFisher Scientific) and with an antibody mixture for different subunits of respiratory chain complexes (MS601; Abcam). The antibodies in this mixture were directed against NDUFB8 of complex I, SDHB of complex II, subunit core 2 of complex III, MT-CO2 of complex IV, and F1 of complex V. Subsequently, the membrane was washed with PBS-T (4 times for 5 min each). After reacting with infrared fluorescence IRDye secondary antibodies (LI-COR) the membrane was washed again with PBS-T (4 times for 5 min each) and PBS (5 min). Protein bands were detected using an infrared imaging system (Odyssey; LI-COR).

Table 2: Applied antibodies for Western blot analysis

Primary Antibody	Dilution	Incubation	Secondary antibody	Dilution	Incubation
Citrate synthase (rabbit)	1:200	1 h, RT	Donkey anti-rabbit IRDye800CW	1:15000	45 min, RT
GAPDH (rabbit)	1:1500	Overnight, 4 °C	Donkey anti-rabbit IRDye800CW	1:15000	45 min, RT
Total OxPhos Complex Kit (mouse)	1:200	1, h RT	Donkey anti-mouse IRDye680	1:15000	45 min, RT

RIPA buffer

50 mM Tris·HCl, pH 8, 150 mM NaCl, 0.2 % Sodium dodecyl sulfate (SDS), 1 % Nonidet P-40, 0.5 % deoxycholate, 1 mM Phenylmethanesulfonylfluoride (PMSF)

Laemmli buffer

(310 mM Tris, 50 mM DTT, 2.5 mM EDTA, 25 % glycerin, 5 % SDS, 5 % bromophenol blue, pH 6.8)

Running buffer

(250 mM Tris, 1M glycin, 1 % SDS, pH 8.3)

Transfer buffer

(20 mM Tris, 150 mM glycin, 20 % methanol, 0.02 % SDS, pH 8.4)

PBS-T
(PBS; 0.1% Tween® 20)

3.5 Complex IV activity

During the OXPHOS process, oxygen is reduced to water at the complex IV (cytochrome c oxidase), by the transfer of electrons from cytochrome c to oxygen. Within the applied activity assay, the O_2 uptake of complex IV can be assessed independent from the OXPHOS process, as complex IV is solubilized from the inner mitochondrial membrane. Therefore, 1 ml frozen adipocytes where homogenized, using a 5 ml potter with 500 µl isolation buffer. After further disruption by an ultrasonic probe (2x 5 sec, 80 % power), the homogenate was centrifuged (16.000 x *g*, 2 min), and the intermediate layer was transferred to a new reaction tube. Protein concentration of the sample was determined by a BCA Protein Assay Kit (ThermoFisher Scientific). Using 250 µg of protein, complex IV activity was assessed by measuring oxygen consumption in a Clarke electrode in 1.5 ml air saturated assay buffer. The buffer additionally included ascorbic acid (20 mM; pH 7, Sigma-Aldrich), as a reducing agent, ADP (5 mM), as an allosteric activator of complex IV, oligomycin as a complex V inhibitor, and cytochrome c (Sigma-Aldrich) as an electron donator. Cytochrome c was titrated in the following steps (µM): 5, 10, 50, 100, 130, 150, 160, 190, and 200. For analysis, maximal oxygen uptake and mean oxygen uptake of the different cytochrome c concentrations were used.

Isolation buffer
(10 mM HEPES, 40 mM KCl, 2 mM EGTA, 10 mM KF, 2 µM oligomycin, 1 mM PMSF, 1 % Tween® 20; pH 7.4)

Assay buffer
(50 mM KH_2PO_4, 2 mM EGTA, 1 % Tween® 20, 2 µM oligomycin, pH 7.4)

3.6 ATP determination

ATP levels in adipocytes were determined using the CellTiter-Glo®Luminescent Cell Viability Assay (Promega, Germany). After centrifugation (200 x *g*, 2 min), 25 µl packed adipocytes were transferred to a 1.5 ml reaction tube containing 100 µl DMEM/F12 + 1 %Pen-Strep. Depending on the amount of available adipose tissue, adipocytes were additionally incubated

with media containing oligomycin (1 µg/ml), 2-deoxy-D-glucose (2-deoxy-D-glc, 100 mM; Sigma-Aldrich) or the combination of both substances. Until the measurement was performed, the adipocytes were stored for 2.5 h in an incubator (5 % CO_2 atmosphere; 37 °C; Binder, Germany). In order to the manufacturer's protocol, the required buffers, an ATP standard series, and the samples had to be equilibrate to room temperature (RT) for 30 min. The ATP standard was transferred to a transparent 96-well plate (Greiner bio-one, Austria). A volume of CellTiter-Glo® Reagent, equal to the volume of ATP standard and samples, was added and incubated under agitation (900 rpm, 12 min) for inducing cell lysis and stabilizing luminescence signal. The reaction tube containing the lyzed adipocytes were centrifuged (400 x *g*, 3 min). Subsequently, 100 µl of the supernatant was transferred to the 96-well plate as well and the luminescence signal of the samples and the ATP standard were measured (Infinite® 200 PRO, Tecan). The ATP concentrations of the unknown samples were calculated by a standard curve referring to the known ATP concentrations. The remaining adipocyte lysate was stored at -80 °C until DNA isolation.

3.7 Lactate determination

For measuring glycolysis in isolated adipocytes, lactate release to the cell culture media was determined. Therefore, L-lactate was measured indirectly by NADH + H^+ which is formed by the conversion of L-lactate to pyruvate by the enzyme LDH with NAD^+ as a cofactor. NADH+ H^+ is absorbing ultraviolet (UV) light at 339 nm and thus, can be measured spectrophotometrically.

Adipocytes were seeded 1:4 diluted in DMEM/F12 + 1 % Pen-Strep. Depending on the amount of available adipose tissue, adipocytes were also incubated with media containing oligomycin (1 µg/ml). After 24 h, adipocytes were removed and frozen at -80°C until DNA isolation. To remove cellular LDH, the supernatant was initially deproteinized by a spin filter with a molecular weight cutoff at 10 kDa (Vivaspin, GE Healthcare). For storage, samples were kept at -80 °C. Samples where thaw on ice. For precipitation of the remaining proteins, 20 µl of the samples were diluted (1:2) with 6 % perchloric acid (Sigma-Aldrich). After vortexing, samples were centrifuged (3000 x *g*, 15 min). Duplicates of 10 µl of the supernatant were transferred to a transparent 96-Well plate (Greiner bio-one, Austria) and 100 µl reagent mix, containing NAD^+ (Sigma-Aldrich) and LDH (Sigma-Aldrich), was added. Samples were incubated for 30 min at RT and absorbance was measured at 399 nm subsequently (Infinite® 200 PRO, Tecan). As

the obtained optical density is proportional to the lactate present in the sample, the amounts of lactate were calculated referring to a lactate standard series.

Hydrazine buffer

(6.8 mM EDTA, 100 mM hydrazine sulphate, 500 mM hydrazine hydrate; pH 9)

Reagent mix per well

100 µl hydrazine buffer, 0.2 mg NAD^+, 1 µl LDH

3.8 DNA isolation and quantification

3.8.1 Mitochondrial DNA quantification

DNA isolation from isolated adipocytes was conducted by a silica- and spin column-based DNA purification Kit (DNeasy Blood & Tissue Kit; Qiagen, Germany). To quantify mtDNA copy number in subjects with different BMI, probe-based quantitative real time PCR was performed on a LightCycler (LightCycler 480; Roche). The applied primers were directed against targets in the mitochondrial (forward 5'-TTC TGG CCA CAG CAC TTA AA-3', reverse 5'-TGG TTA GGC TGG TGT TAG GG-3') and nuclear genome (forward 5'-GCA GGC ATT CCT GGA AGA G-3', reverse 5'-TGT GTG CCC TAC ACA ATG C-3'). The nuclear primer pair amplifies a 78 bp fragment of chromosome 12 (713,966 – 714,043) with no annotated genes within > 30 kb in either direction. The mitochondrial primer pair amplifies a 71 bp fragment of the mitochondrial genome (318 – 388) close to the origin of replication and 257 bp upstream of the phenylalanine tRNA gene (human genome build GRCh38/hg18) (Genome Bioinformatics Group, 2017). With respect to both primer pairs, binding outside their respective unique target region with special attention to the multiple nuclear copies of mitochondrial genome fragments was excluded (Primer pairs designed by Dr. Tobias Fromme). Every sample was measured in triplicates. Prior to plot mtDNA copy numbers against donor's BMI values, the ratio of mtDNA to nuclear DNA was calculated (mtDNA/nDNA).

3.8.2 Total DNA quantification

For normalization purposes, adipocytes used for respiratory, ATP, and lactate determination, were frozen at -80 °C. Samples were thawed on ice and vortexed vigorously. 400 µl of lysis buffer was added to adipocytes originated from ATP, and lactate measurements. Duplicates

of 100 µl adipocyte suspension were diluted 1:5 in lysis buffer with proteinase K (Qiagen). After digestion for 1 h (65 °C, 1,000 rpm) and proteinase K inactivation for 10 min (95 °C, 1,000 rpm), samples were put on ice and 1,125 µl of phenol:chloroform:isoamyl alcohol (25:24:1; ROTH) was added. Samples were vortexed and centrifuged for phase separation (16,000 x *g*, 5 min). Hydrophilic phase was transferred to a new reaction tube. DNA concentrations were determined in duplicates using Quant-iT™ PicoGreen® dsDNA Assay Kit (ThermoFisher Scientific) and calculated referring to an adipocyte human genomic DNA standard series of known concentrations. The PicoGreen® reagent contains fluorophores that become fluorescent through binding to dsDNA and can be measured at 520 nm (Infinite® 200 PRO, Tecan).

Lysis buffer
(10 mM Tris HCl pH 8.3, 50 mM KCl, 0.45 % Nonidet P-40, 0.45 % Tween® 20, 0.2 mg/ml proteinase K)

3.9 Statistical analysis

Statistical analyses were performed with GraphPad Prims version 4 (GraphPad Software, La Jolla, USA) and R Studio (RStudio, Inc. Boston; USA). Boxplots are defined as follows: the vertical line indicates the median; the inter quartile range (IQR) determines the width of the box; the upper and lower quartile (UQ, LQ) margins the box; the whiskers indicate values within 1.5*IQR; outliers are plotted individually, when the values are greater than UQ+1.5*IQR, or lower than the LQ-1.5*IQR.

4 RESULTS

4.1 Oxygen uptake of isolated adipocytes

In order to characterize adipocyte mitochondrial respiration, adipocytes from the subcutaneous and the visceral depot were isolated, and oxygen consumption rates were determined by high-resolution respirometry during different respiratory states. The cohort included subjects with a wide range of BMI values, different ages, as well as individuals with different diabetic states including also individuals with no signs for any disturbances within the glucose homeostasis. The baseline characteristics of the included subjects are summarized in Subject's details Table 26 (Appendix).

4.1.1 Oxygen uptake of isolated adipocytes in association to donor's BMI

All values reflecting oxygen uptake were normalized to the corresponding DNA amount of the measured adipocytes, and therefore, express oxygen uptake per cell. Furthermore, within the regression analysis, data were adjusted for age, that had been found to be associated with mitochondrial dysfunction (Chistiakov et al., 2014), particularly in adipose tissue (Hallgren et al., 1989). OXPHOS capacity (also called state3 respiration) was assessed by adding the complex I substrates malate and pyruvate, the complex II substrate succinate, as well as ADP in excess. Therefore, oxygen uptake is depending on the capacity of the OXPHOS process (Chance and Williams, 1955; Gnaiger, 2014). In subcutaneous adipocytes oxygen uptake limited by OXPHOS capacity was significantly negatively associated to donor's BMI ($p < 0.05$; Figure 5A, Table 3). Although in visceral adipocytes the estimated coefficient for BMI was negative as well, no significant association was observed between OXPHOS capacity and BMI (Table 3). LEAK respiration (also called state4o respiration), which was measured adding the ATP-synthase inhibitor oligomycin, neither was in subcutaneous nor in visceral adipocytes associated with donor's BMI (Figure 5B, Table 3). The ratio of oxygen uptake during OXPHOS capacity to LEAK respiration indicates the respiratory control ratio (RCR). High values of RCR are linked to a high capacity to oxidize substrates as well as ATP turnover and an intact inner mitochondrial membrane. Although there are no absolute values for RCR which indicates mitochondrial dysfunction, changes concerning the OXPHOS process, potentially conduce alterations in the RCR (Brand and Nicholls, 2011). Similar to the results of LEAK respiration, no statistically significant association of the RCR and donor's BMI were found in visceral and

subcutaneous adipocytes (Figure 5C; Table 3). Free OXPHOS capacity (Gnaiger, 2014) (also stated as ATP-linked respiration) was calculated by subtracting oxygen consumption during LEAK respiration from oxygen consumption during OXPHOS capacity. Again, a negative association between BMI and free OXPHOS capacity was only seen in adipocytes derived from the subcutaneous ($p < 0.05$; Figure 5D; Table 3), but not in those from the visceral depot (Table 3). To determine oxygen consumption rates exclusiveley depending on the electron transfer system (ETS), mitochondrial respiration was uncoupled from complex V by titration of the ionophore FCCP, which enables the transport of protons across the inner mitochondrial membrane. In addition, oxygen uptake limited by ETS capacity was inversely associated with donor's BMI values of subcutaneous adipocytes ($p < 0.029$; Figure 5E; Table 3) but not with those of visceral adipocytes (Table 3).

In summary, the results suggest that with increasing BMI values, the OXPHOS capacity, free OXPHOS capacity, as well as the ETS capacity are decreasing per cell within subcutaneous, but not visceral adipocytes.

Table 3: Multiple regression analysis: Adipocyte oxygen consumption and donor's BMI values adjusted for age

respiratory state	fat depot (n)	coefficient BMI	R^2	*p*-value	
OXPHOS capacity	vc (47)	-0.142	0.01	n.s.	0.629
	sc (40)	-0.577	0.18	*	**0.027**
LEAK respiration	vc (47)	-0.022	0.02	n.s.	0.841
	sc (40)	-0.113	0.11	n.s.	0.367
RCR	vc (47)	-0.018	0.02	n.s.	0.393
	sc (40)	-0.009	0.15	n.s.	0.294
free OXPHOS capacity	vc (47)	-0.120	0.01	n.s.	0.594
	sc (40)	-0.465	0.16	*	**0.017**
ETS capacity	vc (47)	-0.081	0.05	n.s.	0.743
	sc (40)	-0.486	0.21	*	**0.029**

A multiple regression analysis with donor's BMI values and respiratory states of adipocytes, adjusted for age, and separated in accordance to the adipose tissue depot of origin, was performed. Estimated coefficients for donor's BMI and multiple R^2 of the model are given. Asterisks indicate if the corresponding coefficient is not equal to zero. Not significant (n.s.); *$p < 0.05$; **$p < 0.01$; ***$p < 0.001$.

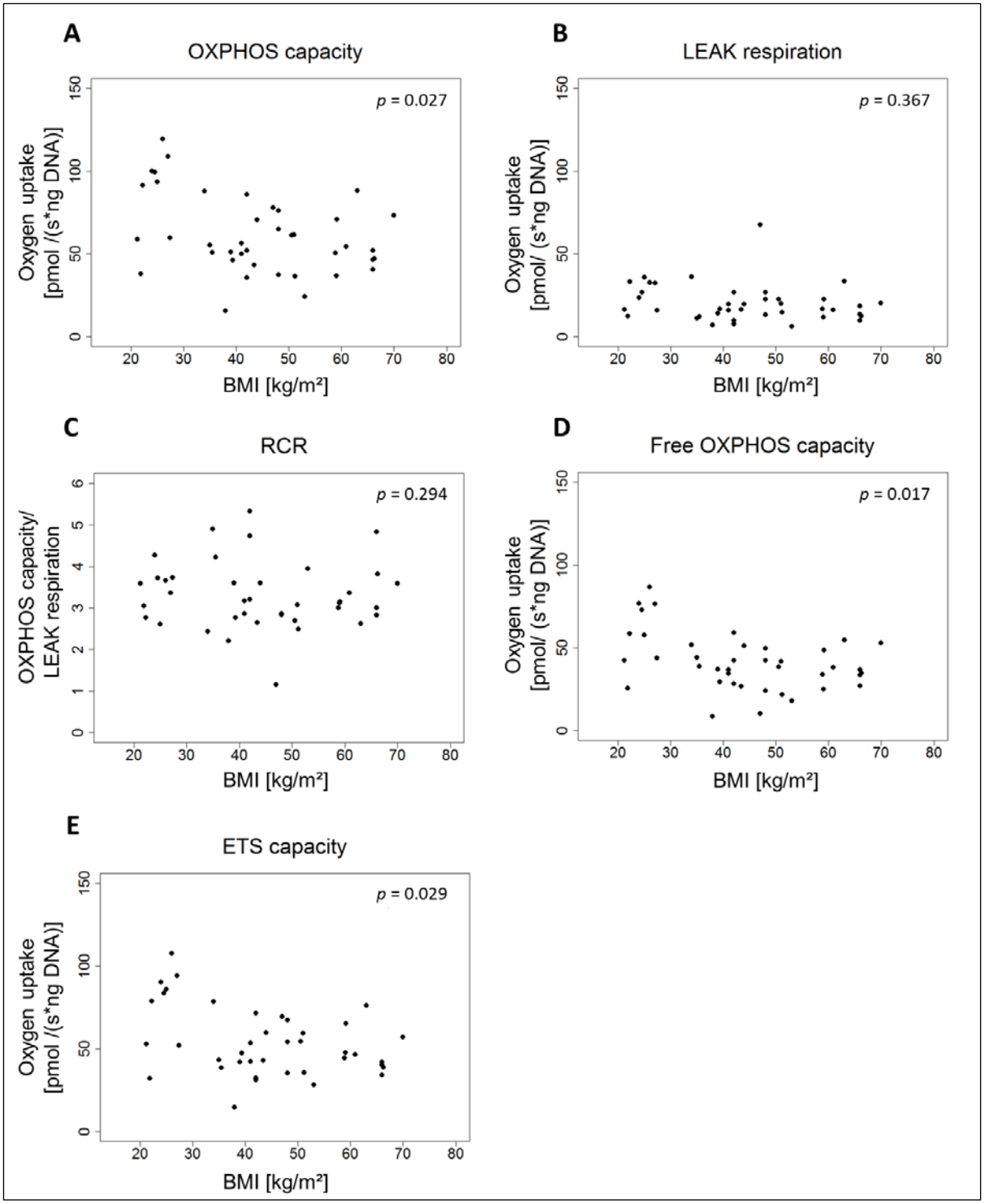

Figure 5: Oxygen uptake of subcutaneous adipocytes during different respiratory states in subjects with varying BMI

Adipocytes were isolated from subcutaneous adipose tissue and permeabilized with digitonin. Oxygen uptake was measured by high-resolution respirometry. Oxygen uptake per s and ng DNA was plotted against donor's BMI. OXPHOS capacity was assessed by adding the complex I and II substrates malate, pyruvate and succinate, as well as ADP in excess (n = 40; A). LEAK respiration was determined by adding the ATP synthase inhibitor oligomycin (n =40; B). RCR was calculated by the ratio of OXPHOS capacity to LEAK respiration (n = 40; C). LEAK respiration values subtracted from OXPHOS capacity values indicate free OXPHOS capacity. (n =40; D). ETS capacity was monitored by the titration with the uncoupling agent FCCP (n =40; E). *P*-values originate from multiple regression analysis, adjusted for donor's age.

4.1.2 Adipocyte oxygen consumption rates of subjects with disturbed glucose homeostasis

Oxygen consumption rates were distinguished between subjects without any disturbances within their glucose homeostasis, and subjects with diabetes or prediabetes, as stated before (see 3.1). To increase the statistical power, pre-diabetic and diabetic individuals were included in the same group, stated as subjects with "disturbances in the glucose homeostasis" (DiGH). Subjects without any impairments within their glucose homeostasis where referred to as "no recognized disturbances within the glucose homeostasis" (ND). To elucidate the role of the diabetic status on oxygen consumption rates of isolated adipocytes in relation to BMI, the impact of the subject's affiliation to DiGH or ND on the association between BMI and oxygen consumption during the different respiratory states was added as an interaction term within a regression analysis adjusted for donor's age. Except for free OXPHOS capacity in visceral adipocytes, no interaction between the diabetic state and the association between BMI values and rates of oxygen uptake could be observed (Table 4). As there was statistically significant evidence that the diabetic status influences the association between BMI and free OXPHOS ($p < 0.05$, Table 4), a linear regression model which included the diabetic status and the subjects age was performed. This analysis did not reveal a significant interaction of the diabetic status with the oxygen uptake during free OXPHOS capacity in visceral adipocytes ($p = 0.83$).

Table 4: Interaction of the diabetic state on the association between adipocyte oxygen consumption and donor's BMI adjusted for age

respiratory state	fat depot (n ND; n DiGH)	coefficient interaction	*p*-value	
OXPHOS capacity	vc (25; 14)	1.18	n.s.	0.150
	sc (20; 14)	0.22	n.s.	0.715
LEAK respiration	vc (25; 14)	-0.04	n.s.	0.894
	sc (20; 14)	0.03	n.s.	0.933
RCR	vc (25; 14)	0.05	n.s.	0.407
	sc (20; 14)	0.01	n.s.	0.690
free OXPHOS capacity	vc (25; 14)	1.22	*	**0.049**
	sc (20; 14)	0.19	n.s.	0.673
ETS capacity	vc (24; 14)	0.99	n.s.	0.600
	sc (20; 14)	0.27	n.s.	0.143

A multiple regression analysis for respiratory states and donor's BMI adjusted for age and the interaction term diabetic status (ND or DiGH) was performed. The results are separated according to the corresponding adipose tissue depot. Estimated coefficients for the interaction terms are given. Asterisks indicate a statistically significant influence from the diabetic status (ND or DiGH) on the association between the respiratory states and the donor's BMI: Not significant (n.s.); *$p < 0.05$; **$p < 0.01$; ***$p < 0.001$.

To further explore if there are differences in oxygen consumption rates with regard to the diabetic status, but to be sure to exclude effects from different BMI values, only subjects with BMI values above 35 kg/m² were compared. Therefore, a regression analysis adjusted for the subject's ages was applied. No statistically significant difference for any respiratory state was observed between the ND and DiGH group (Table 5; Figure 6; Figure 7).

Table 5: Multiple regression analysis: Adipocyte oxygen consumption of subjects with BMI ≥ 35 kg/m²and different diabetic states

respiratory state	fat depot (n ND; n DiGH)	coefficient diabetic state	*p*-value	
OXPHOS capacity	vc (10; 13)	2.44	n.s.	0.824
	sc (11; 12)	-11.29	n.s.	0.132
LEAK respiration	vc (10; 13)	-3.58	n.s.	0.337
	sc (11; 12)	-6.65	n.s.	0.219
RCR	vc (10; 13)	0.38	n.s.	0.315
	sc (11; 12)	0.17	n.s.	0.636
free OXPHOS capacity	vc (10; 13)	6.03	n.s.	0.489
	sc (11; 12)	-6.64	n.s.	0.371
ETS capacity	vc (10; 13)	-0.58	n.s.	0.951
	sc (11; 12)	-5.01	n.s.	0.422

A multiple regression analysis for respiratory states and the diabetic state (ND or DiGH) adjusted for age was performed for subjects with BMI ≥ 35 kg/m². The results are separated according to the corresponding adipose tissue depot. Estimated coefficients for donor's diabetic states and multiple R^2 of the model are given. Asterisks indicate a statistically significant influence from the diabetic state (ND or DiGH) on the association between the respiratory states and the donor's BMI: Not significant (n.s.); *$p < 0.05$; **$p < 0.01$; ***$p < 0.001$.

Boxplots of the two groups for the different respiratory states are shown in Figure 6 for the visceral depot and in Figure 7 for the subcutaneous depot. From these analyzes no differences between the respiratory measurements of the group including subjects with prediabetes or diagnosed/manifest diabetes compared to the group including subjects without any disturbances within their glucose homeostasis can be deduced.

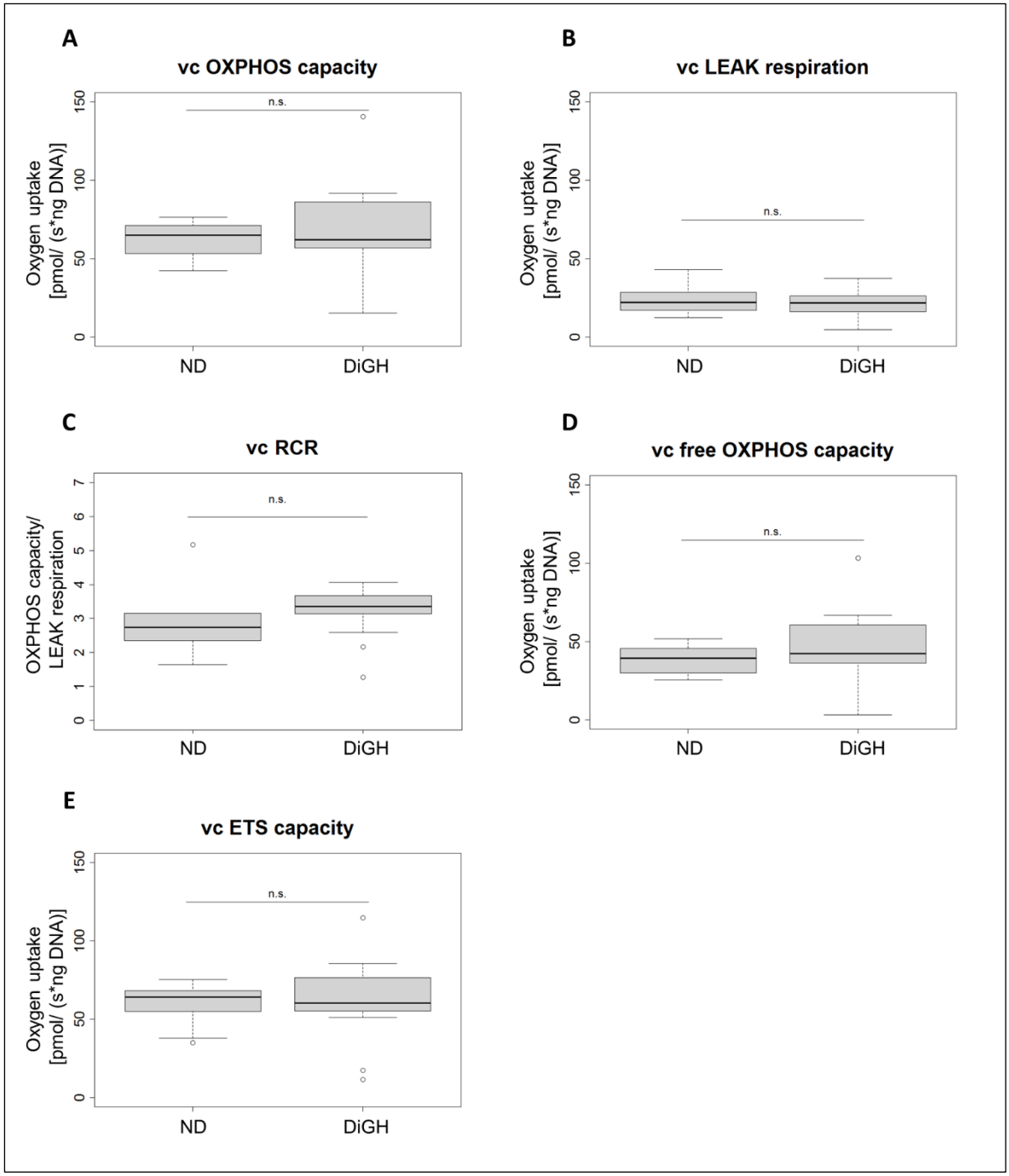

Figure 6: Comparison of visceral adipocytes respiratory states of subjects with different diabetic status

A multiple regression analysis for respiratory states, adjusted for age, and the diabetic status (ND or DiGH) was performed for visceral adipocytes of subjects with BMI ≥ 35 kg/m² (ND: n = 10; DiGH: n = 13). Asterisks indicate statistically significant differences between the two groups (ND vs. DiGH): Not significant (n.s.); *$p < 0.05$; **$p < 0.01$; ***$p < 0.001$.

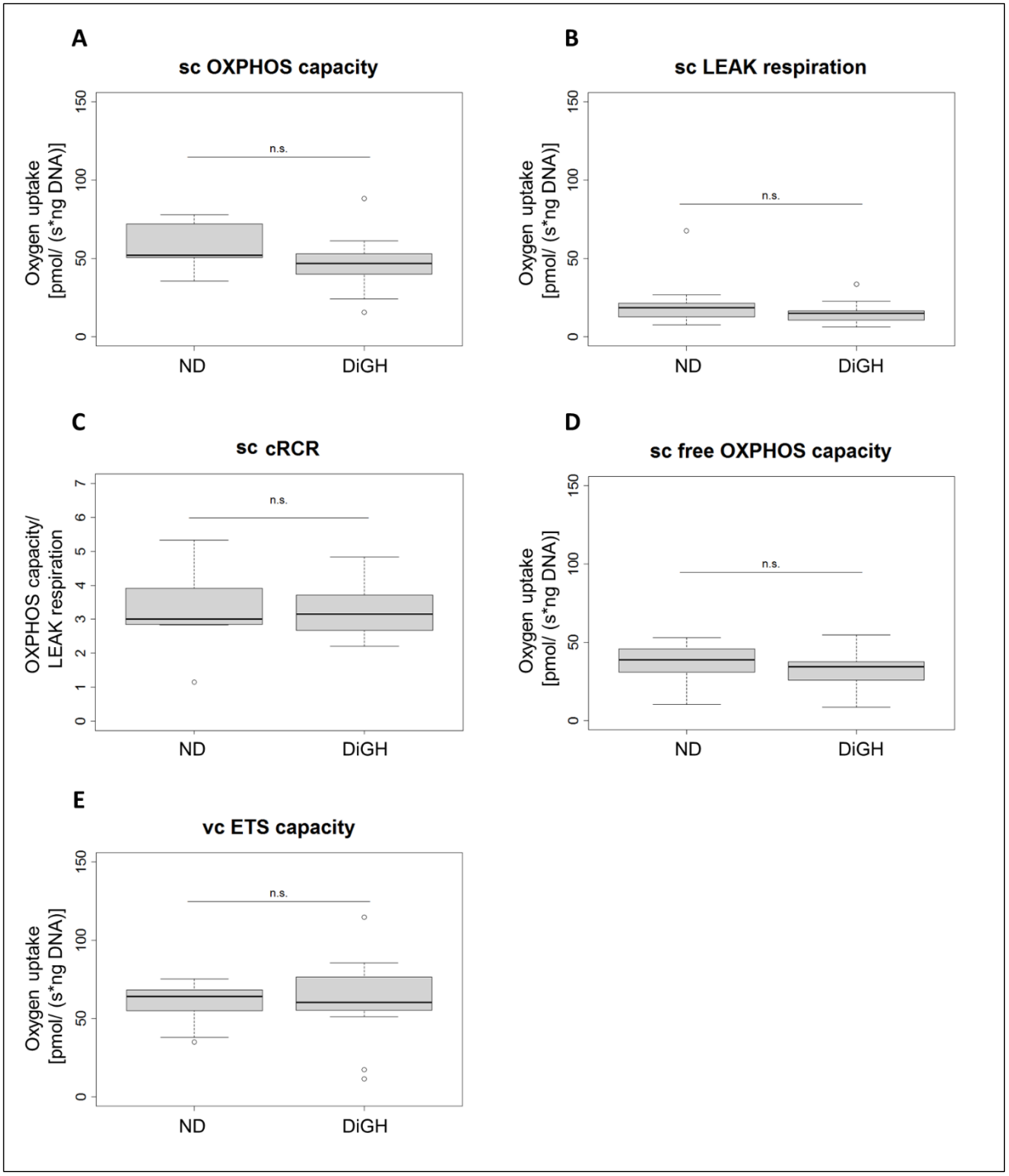

Figure 7: Comparison of subcutaneous adipocytes respiratory states of subjects with different diabetic status

A multiple regression analysis for respiratory states, adjusted for age, and the diabetic status (ND or DiGH) was performed for visceral adipocytes of subjects with BMI ≥ 35 kg/m² (ND: n = 11; DiGH: n = 12). Asterisks indicate statistically significant differences between the two groups (ND vs. DiGH): Not significant (n.s.); *$p < 0.05$; **$p < 0.01$; ***$p < 0.001$.

4.1.3 Adipocyte oxygen uptake with special regard on the adipose tissue depot of origin

With the attempt to analyze if there is an association between oxygen uptake of adipocytes from the subcutaneous and the visceral depot within one subject, Pearson's product-moment correlation was performed. Except for the RCR (Figure 8C), a statistically significant correlation between adipocytes of the two depots was found for all other determined respiratory states within the same subject (Figure 8A, B, D, E). The strongest correlation between the subcutaneous and the visceral depot was found for oxygen uptake during LEAK respiration ($r = 0.71$; $p < 0.001$, Figure 7B).

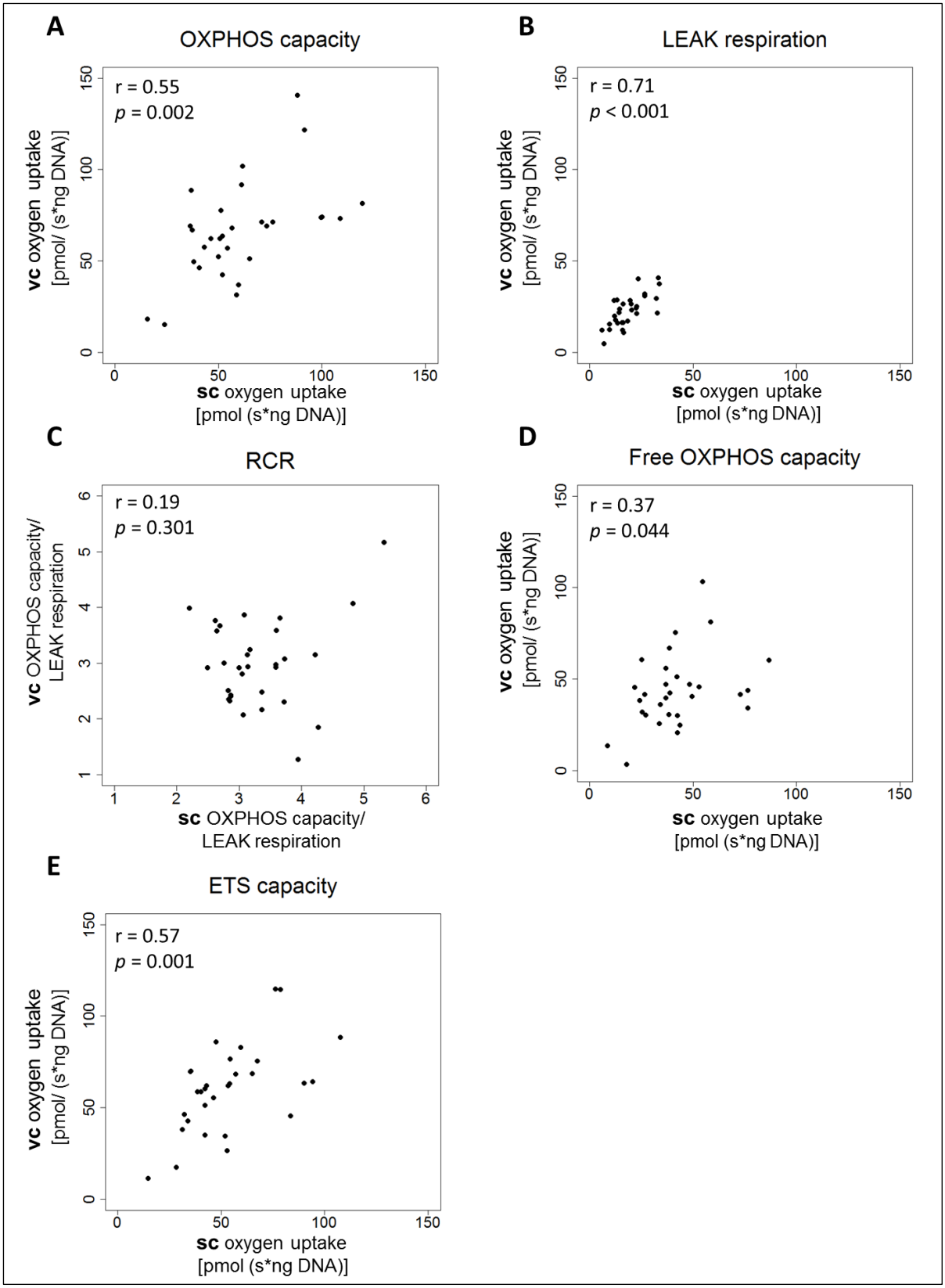

Figure 8: Association between visceral and subcutaneous adipocyte oxygen uptake during different respiratory states

Pearson's product-moment correlation was performed for analyzing the association between subcutaneous and visceral adipocyte oxygen uptake during different respiratory states within the same subject (n = 30).

Besides the examination of the link between oxygen consumption rates of adipocytes from the two depots, also differences between the rates were analyzed. Therefore, a paired Student's *t*-test was performed. Hereby, a significant difference has only been observed between oxygen uptake of visceral and subcutaneous adipocytes during LEAK respiration ($p = 0.002$; Figure 9B). All other respiratory states did not exhibit differences between the two depots (Figure 9A, C-E; Table 6).

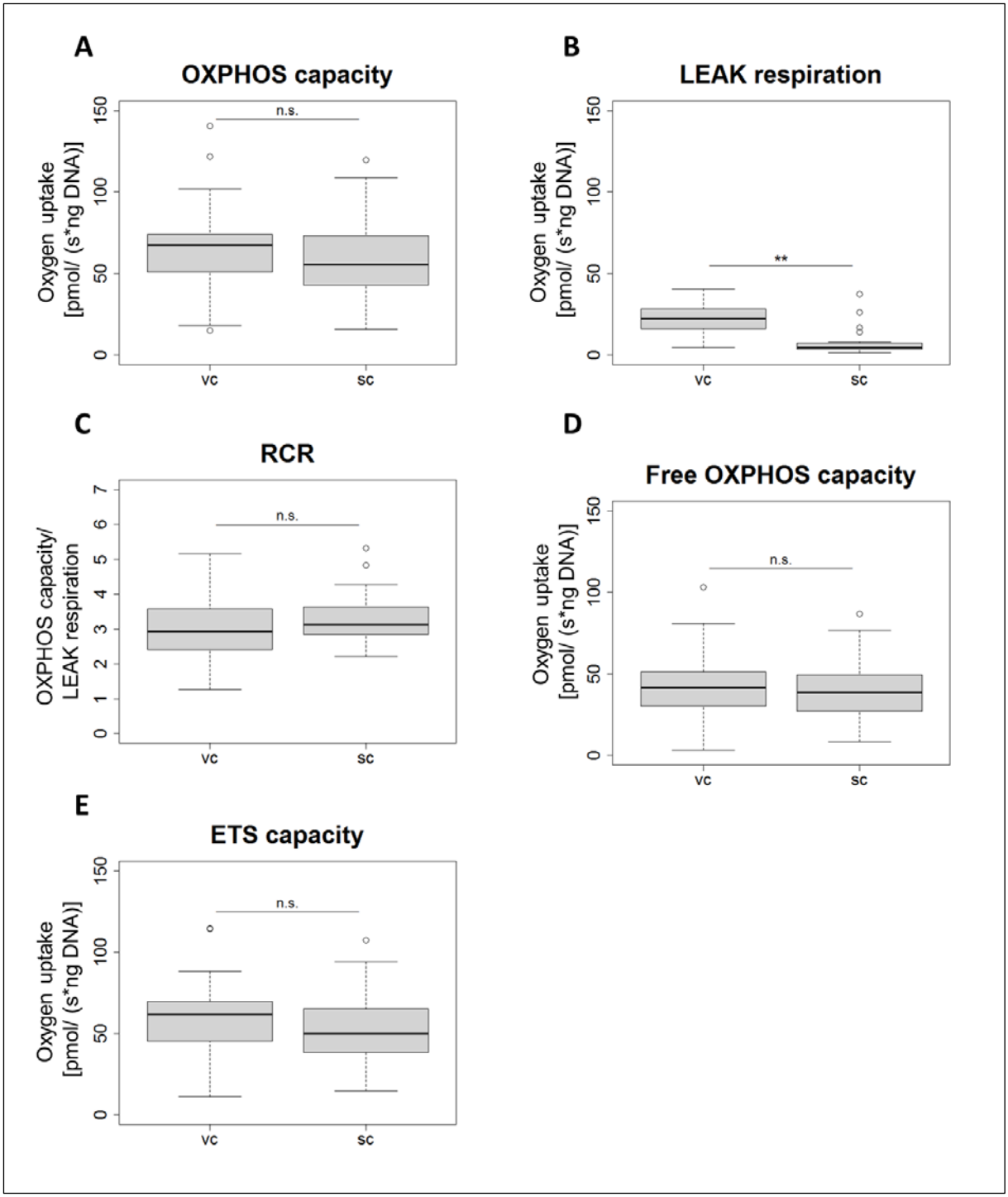

Figure 9: Comparison of respiratory states of visceral and subcutaneous adipocytes

Differences between oxygen consumption rates of visceral and subcutaneous adipocytes were determined using Student's paired *t*-test (n = 30). Asterisks indicate significant differences between the two depots (vc vs. sc): Not significant (n.s.); *$p < 0.05$; **$p < 0.01$; ***$p < 0.001$.

Table 6: Comparison of oxygen uptake between visceral and subcutaneous adipocytes

respiratory state (n)	mean vc	mean sc	*p*-value	
OXPHOS capacity (30)	66.12 (±26.56)	60.68 (±24.98)	n.s.	0.233
LEAK respiration (30)	22.57 (± 8.78)	18.67 (± 7.73)	**	**0.002**
RCR (30)	2.99 (±0.79)	3.31 (±0.79)	n.s.	0.068
free OXPHOS capacity (30)	43.55 (±20.26)	42.01 (±18.27)	n.s.	0.844
ETS capacity (30)	60.25 (±24.00)	53.34(±21.57)	n.s.	0.085

Differences between oxygen consumption rates of visceral and subcutaneous adipocytes were analyzed using Student's paired *t*-test (n = 30). Values are expressed as means (±SD). Only LEAK respiration differed statistically significant between the two depots. Asterisks indicate significant differences between the two depots (vc vs. sc): Not significant (n.s.); *p < 0.05; **p < 0.01; ***p < 0.001.

In order to gain further insights into the effect of donor's BMI on adipocyte bioenergetics, the cohort was divided into one group including lean and overweight subjects with BMI values < 30 kg/m², and another group with obese subjects referring to their BMI values ≥ 30 kg/m². Following this, differences between adipocytes from subcutaneous and visceral adipose tissue depot were compared again. OXPHOS, free OXPHOS and ETS capacity show opposite behavior of visceral and subcutaneous adipocytes between the two groups (Table 7, Figure 10A, D, and E). Except for the determined RCR, obese subjects showed lower oxygen consumption rates within the determined respiratory states (Figure 10A, B, D, and E). Subjects with a BMI below 30 kg/m², showed higher oxygen consumption rates for adipocytes from the subcutaneous depot, except for LEAK respiration (Figure 10B). Although these differences were only statistically significant for the RCR, also OXPHOS capacity ($p = 0.091$) and free OXPHOS capacity ($p = 0.051$) showed trends towards higher subcutaneous oxygen uptake rates.

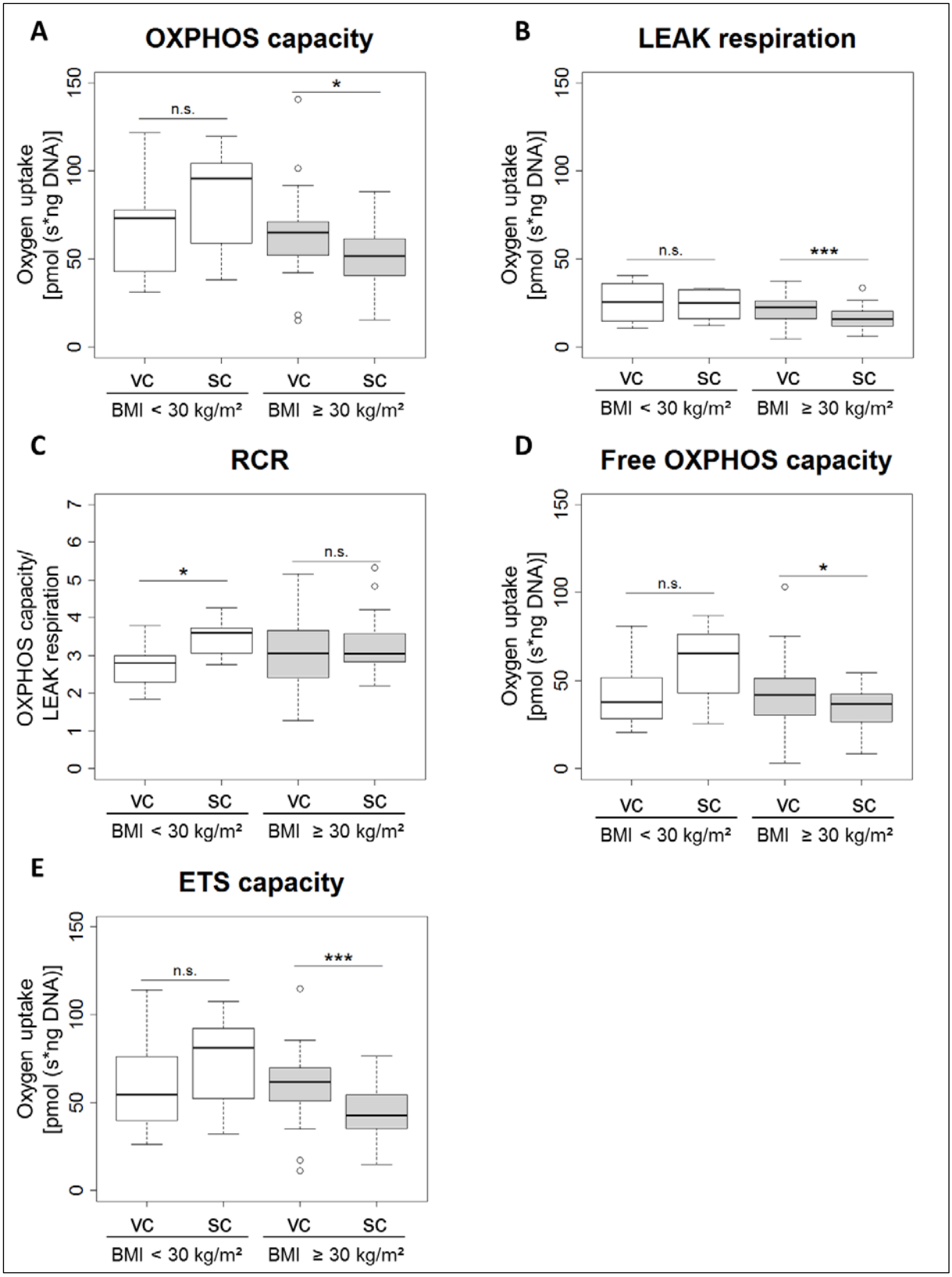

Figure 10: Comparison of oxygen uptake of visceral and subcutaneous adipocytes separated by donor's BMI

Subjects were divided into two groups according to their BMI. Data are shown as boxplots. White boxplots indicate subjects with BMI < 30 kg/m² (n = 8); grey boxplots subjects with BMI ≥ 30 kg/m² (n = 22). Differences between oxygen consumption rates of visceral and subcutaneous adipocytes were analyzed using Student's paired *t*-test or Wilcoxon signed-rank tests, if variances were not equal. Asterisks indicate statistically significant differences between the two depots (vc vs. sc): Not significant (n.s.); *$p < 0.05$; **$p < 0.01$; ***$p < 0.001$.

Table 7: Comparison of oxygen uptake of visceral and subcutaneous adipocytes, separated by the donor's BMI

respiratory state (n BM I< 30; n BMI ≥ 30)	BMI < 30		*p*-value		BM ≥ 30 kg/m²		*p*-value	
	mean vc (±SD)	mean sc (±SD)			mean vc (±SD)	mean sc (±SD)		
OXPHOS capacity (8; 22)	67.69 (±28.91)	84.50 (±28.74)	n.s.	0.091	65.55 (±26.39)	52.02 (±17.08)	*	**0.004**
LEAK respiration (8; 22)	25.50 (±11.82)	24.14 (± 8.38)	n.s.	0.680	21.51 (± 7.45)	16.60 (± 6.60)	***	**< 0.001**
RCR	2.70 (±0.60)	3.47 (±0.46)	*	**0.020**	3.11 (±0.83)	3.24 (±0.76)	n.s.	0.507
free OXPHOS capacity (8; 22)	42.18 (±19.90)	60.37 (±21.38)	n.s.	0.051	44.05 (±20.83)	35.33 (±11.55)	*	**0.046**
ETS capacity (8; 22)	60.21 (±29.20)	73.96 (±25.59)	n.s.	0.167	60.27 (±22.60)	45.84(±14.26)	***	**< 0.001**

Subjects were divided into two groups according to their BMI. Differences between oxygen consumption rates of visceral and subcutaneous adipocytes were performed using the Student's paired *t*-test or the Wilcoxon signed-rank tests, if variances were not equal. Values are expressed as means (±SD). Asterisks indicate statistically significant differences between the two depots (vc vs. sc): Not significant (n.s.); *$p < 0.05$; **$p < 0.01$; ***$p < 0.001$.

4.2 Oxygen uptake of isolated mitochondria in association to donor's BMI

To gain further insights into mitochondrial function of white adipose tissue in obesity, without potential interference of mitochondrial number and adipocyte size, also oxygen uptake of isolated mitochondria was investigated. Therefore, mitochondria were isolated from subcutaneous adipocytes of female donor's with a wide range of BMI values (Appendix: Table 26). Oxygen uptake of isolated mitochondria was measured in a Clarke-Electrode. To evaluate the association between BMI and oxygen uptake during the different respiratory states, a multiple linear regression analysis adjusted for the donor's age was performed (see Table 8).

During OXPHOS capacity, with succinate as a substrate, oxygen uptake was significant inversely correlated to the donor's BMI ($p < 0.01$; Figure 11A, Table 8). LEAK respiration (also stated as state 4o) was examined by adding oligomycin to inhibit complex V. In contrast to respiration during OXPHOS capacity, there was no correlation between oxygen uptake during LEAK respiration and the corresponding BMI values (Figure 11B), which is indicating that membrane integrity does not differ between adipocyte mitochondria derived from lean and obese subjects. To detect free OXPHOS capacity, which is only linked to ATP production, LEAK respiration values were subtracted from OXPHOS capacity values. The association of respiration during free OXPHOS capacity and BMI exhibited a highly significant inverse association ($p < 0.001$; Figure 11C; Table 8). RCR, assessed by the ratio of respiration during OXPHOS capacity to LEAK respiration, also showed an inverse relation to donor's BMI ($p < 0.05$; Figure 11D; Table 8), even though the correlation was not as clear as for OXPHOS and free OXPHOS capacity.

Table 8: Multiple regression analyses: Oxygen consumption rates of isolated mitochondria and donor's BMI adjusted for age

respiratory state (n)	coefficient BMI	R^2	*p*-value	
OXPHOS capacity (16)	-4.39	0.42	*	**0.026**
LEAK respiration (13)	-0.36	0.18	n.s.	0.262
free OXPHOS capacity (log) (13)	-0.18	0.66	***	**< 0.001**
RCR (16)	-0.38	0.53	*	**0.035**

A linear multiple regression analysis with donor's BMI and respiratory states was performed. Estimated coefficient for donor's BMI and multiple R^2 of the model are given. Asterisks indicate if the corresponding coefficient is not equal to zero. Not significant (n.s.); *$p < 0.05$; **$p < 0.01$; ***$p < 0.001$.

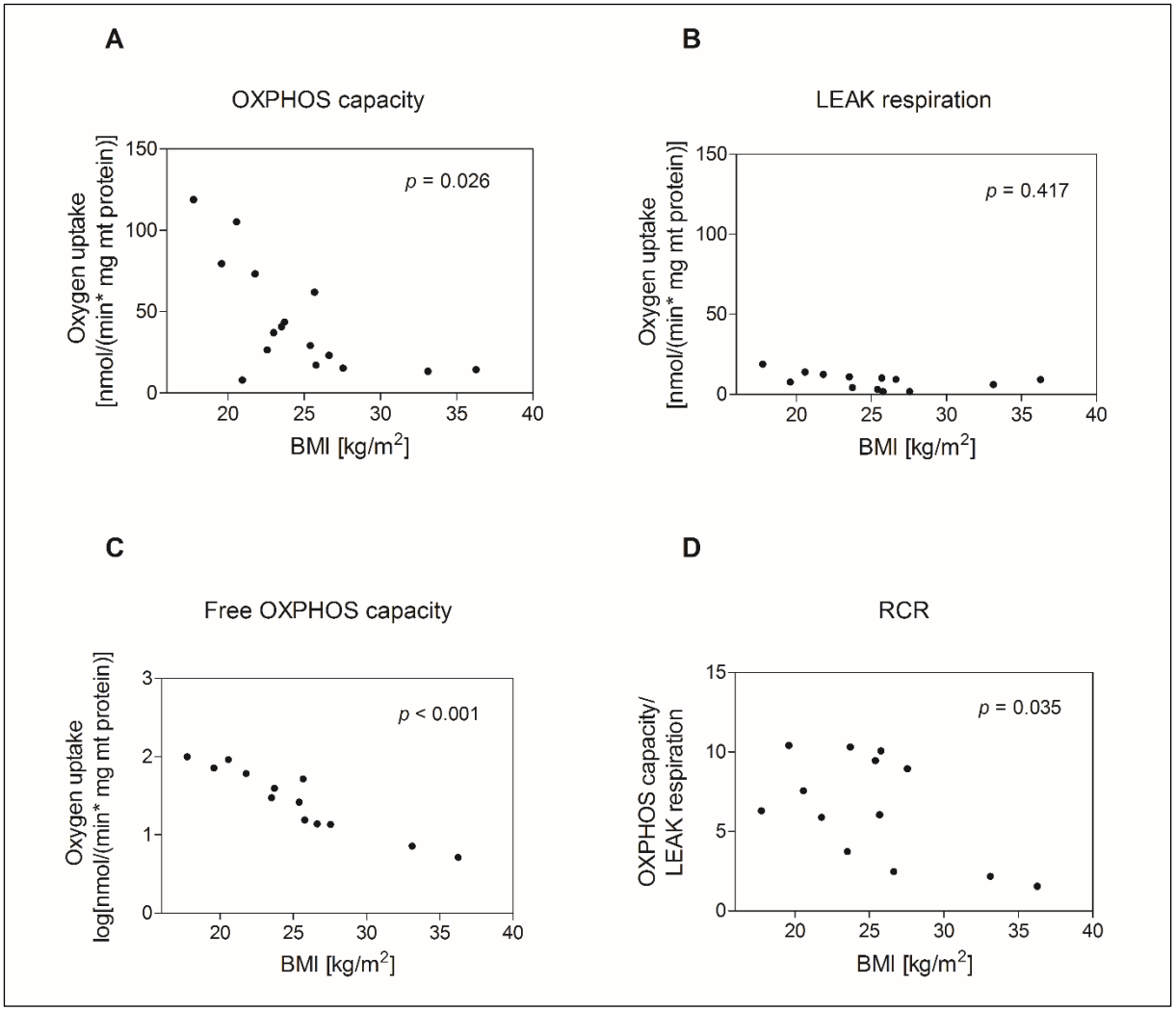

Figure 11: Mitochondrial respiration in association to donor's BMI

Mitochondria were isolated from subcutaneous adipocytes derived from female subjects. Oxygen uptake was measured using a Clark-type oxygen electrode. Oxygen uptake per min and mg mitochondrial protein was plotted against donor's BMI. OXPHOS capacity was assessed by adding the complex II substrate succinate and ADP in excess (n = 16; A). LEAK respiration was monitored by adding the ATP synthase inhibitor oligomycin (n = 13; B). LEAK respiration values subtracted from OXPHOS capacity values indicated free OXPHOS capacity (n = 13; C). The ratio of OXPHOS capacity to LEAK respiration indicated the RCR (n = 13; D). Due to technical issues, oxygen consumption rates during LEAK respiration were available only for 13 of 16 subjects. *P*-values originate from multiple regression analysis, adjusted for age.

4.3 Subcutaneous adipocyte OXPHOS protein expression in obese and non-obese subjects

In order to screen respiratory chain complexes with regard to the subjects BMI, the amounts of single respiratory chain complex subunits were evaluated by Western blot analysis. Therefore, whole adipocyte protein lysates from obese (mean BMI = 32.38 ± 4.2; n = 9) and non-obese (mean BMI = 22.58 ± 2.3; n = 11) female subjects were analyzed. The amounts of respiratory chain complex proteins were detected simultaneously and normalized using

GAPDH as a loading control and CS as an indicator for the mitochondrial content. The detection of complex I revealed significantly higher protein amounts in adipocytes of control subjects (NDUFB8, $p < 0.05$; Figure 12A). Furthermore, protein expression of Complex IV was reduced in obese subjects (MTCO2, $p < 0.05$; Figure 12D). Even though the median protein amounts of complexes II, III, and V were consistently lower in adipocytes from obese compared with those from control subjects, the differences were not statistically significant (Figure 12B, C and E).

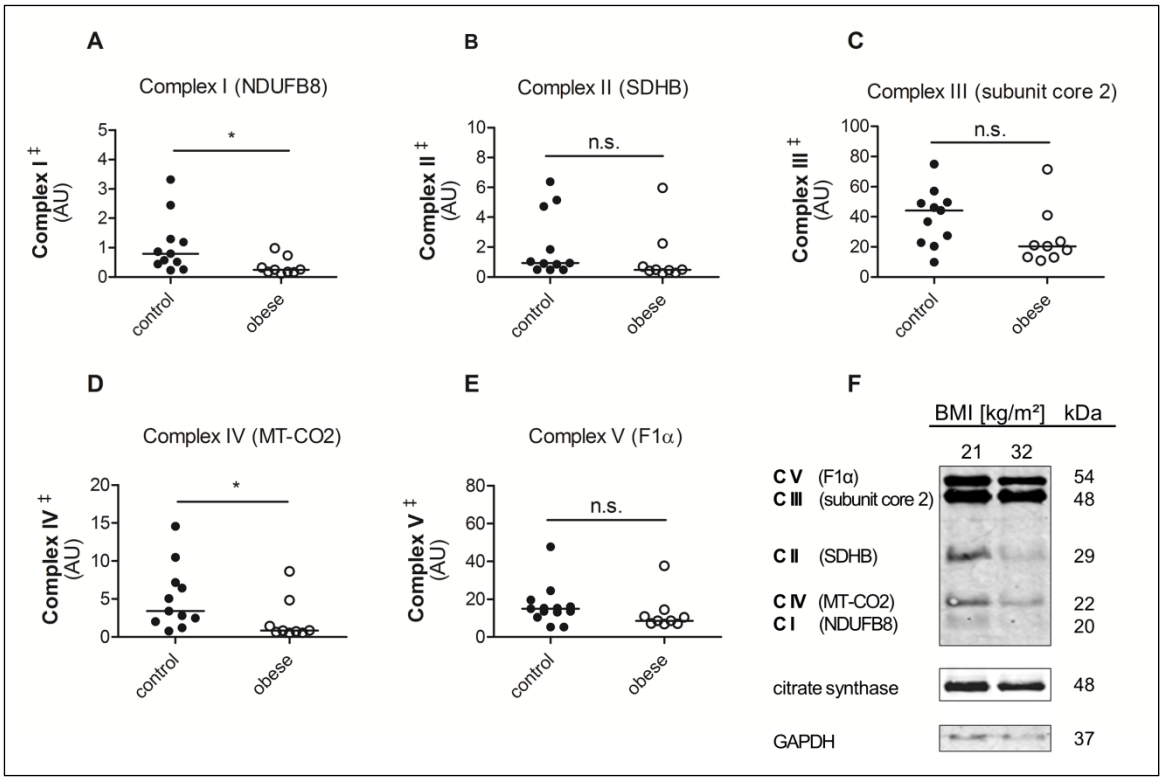

Figure 12: Comparison of protein amounts of respiratory chain complexes between control and obese subjects
Proteins were isolated from human adipocytes from obese (BMI ≥ 26 kg/m²; n = 11) and control (BMI < 26 kg/m²; n = 9) female subjects. Via Western blot analysis respiratory chain complexes were simultaneously detected A-E: ‡band intensities of detected complexes were normalized to GAPDH and CS. Differences between protein amounts were analyzed using a two-tailed unpaired Mann-Whitney test. F: representative Western blot. Arbitrary units (AU). Lines represent medians. Asterisks indicate statistically significant differences between the two groups: Not significant (n.s.); *$p < 0.05$; **$p < 0.01$; ***$p < 0.001$.

4.4 Subcutaneous adipocyte complex IV activity

Western blot analysis revealed lower protein abundance of the complex IV subunit MT-CO2. To obtain further insights into the basis of an impaired mitochondrial respiration with increasing BMI values also the activity of complex IV in subcutaneous adipocytes was investigated. Therefore, the oxygen consumption rates of complex IV, solubilized from the

inner mitochondrial membrane and independent from the OXPHOS process, with cytochrome c as a substrate were assessed by a Clarke electrode. For analysis, the mean complex IV activity as well as the maximal complex IV activity was determined. Through maximal activity also differences within the spare complex IV activity in subjects with different BMIs were addressed. Mean as well as maximal complex IV activity per mg total protein did not show an association with the donor's BMI (n = 20; Figure 13A and B). Whereas the complex IV activity normalized to CS, and therefore to mitochondrial content, showed for mean (p = 0.01, n = 20; Figure 13 C) and maximal complex IV activity (p = 0.03, n = 20; Figure 13D) a significant positive association to the subjects BMI. To further explore a possible compensatory action of complex IV, its activity was associated with its protein abundance revealed from Western blot analysis within the same subject. No association of mean or maximal complex IV activity and the corresponding complex IV protein abundance was detected (n = 20; Figure 13E and F). Taken these results together, an increased subcutaneous adipose tissue complex IV activity per mitochondrion with increasing BMI can be hypothesized, although lower protein levels of complex IV are not accompanied by an increase in complex IV activity. Furthermore, spare activity and mean activity show the same relation to donor's BMI values and complex IV protein abundance (Figure 13).

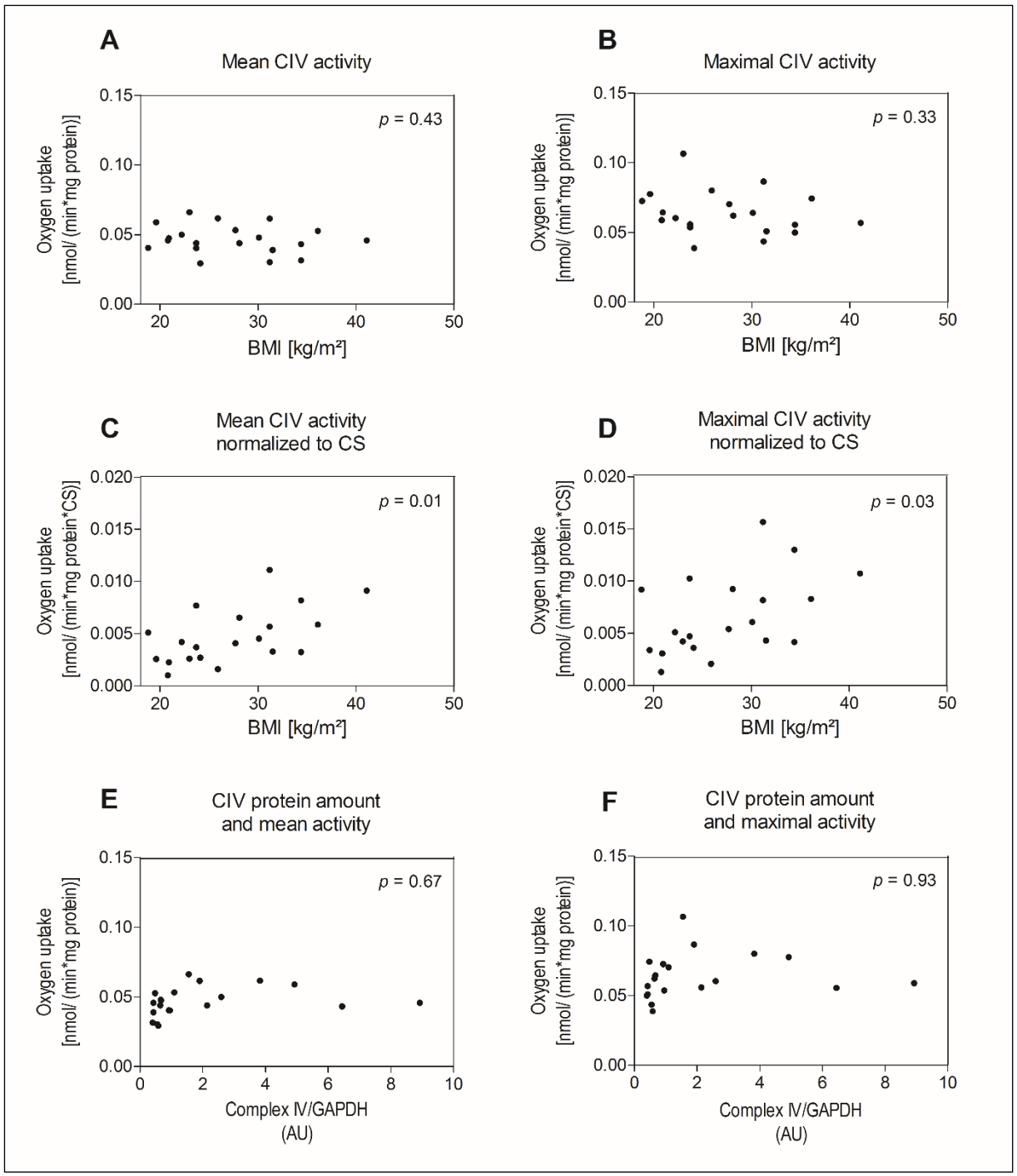

Figure 13: Complex IV activity in subcutaneous adipocytes of subjects with different BMI

Complex IV (CIV) of isolated subcutaneous adipocytes (n = 20) was solubilized from the inner mitochondrial membrane. A total of 250 µg protein was transferred to a Clarke electrode. Oxygen consumption was measured in the presence of ascorbic acid, ADP, Oligomycin and different concentrations cytochrome c. Multiple regression analyses were performed using the mean oxygen consumption during different cytochrome c concentrations (between 5 and 200 µM; A, C, E), and the maximal oxygen consumption of each sample (B, D, F). A-B: Mean and maximal CIV activity was plotted agianst donor's BMI. C-D: Mean and maximal CIV activity was normalized to CS protein abundance and plotted against donor's BMI. E-F: Abundance of CIV, determined by Western blot analysis (see also chapter 4.3), was plotted against mean and maximal CIV activity within the same subject.

Table 9: Multiple regression analyses: complex IV activity

model		coefficient	R^2	*p*-value	
BMI	mean CIV activity	-3.08e-03	0.13	n.s.	0.43
	mean CIV activity/CS	2.42e-04	0.33	*	**0.01**
CIV protein abundance	mean CIV activity	5.43e-03	0.11	n.s.	0.67
BMI	maximal CIV activity	-5.90e-03	0.10	n.s.	0.33
	maximal CIV activity/CS	3.01e-04	0.24	*	**0.03**
CIV protein abundance	maximal CIV activity	1.88e-03	0.05	n.s.	0.93

A linear multiple regression analysis with donor's BMI or complex IV protein abundance and complex IV activity in isolated subcutuaneous adipocytes adiadjusted for donor's age was performed (n = 20). Estimated coefficient for BMI or complex IV abundance and multiple R^2 of the are given. Asterisks indicate if the corresponding coefficient is not equal to zero. Not significant (n.s.); *p < 0.05; **p < 0.01; ***p < 0.001.

4.5 Markers for mitochondrial content in subcutaneous adipocytes are associated to subject's BMI

To investigate whether there are not only differences in mitochondrial function in relation to donor's BMI, but also in mitochondrial content per se, CS protein expression and the mtDNA content were examined. Therefore, nDNA and mtDNA copy numbers were determined with probe-based quantitative real time PCR. MtDNA copy numbers were normalized to the corresponding nDNA copy numbers. The correlation analysis of mtDNA with BMI demonstrated a significantly inverse relationship (r = -0.59; $p < 0.05$; n = 17 Figure 14A). According to that, also CS protein expression of whole adipocyte protein lysate, normalized to GAPDH as a loading control, resulted in an inverse association to the donor's BMI (r = -0.45; $p < 0.05$; n = 20; Figure 14B). The amount of mtDNA and CS was not associated to the donor's age (data not shown).

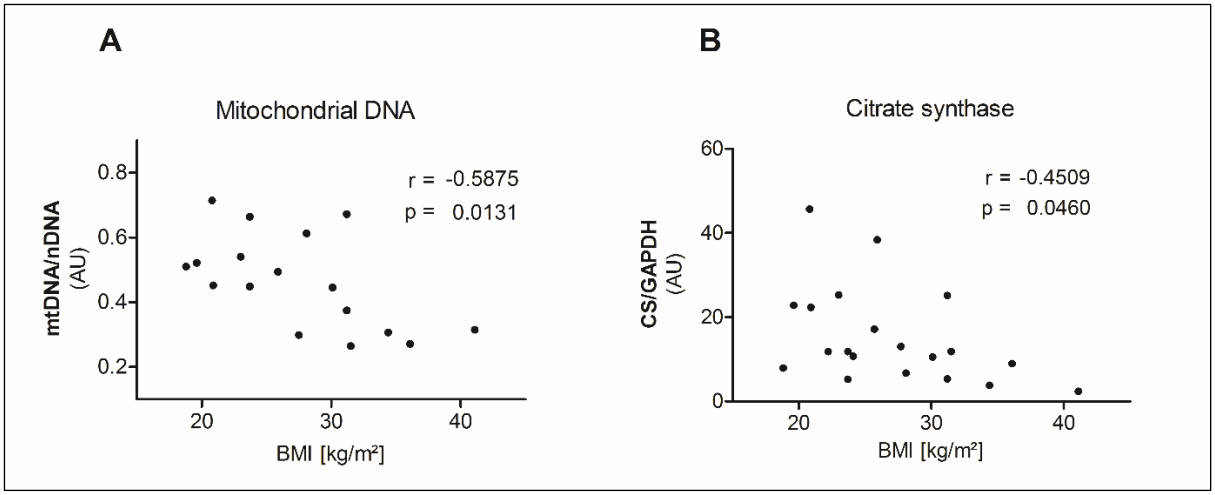

Figure 14: Markers for mitochondrial content in adipocytes of subjects with different BMI

Pearson's product-moment correlation was performed for analyzing the association between parameters of mitochondrial content and donor's BMI. Individual donors are represented by dots. DNA was isolated from adipocytes. mtDNA and nDNA was quantified using probe-based real-time PCR. A: The ratio of mtDNA and nDNA was plotted against donor's BMI (n = 17). B: CS protein amounts of adipocytes whole protein lysates were detected via Western blot analysis and plotted against donor's BMI (n = 20).

4.6 Mitochondrial yield and respiratory control ratio of small and large subcutaneous adipocytes

Obesity goes along with adipocyte hypertrophy. Thus, differences in mitochondria derived from large compared to small adipocytes were examined. Therefore, mitochondria were isolated from five female subjects with different BMI values (21.8, 22.6, 26.7, 33.1, 36.3 kg/m²). Cell size determination of the isolated adipocytes showed a median diameter of 92 µm [27,151] for the TF, 81 µm [22, 135] for FI, and 113 µm [43, 184] for FIV. Mitochondrial yield (pg/cell) was significantly higher in large adipocytes (FIV; mean: 306 ± 135 pg/cell) compared to small adipocytes (FI; 52± 21 pg/cell) or the TF (99± 18 pg/cell), which indicates that mitochondrial content rises with the size of adipocytes. The mitochondrial yield of small adipocytes (FI) appeared to be lower compared to the TF, but this difference was not statistically significant (Figure 15A). In terms of RCR values, no difference between mitochondria of the three was observed (Figure 15B). Along with that, the RCR values of FI and FIV where clearly associated to each other within the same subject ($r = 1.00$; $p < 0.05$; Table 15B) which indicates a similar mitochondrial function across adipocytes independently from adipocytes sizes.

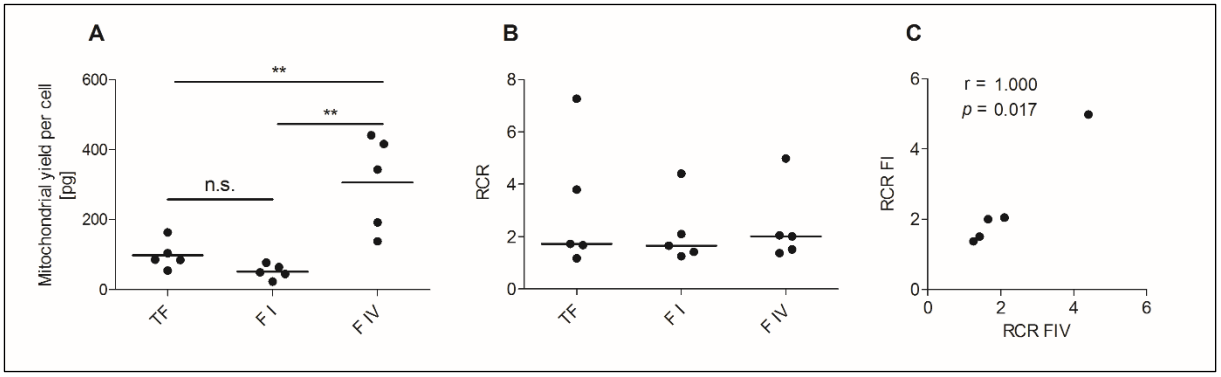

Figure 15: RCR values of mitochondria from the total fraction, fraction I and IV

Mitochondria were isolated from adipocytes of the TF, FI, and FIV. RCR values (calculated by the ratio of OXPHOS capacity to LEAK respiration) were determined by a Clark-type oxygen electrode. Differences between TF, FI, and FIV were analyzed using a one-way ANOVA. A: Comparison of mitochondrial yield per cell. B: Comparison of RCR values. C: RCR values of FI and FIV within the same subjects were correlated and analyzed by Spearman's rank correlation coefficient. Asterisks indicate statistically significant differences between the different fractions: Not significant (n.s.); *$p < 0.05$; **$p < 0.01$; ***$p < 0.001$.

4.7 Lactate release of isolated adipocytes

In order to gain further knowledge about the bioenergetics of human adipocytes in the context of obesity and with regard to the subcutaneous and the visceral depot, lactate release was determined to draw conclusions about the role of glycolysis.

4.7.1 Lactate release is increasing after the inhibition of the OXPHOS process

Lactate release of visceral and subcutaneous adipocytes were measured in a basal state and after the incubation with oligomycin. As oligomycin is inhibiting complex V, ATP cannot be synthesized by OXPHOS anymore. Consequently, both depots show a statistically significant increase of lactate release ($p < 0.01$; Figure 16; Table 10) after the incubation with oligomycin compared to the basal lactate release, indicating a compensatory ATP production by glycolysis.

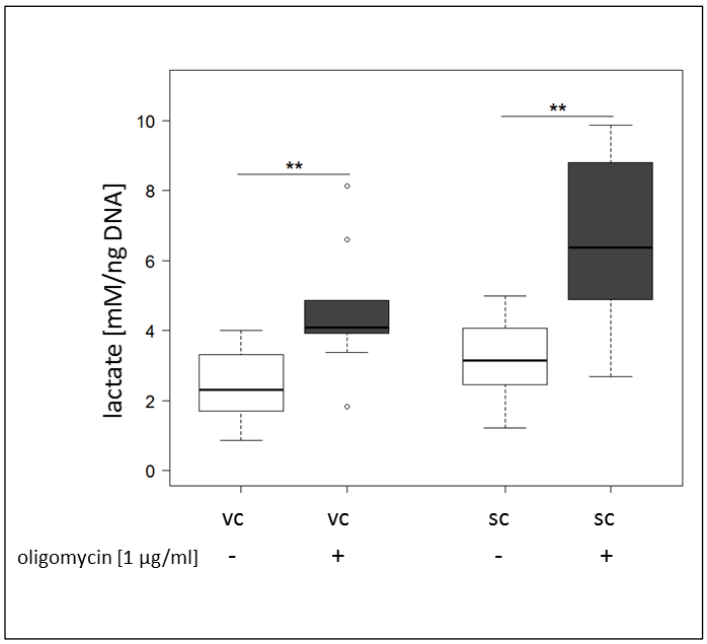

Figure 16: Lactate release of visceral and subcutaneous adipocytes: basal and after the inhibition of the ATP-synthase with oligomycin

Lactate release of visceral (n = 9) and subcutaneous (n = 10) adipocytes was measured after the incubation with and without the ATP-synthase inhibitor oligomycin for 24 h. Lactate was measured indirectly by NADH + H^+ which is formed by the conversion of L-lactate to pyruvate. NADH+ H^+ is absorbing ultraviolet (UV) light at 339 nm and thus, can be measured spectrophotometrically. Differences were analyzed by Student's paired *t*-test. Asterisks indicate statistically significant differences between the two conditions: Not significant (n.s.); *$p < 0.05$; **$p < 0.01$; ***$p < 0.001$.

Table 10: Lactate release of visceral and subcutaneous adipocytes: basal and after the inhibition of the ATP-synthase

fat depot (n)	lactate basal (nM/DNA) mean (±SD)	lactate + oligomycin (nM/DNA) mean sc (±SD)	*p*-value	
vc (9)	2.32 (±1.18)	4.61 (±1.83)	**	**0.004**
sc (10)	2.91 (±1.24)	6.58 (±2.41)	**	**0.002**

Differences between adipocyte lactate release with and without oligomycin-treatment were assessed using a Wilcoxon signed-rank test. Values are expressed as means (±SD). Asterisks indicate statistically significant differences between the two treatments: Not significant (n.s.); *$p < 0.05$; **$p < 0.01$; ***$p < 0.001$.

4.7.2 Adipocyte lactate release in association to donor's BMI

Adipocytes response to an impaired OXPHOS process with an increase in lactate release (shown in 4.7.1), and therefore, an increase of ATP production by glycolysis. As OXPHOS capacity is decreased with increasing BMI values at least in subcutaneous adipocytes (see 4.1.1 and 4.5), a multiple regression analysis, adjusted for age, including BMI and lactate release was performed. Hereby, a link between BMI and basal lactate release (vc: $p = 0.04$; sc: $p = 0.01$; Figure 17A and B; Table 11), as well as for lactate release of oligomycin treated adipocytes (vc: $p = 0.002$; sc: $p = 0.01$; Figure 17C and D; Table 11) was demonstated. Lactate concentration during the incubation with oligomycin, subtracted from basal lactate concentration (delta lactate release) indicate to which extent glycolysis is increased above basal lactate release when mitochondrial ATP production is inhibited, and therefore, indicates the "spare capacity" of glycolysis. Hereby, only delta lactate release of subcutaneous

adipocytes was linked to donor's BMI ($p = 0.02$; Figure 17F; Table 11), whereas the link between delta lactate release of visceral adipocytes and BMI was not statistically significant ($p = 0.11$; Figure 17E; Table 11). Taken together, these results indicate that basal and oligomycin treated adipocyte's lactate release, and therefore ATP production from the process of glycolysis, is increasing with increasing BMI values, irrespective of adipocytes depot origin. Whereas, the capability to increase adipocyte lactate release after the inhibition of mitochondrial ATP production is only associated with BMI values in subcutaneous adipocytes.

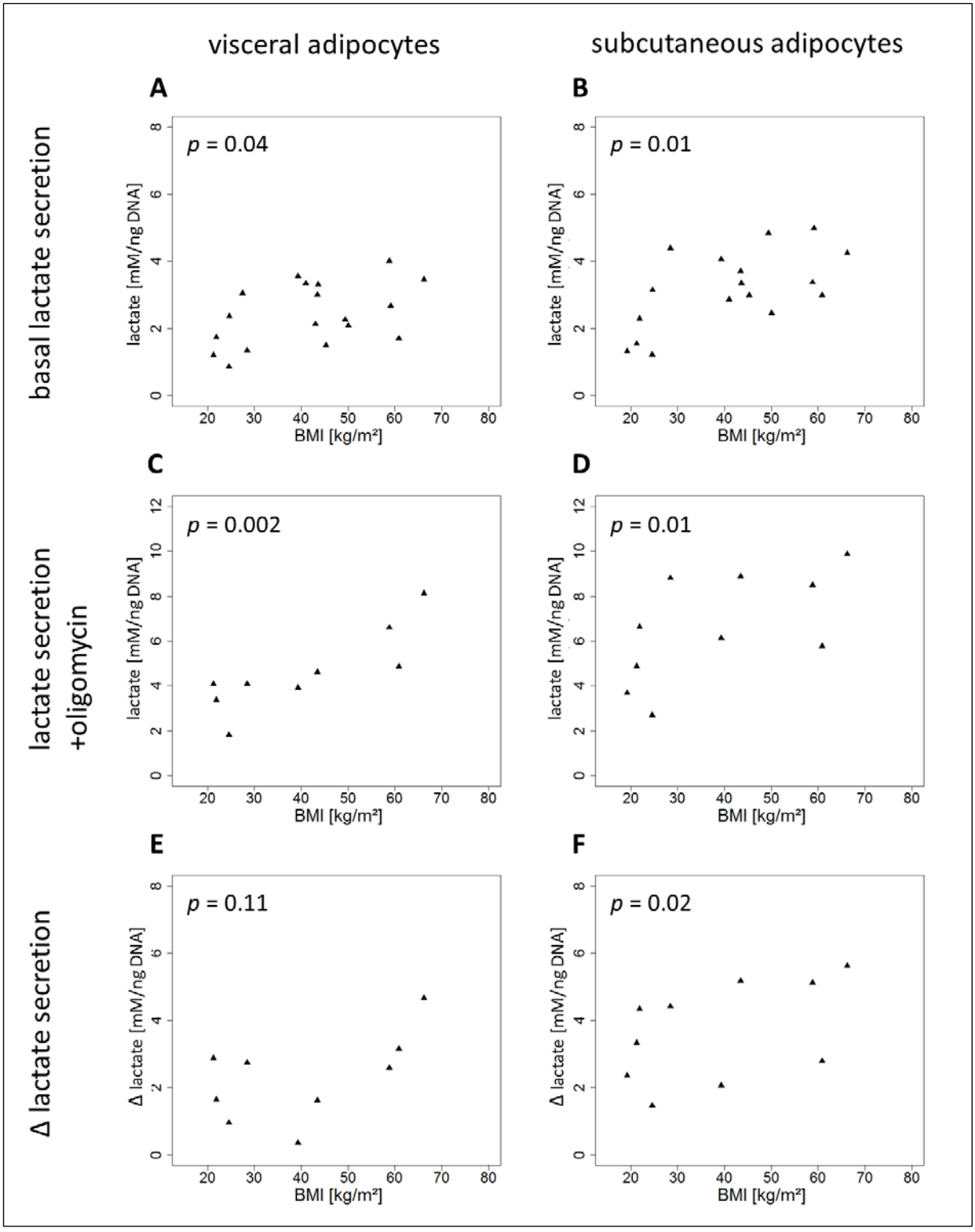

Figure 17: Lactate release of visceral and subcutaneous adipocytes in association to donor's BMI

Lactate release of visceral and subcutaneous adipocytes was plotted against donr's BMI. Lactate release was determined with and without adding the ATP-synthase inhibitor oligomycin (A-D; n = 9-18). Delta lactate was determined by subtracting the oligomycin treated adipocyte's lactate release from basal lactate release into the media and indicates the individual increase in lactate release after inhibiting OXPHOS (E, F; n = 9-10). *P* values originate from multiple regression analysis, adjusted for age.

Table 11: Multiple regression analysis: lactate release and donor's BMI adjusted for age

condition	fat depot (n)	coefficient BMI	R^2	*p*-value	
basal lactate	vc (18)	0.033	0.26	*	**0.040**
	sc (17)	0.047	0.39	*	**0.010**
lactate + oligomycin	vc (9)	0.096	0.81	**	**0.002**
	sc (10)	0.095	0.70	*	**0.011**
delta lactate	vc (9)	0.045	0.37	n.s.	0.113
	sc (10)	0.049	0.75	*	**0.016**

A multiple regression analysis with donor's BMI and lactate release, adjusted for age and separated in accordance to the adipose tissue depot of origin, was performed. Estimated coefficient for donor's BMI and multiple R^2 of the model are given. Asterisks indicate if the corresponding coefficient is not equal to zero. Not significant (n.s.); *p < 0.05; **p < 0.01; ***p < 0.001.

4.7.3 Adipocyte lactate release in association to OXPHOS capacities

An increase in BMI was found to be accompanied by a decrease of subcutaneous adipocyte mitochondrial respiration (4.1.1 and 4.2). In 4.7.2 it has further been shown that an increase in BMI is associated with an increase in lactate release. Thus, it was also examined if there is a direct link between OXPHOS and lactate release. Hereby, a multiple regression analysis, adjusted for age, with basal lactate release, lactate release with oligomycin, and delta lactate release for OXPHOS capacity and free OXPHOS capacity was applied. Except from basal lactate release of visceral adipocytes, all estimated coefficients were negative within the model including OXPHOS capacity and hence, imply an inverse link between lactate release rates and oxygen uptake limited by OXPHOS capacity. However, the associations within these models showed only borderline significance for an inverse association between subcutaneous OXPHOS capacity and lactate release after the treatment with oligomycin ($p = 0.08$; Figure 18D; Table 12).

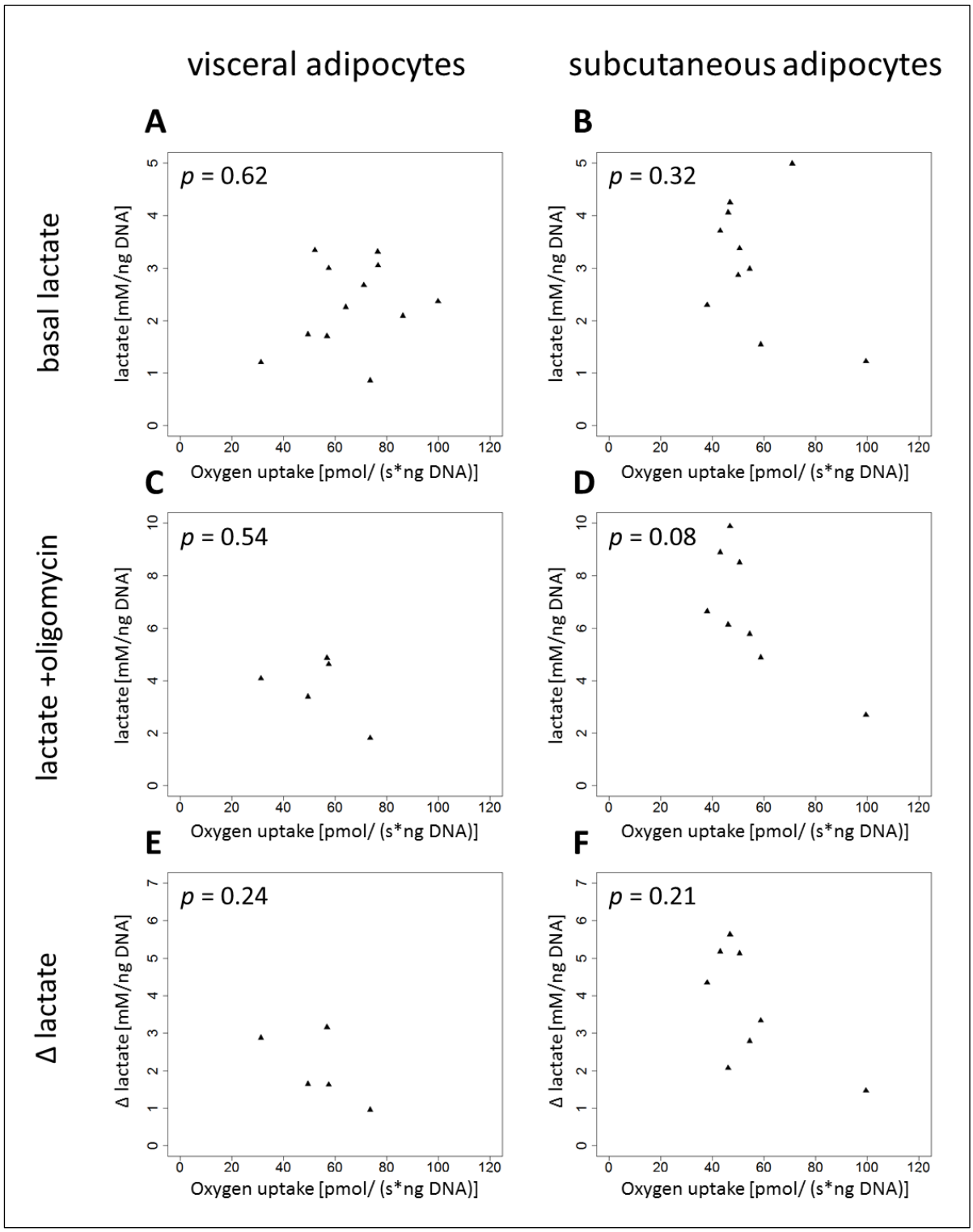

Figure 18: Lactate release of adipocytes and OXPHOS capacity

Oxygen uptake, limited by OXPHOS capacity, was plotted against basal lactate release (A, n = 12 and B, n = 10), lactate release under oligomycin (C, n = 5 and D n = 8) and delta lactate release (E, n = 5 and F, n = 8). OXPHOS capacity was assessed by adding the complex I and II substrate malate, pyruvate and succinate as well as ADP in excess. *P*-values originate from multiple regression analysis, adjusted for age.

Similar results were observed for the models that included free OXPHOS capacity. Also hereby, only visceral basal lactate release resulted in a positive coefficient within a model for free OXPHOS capacity. All other coefficients determined were negative. However, only for the inverse association within subcutaneous adipocytes between lactate release after the inhibition of mitochondrial ATP production and free OXPHOS capacity borderline significance was observed ($p = 0.08$; Figure 19D; Table 12) all other models were not statistically significant.

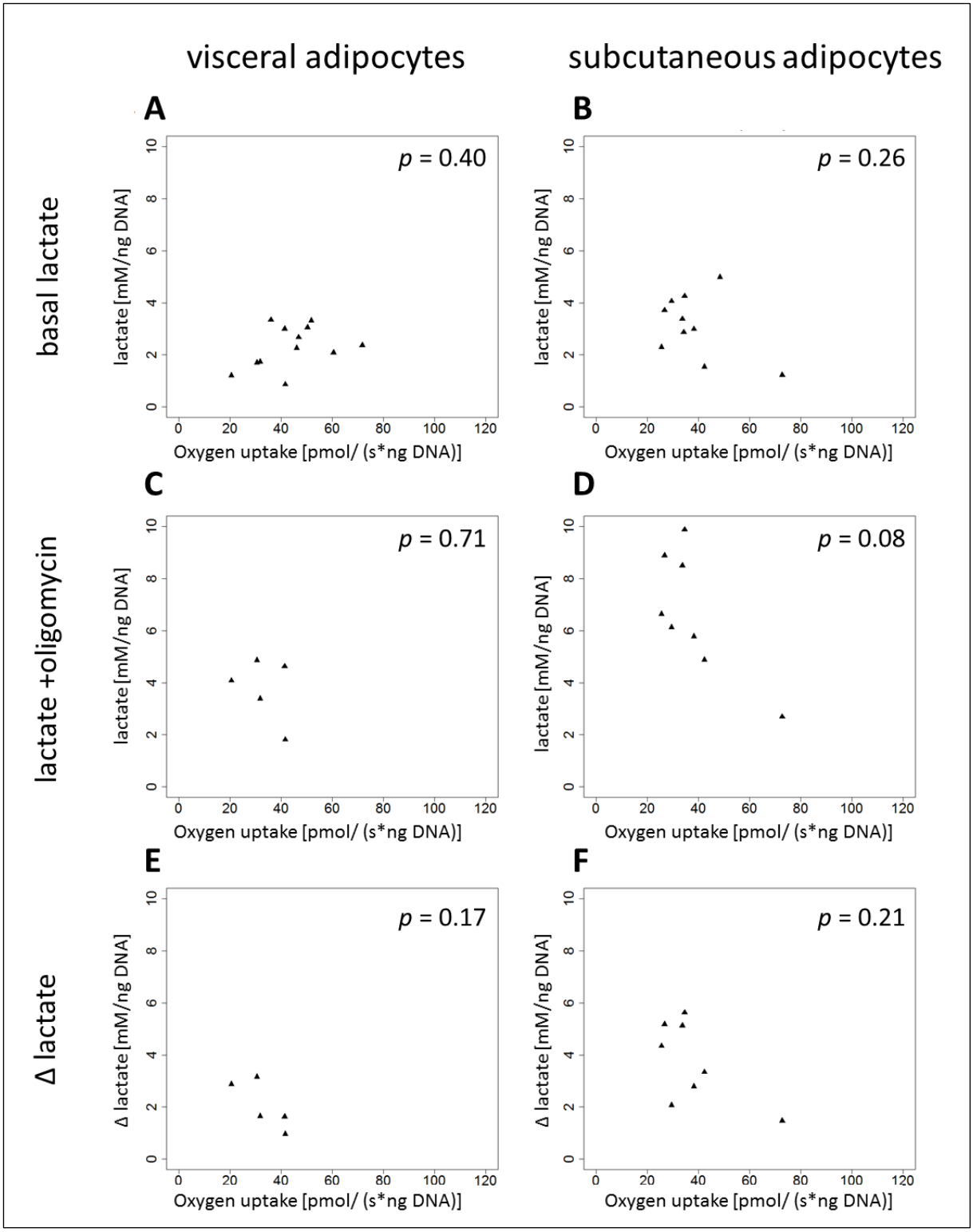

Figure 19: Adipocyte lactate release and free OXPHOS capacity

Oxygen uptake, limited by free OXPHOS capacity, was plotted against basal lactate release (A, n = 12 and B, n = 10), lactate release under oligomycin (C, n = 5 and D n = 8) and delta lactate (E, n = 5 and F, n = 8). Free OXPHOS capacity was assessed by subtracting oxygen uptake during LEAK respiration from oxygen uptake limited by OXPHOS capacity. *P*-values originate from multiple regression analysis adjusted for age.

Table 12: Multiple regression analysis: Adipocyte lactate release and OXPHOS

respiratory state	condition	fat depot (n)	coefficient respiratory state	R^2	*p*-value	
OXPHOS capacity	basal lactate	vc (12)	0.01	0.11	n.s.	0.62
		sc (10)	-0.03	0.14	n.s.	0.32
	lactate + oligomycin	vc (5)	-0.05	0.26	n.s.	0.54
		sc (8)	-0.09	0.58	n.s.	0.08
	delta lactate	vc (5)	-0.06	0.59	n.s.	0.24
		sc (8)	-0.03	0.66	n.s.	0.21
free OXPHOS capacity	basal lactate	vc (12)	0.02	0.16	n.s.	0.40
		sc (10)	-0.04	0.18	n.s.	0.26
	lactate + oligomycin	vc (5)	-0.04	0.14	n.s.	0.71
		sc (8)	-0.11	0.57	n.s.	0.08
	delta lactate	vc (5)	-0.10	0.69	n.s.	0.17
		sc (8)	-0.04	0.66	n.s.	0.21

A multiple regression analysis with adipocyte lactate release depending on oxygen uptake limited by OXPHOS capacity and free OXPHOS capacity adjusted for age and separated in accordance to the adipose tissue depot of origin was performed. Estimated coefficient for donor's oxygen uptake of the corresponding respiratory state and multiple R^2 of the model are given. Asterisks indicate if the corresponding coefficient is not equal to zero. Not significant (n.s.); *$p < 0.05$; **$p < 0.01$; ***$p < 0.001$.

Taken together, the models did not show any statistically significant associations between lactate release and the determined oxygen uptake during OXPHOS and free OXPHOS capacity. Nevertheless, borderline significance was found when associating lactate release after the inhibition of mitochondrial ATP production by oligomycin and oxygen uptake limited by OXPHOS and free OXPHOS capacity.

4.7.4 Adipocyte lactate release with special regard on the adipose tissue depot of origin

With the attempt to determine whether there are differences between lactate release of visceral and subcutaneous adipocytes, Student's paired *t*-test was performed. Hereby, significantly higher released levels of lactate were found in subcutaneous compared with visceral adipocytes, when all subjects were included in the analysis (Figure 20; Table 13).

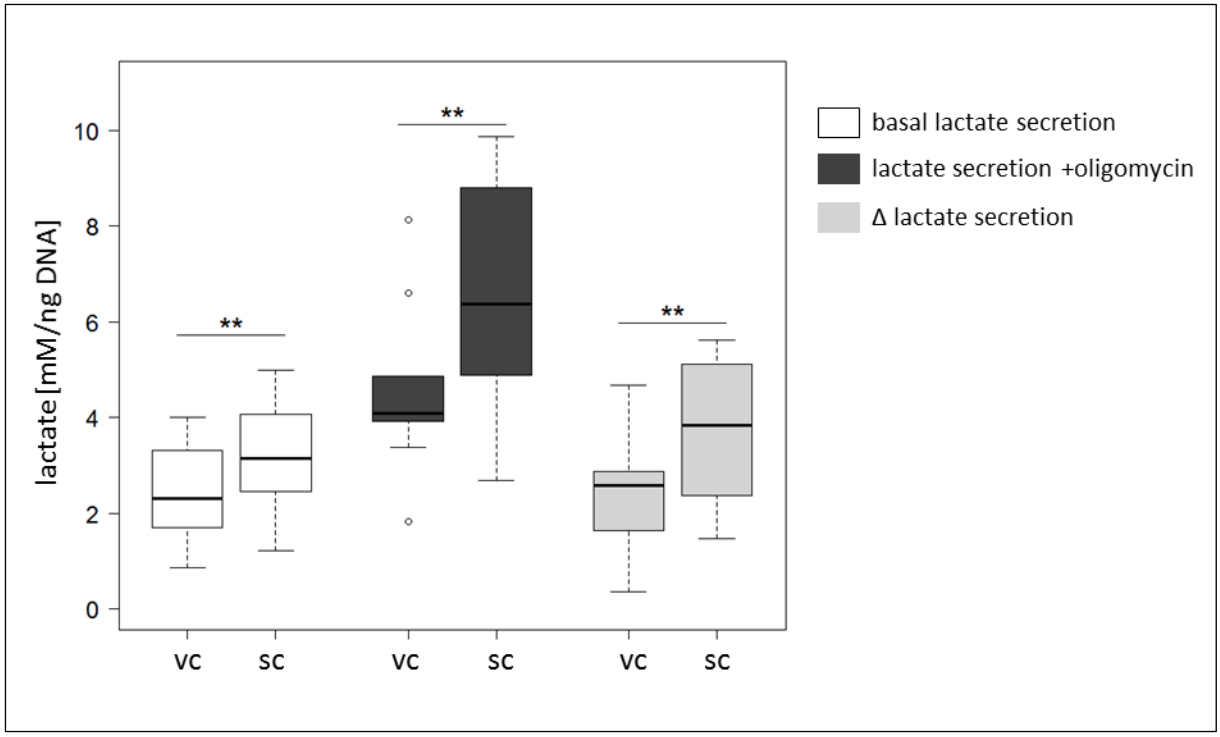

Figure 20: Lactate release of visceral and subcutaneous adipocytes

Differences between lactate release of visceral and subcutaneous adipocytes were analyzed using Student's paired *t*-test (n = 9-16). Asterisks indicate statistically significant differences between the two depots (vc vs. sc): Not significant (n.s.); *p < 0.05; **p < 0.01; ***p < 0.001.

Table 13: Comparison of visceral and subcutaneous lactate release

condition (n)	mean vc (±SD)	mean sc (±SD)	*p*-value	
lactate basal (16)	2.40 (±0.97)	3.28 (±1.08)	**	0.004
lactate with oligomycin (9)	4.61 (±1.83)	6.90 (±2.31)	**	0.002
delta lactate (9)	2.29 (±1.30)	3.81 (±1.47)	**	0.007

Differences between lactate release of visceral and subcutaneous adipocytes were assessed using Student's paired *t*-test (n = 9-16). Values are expressed as means (±SD). Asterisks indicate statistically significant differences between the two depots (vc vs. sc): Not significant (n.s.); *$p < 0.05$; **$p < 0.01$; ***$p < 0.001$.

When the cohort was divided according to the BMI, the observed difference between the visceral and the subcutaneous depot only persisted in obese subjects with BMI values of 30 kg/m² or greater. Nevertheless, also lactate release of subjects with BMI values below 30 kg/m² showed consistently higher lactate release of subcutaneous compared with visceral adipocytes, although those differences were not statistically significant (Figure 18; Table 12).

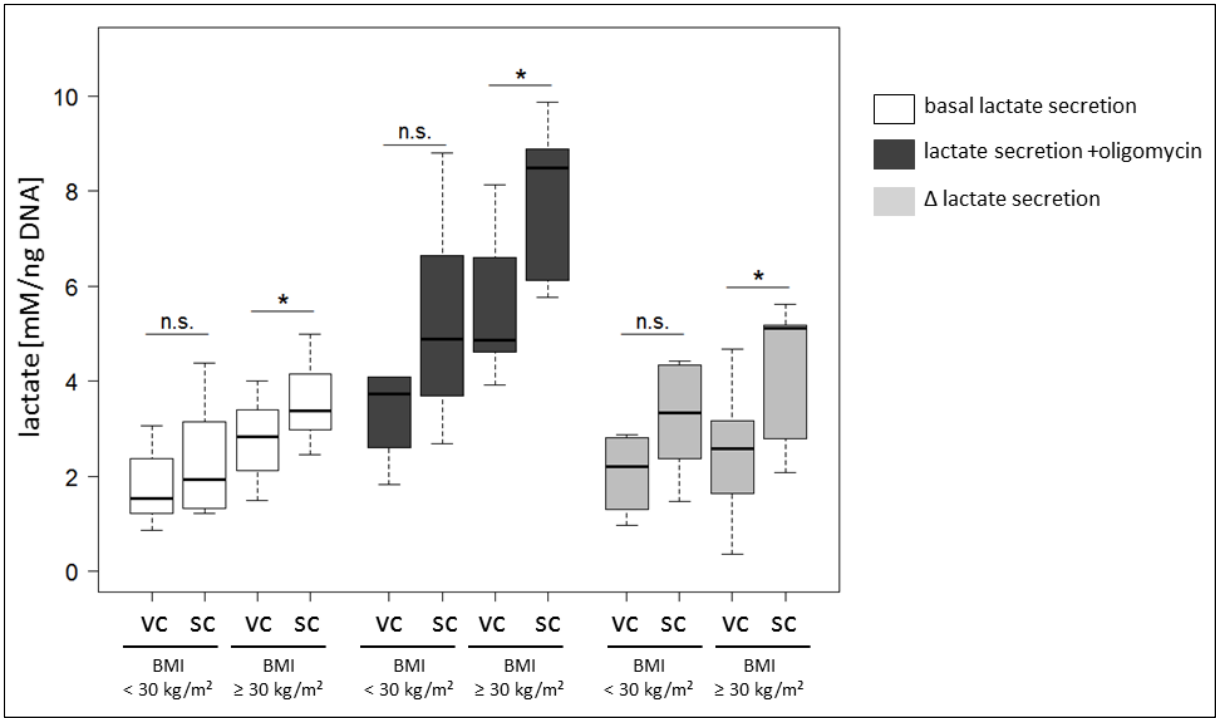

Figure 21: Lactate release of visceral and subcutaneous adipocytes separated by donor's BMI

Subjects were divided into two groups according to their BMI (n = 4-11). Differences between visceral and subcutaneous lactate release was analyzed by the Student's paired *t*-test. Asterisks indicate statistically significant differences between the two depots (vc vs. sc): Not significant (n.s.); $*p < 0.05$; $**p < 0.01$; $***p < 0.001$.

Table 14: Comparison of visceral and subcutaneous lactate release separated by donor's BMI

condition (n)	BMI < 30 kg/m²		*p*-value	BM ≥ 30 kg/m²		*p*-value
	mean vc (±SD)	mean sc (±SD)		mean vc (±SD)	mean sc (±SD)	
lactate basal (5; 11)	1.50 (±0.58)	2.52 (±1.28)	n.s. 0.119	2.81 (±0.82)	3.62 (±0.83)	* **0.026**
lactate with oligomycin (4; 5)	3.34 (±1.07)	5.75 (±2.60)	n.s. 0.086	5.65 (±1.71)	7.83 (±1.79)	* **0.017**
delta lactate (4; 5)	2.05 (±0.92)	3.39 (±1.37)	n.s. 0.087	2.48 (±1.62)	4.15 (±1.61)	n.s. 0.066

Subjects were divided into two groups according to their BMI. Differences of visceral and subcutaneous lactate release were analyzed by Student's paired *t*-test. Asterisks indicate statistically significant differences between the two depots (vc vs. sc): Not significant (n.s.); *$p < 0.05$; **$p < 0.01$; ***$p < 0.001$.

Further insights into lactate release of subcutaneous and visceral adipocytes where drawn from Pearson's product-moment correlation analysis. Hereby, only lactate release with oligomycin showed a significant correlation between visceral and subcutaneous adipocytes (r = 0.77; *p* = 0.02; Figure 22A). However, also basal lactate release (r = 0.49; *p* = 0.05; Figure 22B) and delta lactate release (r = 0.59; *p* = 0.09; Figure 22C) showed borderline significance for a link between adipocytes from the visceral and the subcutaneous depot within the same subject.

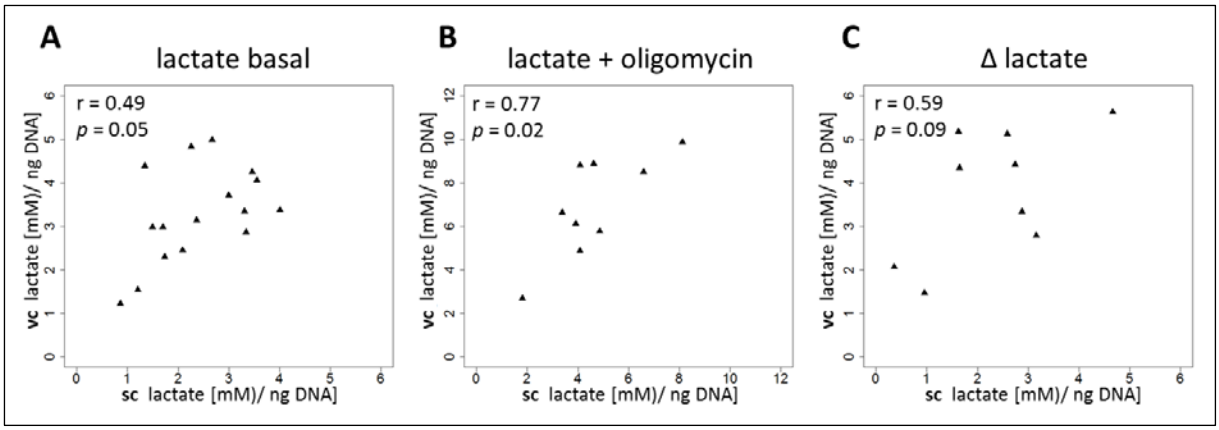

Figure 22: Association between visceral and subcutaneous lactate release

Pearson's product-moment correlation was performed for analyzing the association between subcutaneous and visceral adipocyte basal lactate release, lactate release with the addition of oligomycin, and delta lactate release (basal lactate release – lactate release under oligomycin) within the same subject (A: n = 17; B and C: n = 9).

Taken together, in comparison with visceral adipocytes, these results suggest higher lactate release of subcutaneous adipocytes in obese subjects not only of basal release, but also after the inhibition of mitochondrial ATP production with oligomycin and the capacity to increase lactate release after the treatment with oligomycin (stated as delta lactate release). Moreover, a link between subcutaneous and visceral adipocyte lactate release can be only demonstrated when lactate release upon oligomycin treatment is correlated. But due to borderline significance also basal lactate as well as the capacity to increase lactate release might be correlated between adipocytes of the two depots.

4.8 ATP levels of isolated adipocytes

With the attempt to further investigate, if impairments in adipocyte mitochondrial respiration go along with changes in the cellular energy balance and to what degree OXPHOS and glycolysis contribute to ATP concentrations, adipocyte ATP levels were determined during

different conditions.

4.8.1 Basal ATP levels of isolated adipocytes in association to donor's BMI

Basal cellular ATP levels were measured luminometrically after the incubation of adipocytes in DMEM/F12 for 2.5 h. Measured ATP levels were associated to donor's BMI. A multiple regression analysis, adjusted for age, revealed a slightly but statistically significant link between BMI and ATP levels in visceral adipocytes (p = 0.02; Figure 23A; Table 15). In contrast to that, a negative estimated coefficient was observed for the association between BMI and ATP levels in subcutaneous adipocytes. However, this links was not statistically significant (p = 0.99; Figure 23B; Table 15).

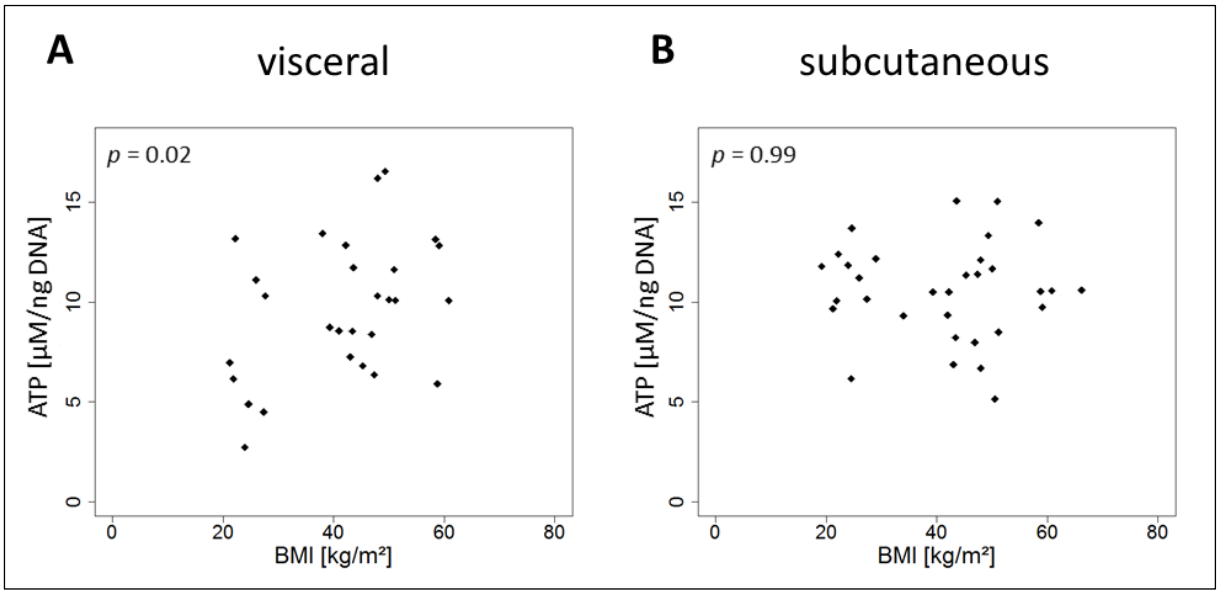

Figure 23: Basal ATP levels in visceral and subcutaneous adipocytes and donor's BMI

Luminometrically determined ATP levels normalized to DNA were plotted against donor's BMI (vc: n = 29; sc: n = 32). *P*-values originate from multiple regression analysis and are adjusted for donor's age.

Table 15: Multiple regression analysis of ATP levels and donor's BMI adjusted for age

model	fat depot (n)	coefficient BMI	R^2	*p*-value	
ATP basal	vc (29)	0.13	0.19	*	**0.02**
	sc (32)	-0.001	0.01	n.s.	0.99

A multiple regression analysis with donor's BMI and ATP levels adjusted for age and separated in accordance to the adipose tissue depot of origin was performed. Estimated coefficient for donor's BMI and multiple R^2 of the model are given. Asterisks indicate if the corresponding coefficient is not equal to zero. Not significant (n.s.); *$p < 0.05$; **$p < 0.01$; ***$p < 0.001$.

4.8.2 Basal ATP levels in association to OXPHOS

A multiple regression analysis, adjusted for the donor's age was performed to reveal if the determined ATP levels are directly associated to the measured mitochondrial OXPHOS and free OXPHOS capacity. As free OXPHOS capacity is adjusted for LEAK respiration and, therefore, only depicts respiration which is linked to ATP production, it could be assumed that the association between ATP levels and free OXPHOS capacity might be stronger than for OXPHOS capacity. However, no link between OXPHOS capacity and cellular ATP levels was observed in visceral ($p = 0.23$; Figure 24A; Table 16) or subcutaneous adipocytes ($p = 0.42$; Figure 24B; Table 16). Although a link between oxygen uptake limited by free OXPHOS capacity and ATP levels was assumed, no statistically significant association was found in visceral ($p = 0.18$; Figure 24C; Table 16) or subcutaneous adipocytes ($p = 0.40$; Figure 24D; Table 16).

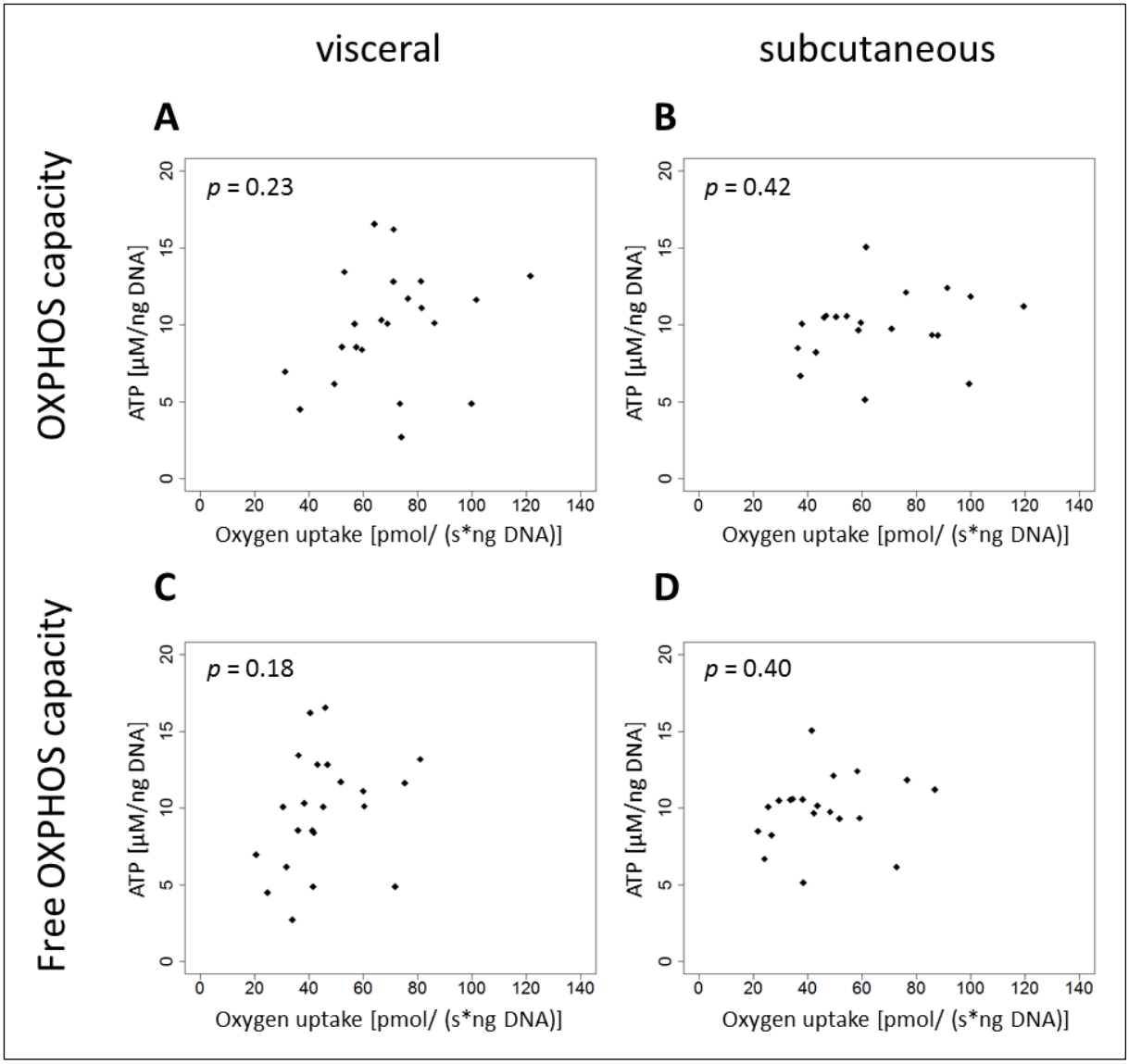

Figure 24: ATP levels and OXPHOS capacity in visceral and subcutaneous adipocytes

Luminometrically determined ATP levels per DNA of visceral and subcutaneous adipocytes were plotted against oxygen uptake limited by OXPHOS capacity (A: n = 22 and B: n = 20) and free OXPHOS capacity (C: n = 22 and D: n = 20). *P*-values originate from multiple regression analysis and are adjusted for donor's age.

Table 16: Multiple regression analysis: ATP levels and OXPHOS capacity in subcutaneous and visceral adipocytes

respiratory state	fat depot (n)	coefficient oxygen uptake	R^2	*p*-value	
OXPHOS capacity	vc (22)	0.05	0.08	n.s.	0.23
	sc (20)	0.02	0.04	n.s.	0.42
free OXPHOS capacity	vc (22)	0.07	0.10	n.s.	0.18
	sc (20)	0.03	0.04	n.s.	0.40

A multiple regression analysis with oxygen uptake rates limited by OXPHOS capacity and free OXPHOS capacity and ATP levels adjusted for age, separated in accordance to the adipose tissue depot of origin was performed. Estimated coefficient for oxygen uptake and multiple R^2 of the model are given. Asterisks indicate if the corresponding coefficient is not equal to zero. Not significant (n.s.); $*p < 0.05$; $**p < 0.01$; $***p < 0.001$.

4.8.3 Basal ATP levels in association to lactate release

Beside the mitochondrial OXPHOS process, also glycolysis is a source for ATP levels. Therefore, also the link between lactate release and cellular ATP concentrations was determined. In visceral as well as subcutaneous adipocytes, the multiple regression analysis revealed a slightly positive but statistically not significant coefficient for basal lactate concentrations (Figure 25; Table 17). Therefore, in the investigated model subcutaneous and visceral adipocyte ATP levels are not linked to basal lactate release.

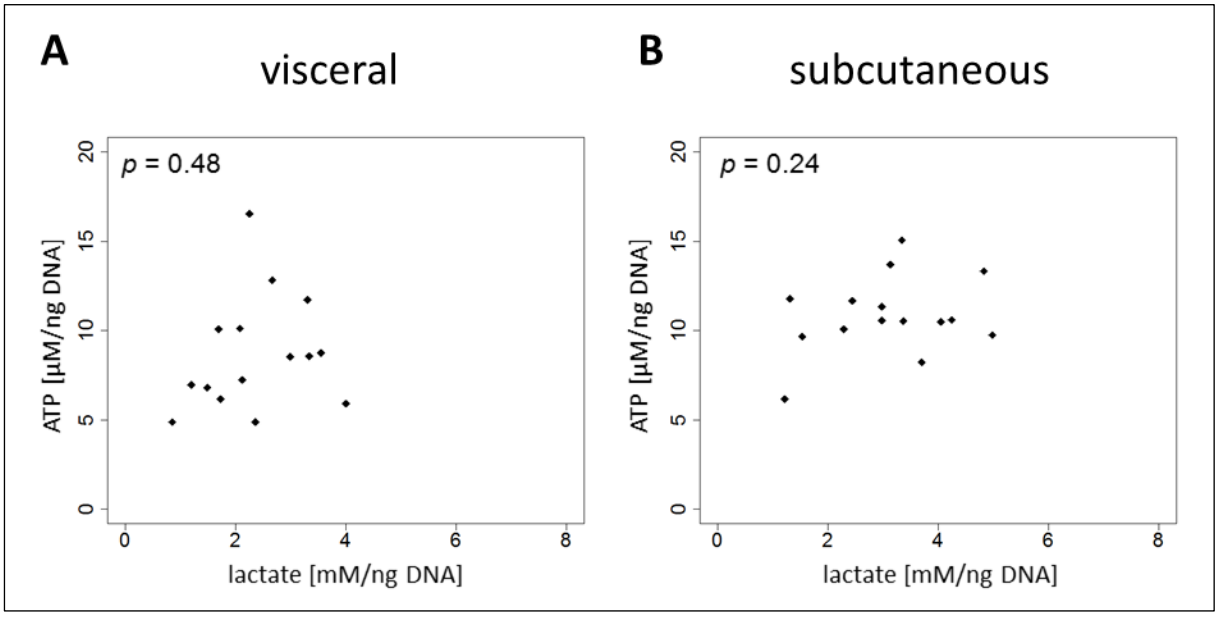

Figure 25: ATP levels and basal lactate release in visceral and subcutaneous adipocytes

Luminometrically determined cellular ATP concentrations per DNA were plotted against basal released lactate levels (vc: n = 15; sc: n = 15). *P* values originate from multiple regression analysis and are adjusted for donor's age.

Table 17: Multiple regression analysis: ATP levels and basal lactate release in subcutaneous and visceral adipocytes

model	fat depot (n)	coefficient lactate	R^2	*p*-value	
basal lactate release	vc (15)	0.73	0.04	n.s.	0.48
	sc (15)	0.57	0.25	n.s.	0.24

A multiple regression analysis with basal released lactate levels and cellular ATP concentrations adjusted for age and separated in accordance to the adipose tissue depot of origin was performed. Estimated coefficient for basal lactate release and multiple R^2 of the model are given. Asterisks indicate if the corresponding coefficient is not equal to zero. Not significant (n.s.); *$p < 0.05$; **$p < 0.01$; ***$p < 0.001$.

4.8.4 Origin of ATP levels in isolated adipocytes

With the attempt to gain further insights into the origin of adipocyte ATP levels, ATP was also measured under the conditions of a suppressed mitochondrial ATP-synthase (oligomycin) and/or glycolysis (2-deoxy-D-glc). All ATP levels within the following analysis were background corrected with ATP levels gained from the combined incubation of oligomycin and 2-deoxy-D-glc, in order to distinguish between ATP origination without any disturbances of preexisting ATP production.

The analysis of visceral adipocytes revealed that ATP levels are significantly decreased after the inhibition of glycolysis with 2-deoxy-D-glc ($p < 0.001$; Figure 26; Table 18). Compared to basal ATP levels the decrease equals to approx. 92 %. In contrast to that, the inhibition of the mitochondrial ATP production with oligomycin, only led to a reduction of 7 % in comparison to basal ATP levels. Furthermore, this reduction was not found to be statistically significant ($p = 0.32$; Figure 26; Table 18). In subcutaneous adipocytes, the inhibition of glycolytic, as well as of mitochondrial ATP production led to a statistically significant decrease of ATP levels compared with basal ATP levels. Nevertheless, the decrease of ATP levels followed by the treatment with 2-deoxy-D-glc accounted for approx. 92 % ($p < 0.001$; Figure 26; Table 18), and was therefore evidently more pronounced as the reduction of ATP levels after the incubation with oligomycin, which accounted for a reduction by around 17 % ($p < 0.001$; Figure 26; Table 18). In summary, these results suggest that adipocyte ATP production is predominantly achieved be glycolysis rather than OXPHOS. Furthermore, this seems to be even more pronounced in visceral adipocytes.

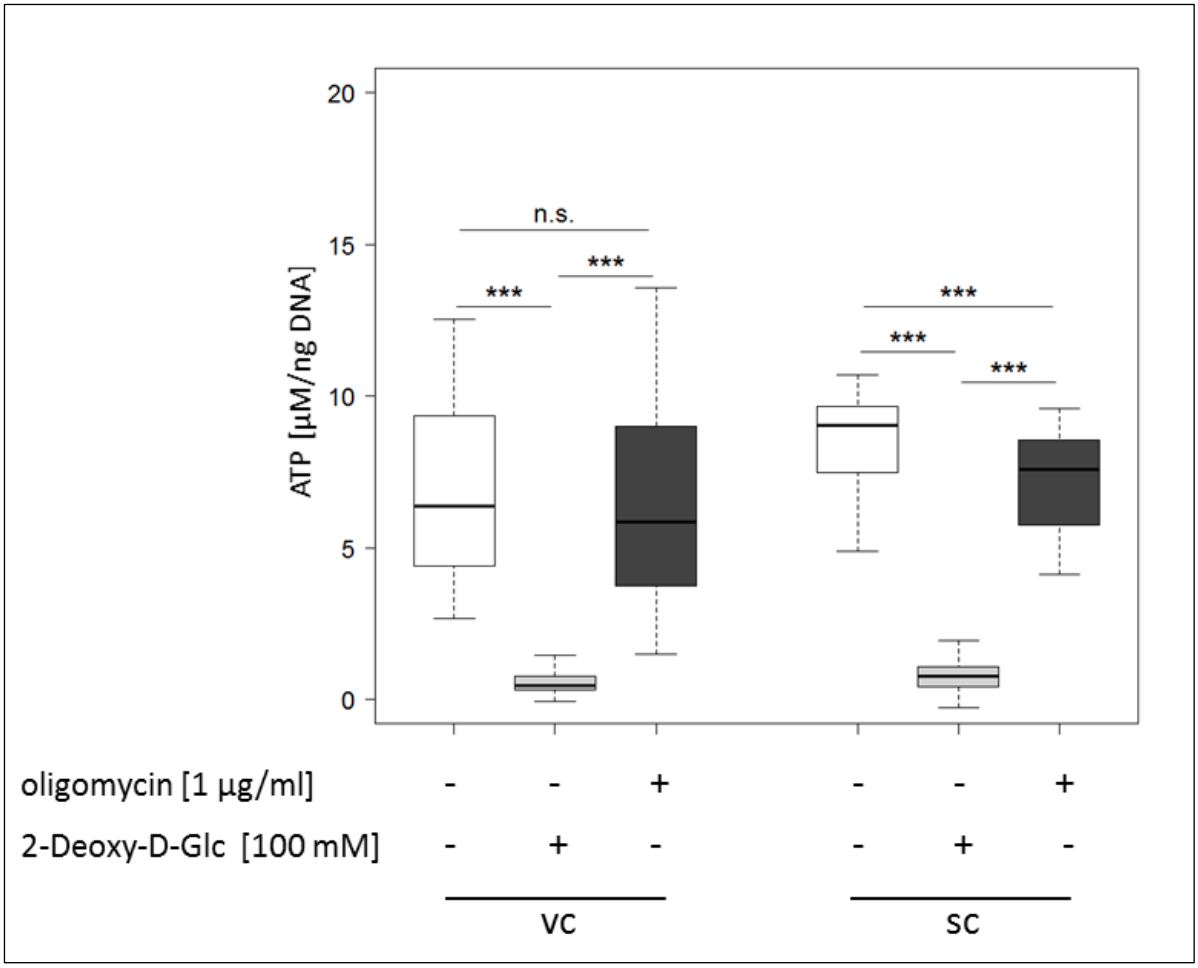

Figure 26: Visceral and subcutaneous adipocyte ATP levels of different origin

Cellular ATP levels normalized to DNA with and without the addition of oligomycin [1 µg/ml] and 2-deoxy-D-glc [100 mM] were determined luminometrically. All ATP levels were corrected with ATP levels gained from the combined incubation of oligomycin and 2-deoxy-D-glc. Asterisks indicate statistically significant differences between the different conditions: Not significant (n.s.); *p < 0.05; **p < 0.01; ***p < 0.001.

Table 18: Visceral and subcutaneous ATP levels of different origin

fat depot (n)	ATP basal mean (±SD)	ATP from OXPHOS mean (±SD)	ATP from glycolysis mean (±SD)	ATP basal vs. ATP from OXPHOS *p*-value		ATP basal vs. ATP from glycolysis *p*-value		ATP from OXPHOS vs. ATP from glycolysis *p*-value	
vc (14)	7.15 (±3.07)	0.57(±0.47)	6.66 (±3.48)	***	**< 0.001**	n.s.	0.32	***	**< 0.001**
sc (13)	8.52 (±1.72)	0.70 (±0.60)	7.10 (±1.99)	***	**< 0.001**	***	**< 0.001**	***	**< 0.001**

Cellular ATP levels per DNA with and without the addition of oligomycin [1 µg/ml] and 2-deoxy-D-glc [100 mM] were determined luminometrically. All ATP levels were corrected with ATP levels gained from the combined incubation of oligomycin and 2-deoxy-D-glc. Differences between different treatments of visceral and subcutaneous adipocytes were performed using the Student's paired *t*-test or the Wilcoxon signed-rank tests, if variances were not equal. Values are expressed as means (±SD). Asterisks indicate statistically significant differences between the different conditions: Not significant (n.s.); *$p < 0.05$; **$p < 0.01$; ***$p < 0.001$.

4.8.4.1 ATP from OXPHOS and glycolysis in association to donor's BMI

Beside the investigation of an association of adipocyte basal ATP levels and BMI, also the link between BMI and ATP levels originated from either OXPHOS or glycolysis were analyzed using multiple regression analysis. As OXPHOS as well as free OXPHOS capacity were found to be decreased with increasing BMI values, at least in subcutaneous adipocytes (4.1.1 and 4.2), a decrease of ATP from OXPHOS and an increase of ATP from glycolysis could be expected. However, ATP from OXPHOS did not show an association with donor's BMI in subcutaneous as well as visceral adipocytes (Figure 27A and B; Table 19). The same was seen for ATP levels derived from glycolysis, when OXPHOS was inhibited by the treatment with oligomycin. A link to donor's BMI was not detected in subcutaneous or visceral adipocytes (Figure 27C and D; Table 19).

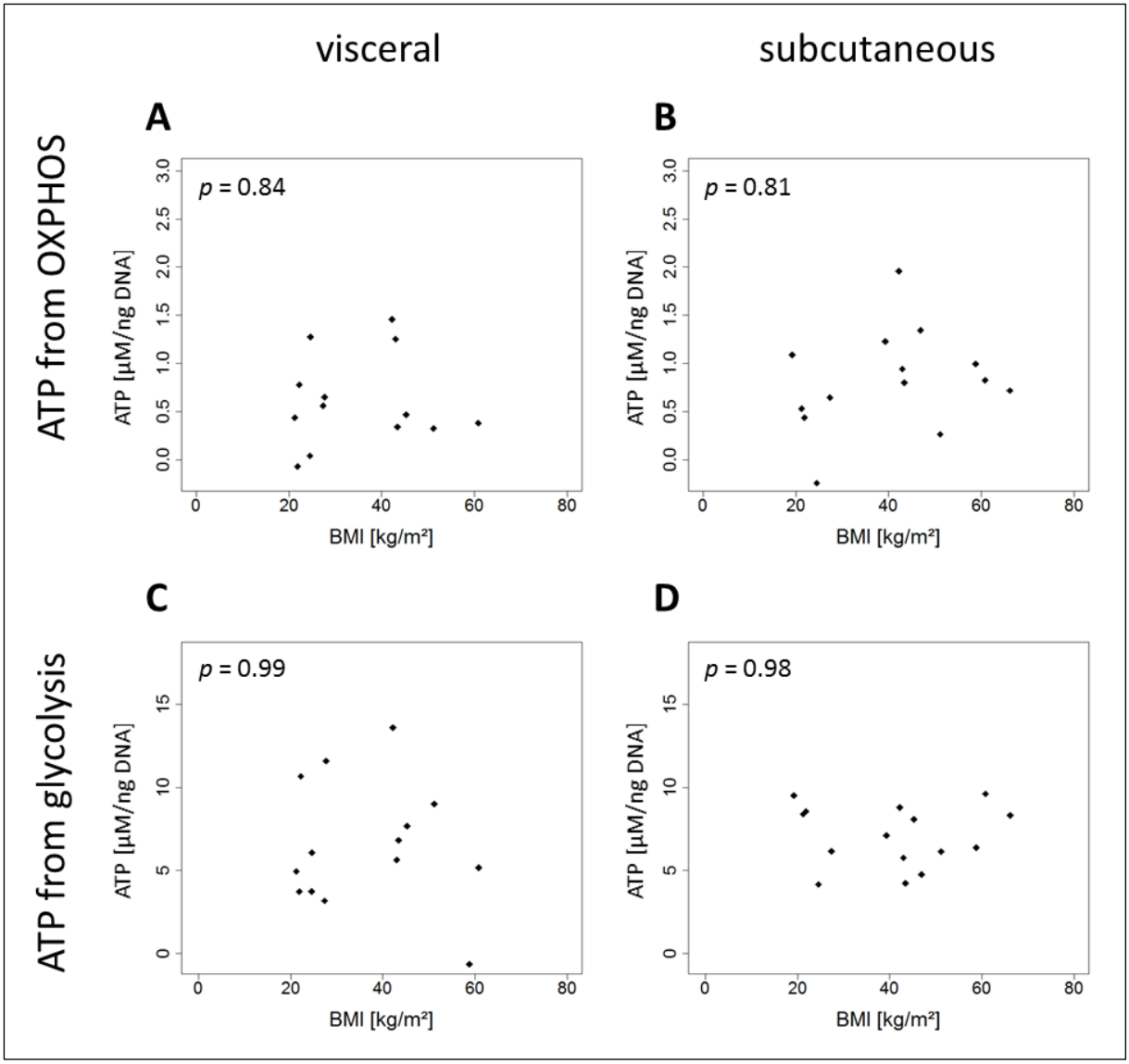

Figure 27: ATP from OXPHOS and glycolysis in association to BMI

Luminometrically determined cellular ATP levels per DNA from OXPHOS (+ 2-deoxy-D-glc [100 mM] A: n = 13 and B: n = 14) and from glycolysis (+ oligomycin [1 µg/ml]) C: n = 14 and D: n = 15) were plotted against donor's BMI. *P*-values originate from multiple regression analysis and are adjusted for donor's age.

Table 19: Multiple regression analysis: ATP of different origin and donor's BMI

ATP origin	fat depot (n)	coefficient BMI	R^2	*p*-value	
ATP from OXPHOS	vc (13)	0.007	0.21	n.s.	0.52
	sc (14)	0.008	0.09	n.s.	0.41
ATP from glycolysis	vc (14)	0.001	0.22	n.s.	0.99
	sc (15)	-0.001	0.08	n.s.	0.98

A multiple regression analysis with donor's BMI and ATP levels from OXPHOS or glycolysis, adjusted for age, and separated in accordance to the adipose tissue depot of origin, was performed. Estimated coefficients for donor's BMI values and multiple R^2 of the model are given. Asterisks indicate if the corresponding coefficient is not equal to zero: Not significant (n.s.); *$p < 0.05$; **$p < 0.01$; ***$p < 0.001$.

In summary, ATP levels of subcutaneous and visceral adipocytes either derived from OXPHOS or from glycolysis were not associated with donor's BMI.

4.8.4.2 ATP levels in association to OXPHOS capacities

If ATP originates from mitochondrial OXPHOS, a link to the determined corresponding OXPHOS as well as free OXPHOS capacity can be assumed. Moreover, glycolytic ATP production might take over, when mitochondrial ATP production from OXPHOS is comprised. Therefore, ATP from glycolysis might be inversely correlated to OXPHOS and free OXPHOS capacity. To test those assumptions, a multiple regression analysis was performed. Hereby, no association between oxygen uptake limited by OXPHOS capacity and ATP levels derived from OXPHOS was observed in visceral adipocytes (p = 0.84; Figure 28A; Table 20). In contrast to that and to the previously made assumptions, a statistically significant inverse association between ATP from OXPHOS and oxygen consumption limited by OXPHOS capacity was observed within subcutaneous adipocytes (p = 0.01; Figure 28B; Table 20). However, when removing the outlier which is lying at the O_2 consumption rate of approx. 100 (Figure 28B), this link is not significant anymore, and even changes from an inverse association (Coefficient: -0.02, Table 20) towards a positive association (Coefficient: 0.003; R^2: 0.67; p = 0.75), although this association was not statistically significant. Analyzing the association between ATP from glycolysis and oxygen uptake limited by OXPHOS capacity, no link either in visceral (p = 0.12; Figure 28C; Table 20), or in subcutaneous adipocytes (p = 0.41; Figure 28D; Table 20) was detected.

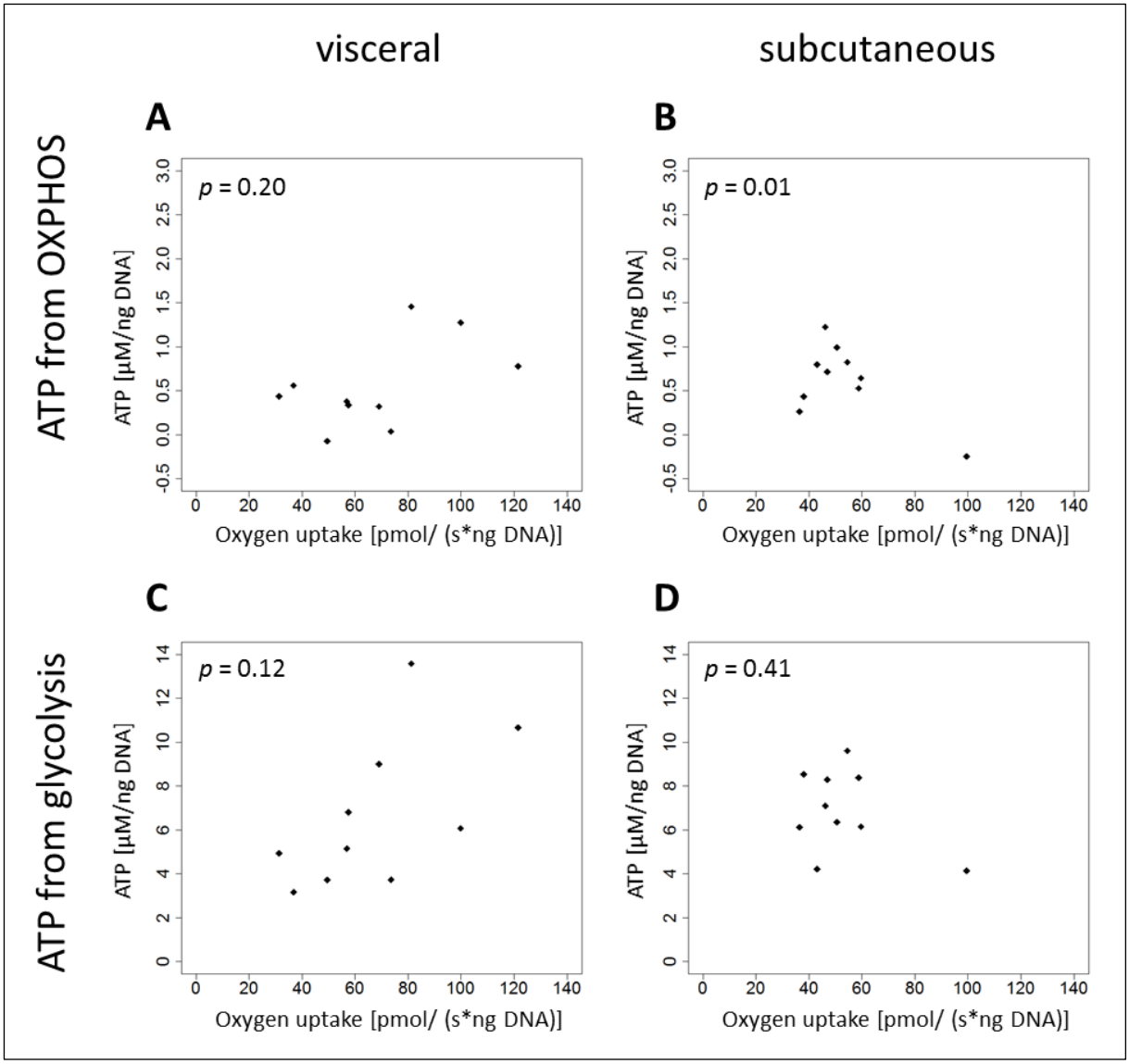

Figure 28: OXPHOS capacity and ATP levels of different origin

Luminometrically determined cellular ATP levels per DNA from OXPHOS (+ 2-deoxy-D-glc [100 mM] A: n = 10 and B: n = 10) and glycolysis (+ oligomycin [1 µg/ml] C: n = 10 and D: n = 10) were plotted against oxygen uptake limited by OXPHOS capacity. *P*-values originate from multiple regression analysis and are adjusted for donor's age.

In visceral adipocytes, there was no link between ATP from OXPHOS and oxygen consumption rates during free OXPHOS capacity observed ($p = 0.02$; Figure 29A; Table 20). Whereas, in subcutaneous adipocytes, again a significantly inverse association between ATP from OXPHOS and oxygen uptake, limited by free OXPHOS capacity, could be shown ($p = 0.02$; Figure 29B; Table 20). Again, this was no longer the case, if the outlier, which is located at the O_2 consumption rate of approx. 80 (Figure 29B), was excluded from the regression analysis. Furthermore, the link is also changing from an inverse association (Coefficient: -0.023, Table 19) towards a positive association (Coefficient: 0.003; R^2: 0.67; p = 0.77). Investigating ATP

derived from glycolysis and the association with oxygen uptake limited by free OXPHOS capacity, neither in visceral (p = 0.25; Figure 29C; Table 20), nor in subcutaneous adipocytes (p = 0.54; Figure 29D; Table 20), a significant link was revealed.

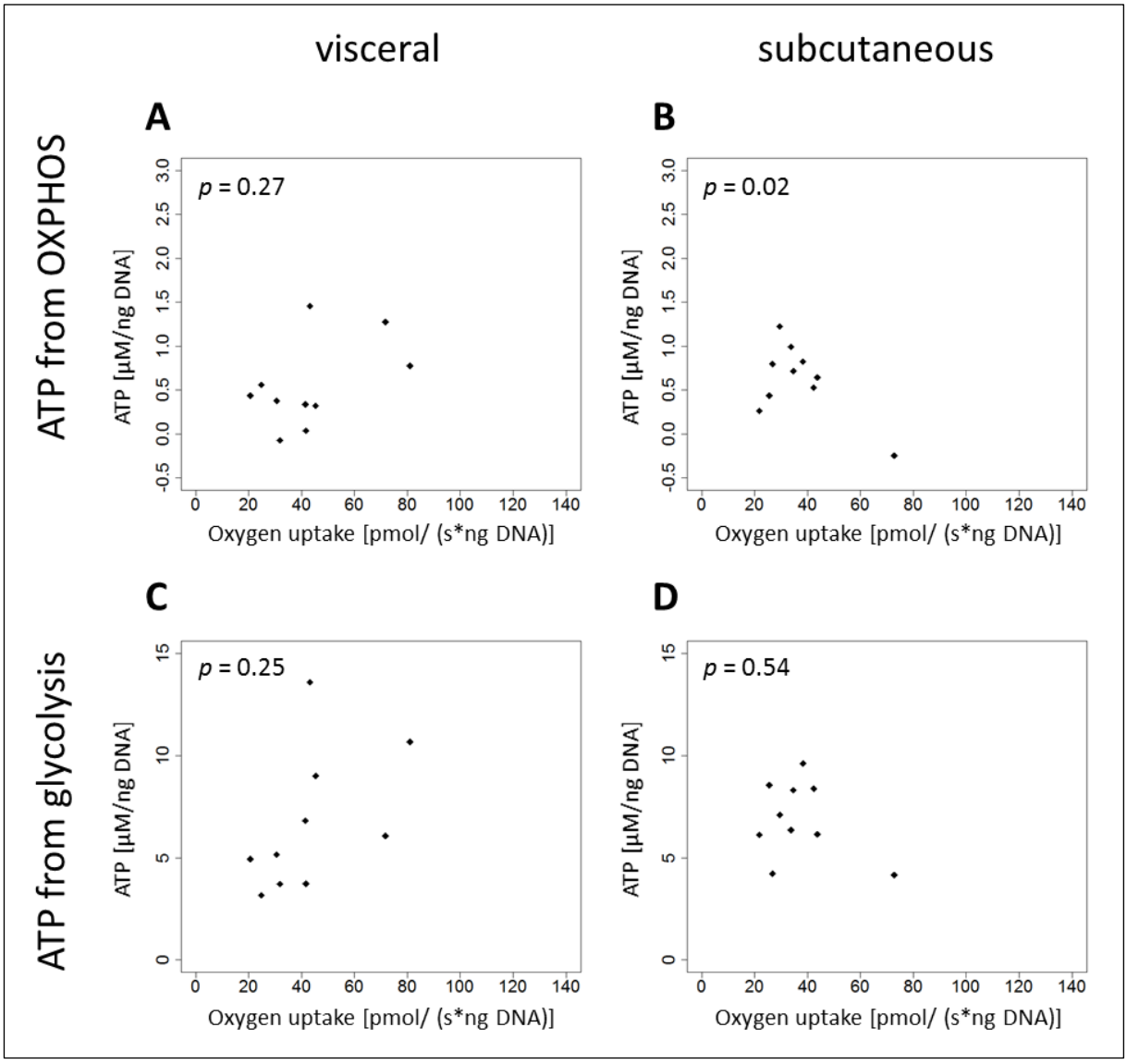

Figure 29: Free OXPHOS capacity and ATP of different origin

Luminometrically determined cellular ATP levels per DNA from OXPHOS (+ 2-deoxy-D-glc [100 mM] A: n = 10 and B: n = 10) and glycolysis (+ oligomycin [1 µg/ml] C: n = 10 and D: n = 10) were plotted against oxygen uptake limited by free OXPHOS capacity. *P* values originate from multiple regression analysis and are adjusted for donor's age.

Table 20: Multiple regression analysis: OXPHOS and free OXPHOS capacity and ATP levels of different origin

respiratory state	ATP origination	fat depot (n)	coefficient respiratory state	R^2	*p*-value	
OXPHOS capacity	ATP from OXPHOS	vc (10)	0.008	0.38	n.s.	0.20
		sc (10)	-0.020	0.62	*	**0.01**
	ATP from glycolysis	vc (10)	0.062	0.50	n.s.	0.12
		sc (10)	-0.035	0.15	n.s.	0.41
free OXPHOS capacity	ATP from OXPHOS	vc (10)	0.010	0.34	n.s.	0.27
		sc (10)	-0.023	0.57	*	**0.02**
	ATP from glycolysis	vc (10)	0.068	0.40	n.s.	0.25
		sc (10)	-0.032	0.05	n.s.	0.54

A multiple regression analysis with ATP levels from OXPHOS or glycolysis and oxygen consumption limited by OXPHOS capacity or free OXPHOS capacity, adjusted for age, and separated in accordance to the adipose tissue depot of origin, was performed. Estimated coefficients for oxygen uptake during the respective respiratory state and multiple R^2 of the model are given. Asterisks indicate if the corresponding coefficient is not equal to zero: Not significant (n.s.); *$p < 0.05$; **$p < 0.01$; ***$p < 0.001$.

Taken together, no clear association between mitochondrial or glycolytic ATP levels and oxygen uptake limited by OXPHOS or free OXPHOS capacity was observed.

4.8.4.3 ATP levels in relation to lactate release

Lactate release which represents the rate of glycolysis might therefore be positively associated to ATP from glycolysis. Analog to ATP from glycolysis and OXPHOS capacities (chapter 4.8.4.2), ATP from OXPHOS might be inversely associated to the determined lactate release. To verify those assumptions, multiple regression analyzes were performed. Hereby, no link between ATP from OXPHOS or glycolysis and basal lactate release, neither in visceral (ATP from OXPHOS: $p = 0.41$; Figure 30A; Table 20; ATP from glycolysis: $p = 0.25$; Figure 30C; Table 20), nor in subcutaneous adipocytes (ATP from OXPHOS: $p = 0.85$; Figure 30B; Table 20; ATP from glycolysis: $p = 0.92$; Figure 30D; Table 20) were observed. The multiple regression analysis including ATP from glycolysis and lactate release revealed a negative estimated coefficient (Coefficient: -1.21, Table 21) which is changing towards a positive estimated coefficient (Coefficient: 0.83; R^2: 0.29; $p = 0.21$) if the outlier, which is lying at the lactate release rate of 4 mM/ng DNA (Figure 30C). The associations though were also not found to be statistically significant.

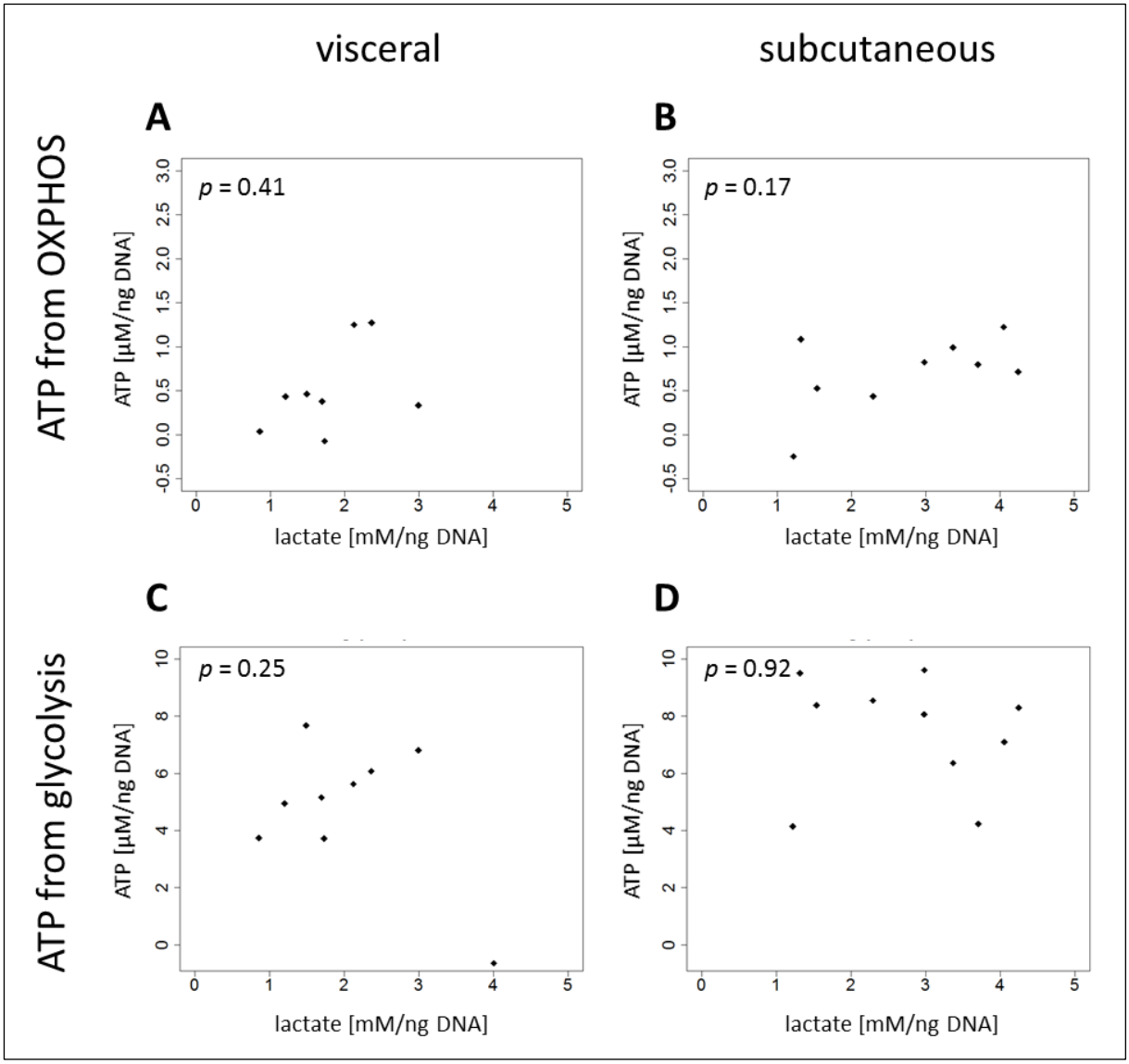

Figure 30: ATP of different origin and basal lactate release

Luminometrically determined cellular ATP levels per DNA from OXPHOS (+ 2-deoxy-D-glc [100 mM] A: n = 8 and B: n = 9) and from glycolysis (+ oligomycin [1 µg/ml] C: n = 9 and D: n = 10) were plotted against basal lactate release. *P* values originate from multiple regression analysis and are adjusted for donor's age.

Table 21: Multiple regression analysis: Basal lactate release and ATP levels of different origin

model	fat depot (n)	coefficient lactate	R^2	*p*-value	
ATP from OXPHOS	vc (8)	0.282	0.20	n.s.	0.41
	sc (9)	0.197	0.29	n.s.	0.17
ATP from glycolysis	vc (9)	-1.207	0.22	n.s.	0.25
	sc (10)	-0.068	0.12	n.s.	0.92

A multiple regression analysis with cellular ATP levels from OXPHOS or glycolysis and basal lactate release, adjusted for age, and separated in accordance to the adipose tissue depot of origin, was performed. Estimated coefficients for lactate release and multiple R^2 of the model are given. Asterisks indicate if the corresponding coefficient is not equal to zero: Not significant (n.s.); *$p < 0.05$; **$p < 0.01$; ***$p < 0.001$.

To further investigate if there might be rather a link between the lactate release after the inhibition of OXPHOS with oligomycin as well as the capacity to increase lactate release after the treatment with oligomycin (delta lactate) with ATP from OXPHOS and glycolysis, another multiple regression analysis including those variables were performed. None of the investigated links were statistically significant. Unexpectedly, the analyses including ATP from OXPHOS showed positive coefficients, whereas ATP from glycolysis showed consistently negative coefficients (Table 22; Appendix: Figure 38; Figure 39).

Table 22: Multiple regression analysis: Lactate release after the treatment with oligomycin and ATP levels of different origin.

model	lactate	fat depot (n)	coefficient lactate	R^2	*p*-value	
ATP from OXPHOS	lactate with oligomycin	vc (5)	0.156	0.73	n.s.	0.16
		sc (9)	0.086	0.21	n.s.	0.26
	delta lactate	vc (5)	0.190	0.66	n.s.	0.20
		sc (9)	0.131	0.13	n.s.	0.40
ATP from glycolysis	lactate with oligomycin	vc (5)	0.862	0.65	n.s.	0.19
		sc (9)	-0.184	0.15	n.s.	0.61
	delta lactate	vc (9)	0.386	0.09	n.s.	0.72
		sc (9)	-0.632	0.24	n.s.	0.36

A multiple regression analysis with ATP levels from OXPHOS or glycolysis and lactate release after the addition of oligomycin, as well as delta lactate, adjusted for age, and separated in accordance to the adipose tissue depot of origin, was performed. Estimated coefficients for lactate release and multiple R^2 of the model are given. Asterisks indicate if the corresponding coefficient is not equal to zero: Not significant (n.s.); *$p < 0.05$; **$p < 0.01$; ***$p < 0.001$.

To sum up, there was no evidence that ATP levels of OXPHOS or glycolysis are linked to either basal lactate release, lactate release when OXPHOS was inhibited or the capacity to increase lactate release as a consequence of the inhibition of mitochondrial ATP production.

4.8.5 Adipocyte ATP levels with special regard on the adipose tissue depot of origin

To further investigate if there are depot specific differences in adipocyte ATP production, basal ATP levels, ATP from OXPHOS, and ATP from glycolysis were compared between the subcutaneous and the visceral depot. Although mean ATP levels were higher in subcutaneous adipocytes during all different treatments, no statistically significant differences were observed (Figure 31; Table 23). Only the difference between basal ATP levels of visceral and

subcutaneous adipocytes reached borderline significance (p = 0.09; Figure 31; Table 23).

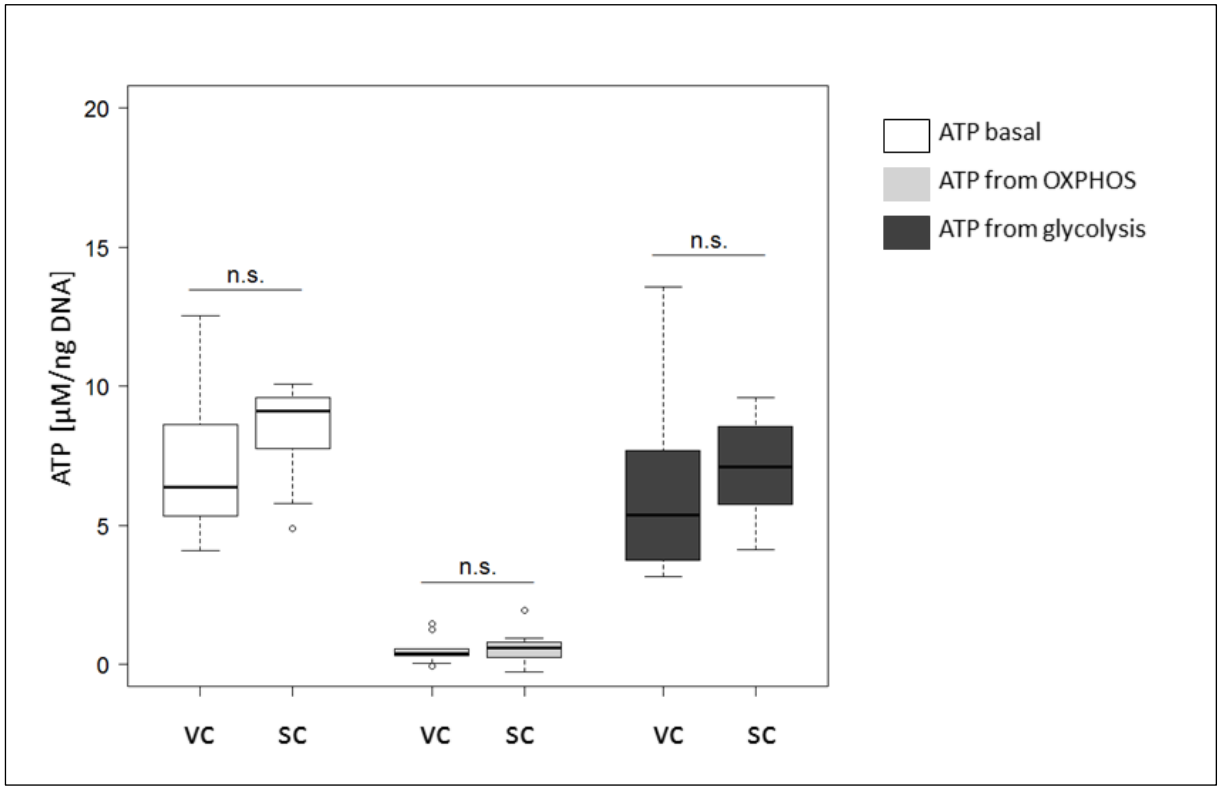

Figure 31 Comparison of visceral and subcutaneous adipocyte ATP production of different origin

Differences between basal, mitochondrial and glycolytic ATP levels of visceral and subcutaneous adipocytes were analyzed using Student's paired *t*-test (n = 10-12). Asterisks indicate statistically significant differences between the two depots (vc vs. sc): Not significant (n.s.); *p < 0.05; **p < 0.01; ***p < 0.001

Table 23: Comparison of visceral and subcutaneous adipocyte ATP production of different origin

condition (n)	mean vc (±SD)	mean sc (±SD)	*p*-value
ATP basal (12)	7.09 (±2.48)	8.47 (±1.65)	n.s. 0.09
ATP from OXPHOS (10)	0.52 (±0.48)	0.58 (±0.64)	n.s. 0.60
ATP from glycolysis (10)	6.34 (±3.15)	6.98 (±1.95)	n.s. 0.38

Differences between ATP levels of visceral and subcutaneous adipocytes were assessed using Student's paired *t-test*. Values are expressed as means (±SD). Asterisks indicate statistically significant differences between the two depots (vc vs. sc): Not significant (n.s.); *p < 0.05; **p < 0.01; ***p < 0.001.

After dividing subjects into two groups according to their BMI (< 30 vs. ≥ 30 kg/m²), different results were observed than comparing ATP levels of subcutaneous and visceral adipocytes of the total cohort. Basal ATP levels of subcutaneous adipocytes originated from lean and overweight subjects were significantly higher compared with those from visceral adipocytes

($p < 0.05$; Figure 32; Table 24). Although not statistically significant, in subjects of this group, ATP levels from glycolysis were lower in visceral compared with subcutaneous adipocytes ($p = 0.051$; Figure 32; Table 24). No differences were observed comparing ATP from OXPHOS in both groups as well as basal ATP and ATP from glycolysis in the group including only obese subjects (Figure 32; Table 24).

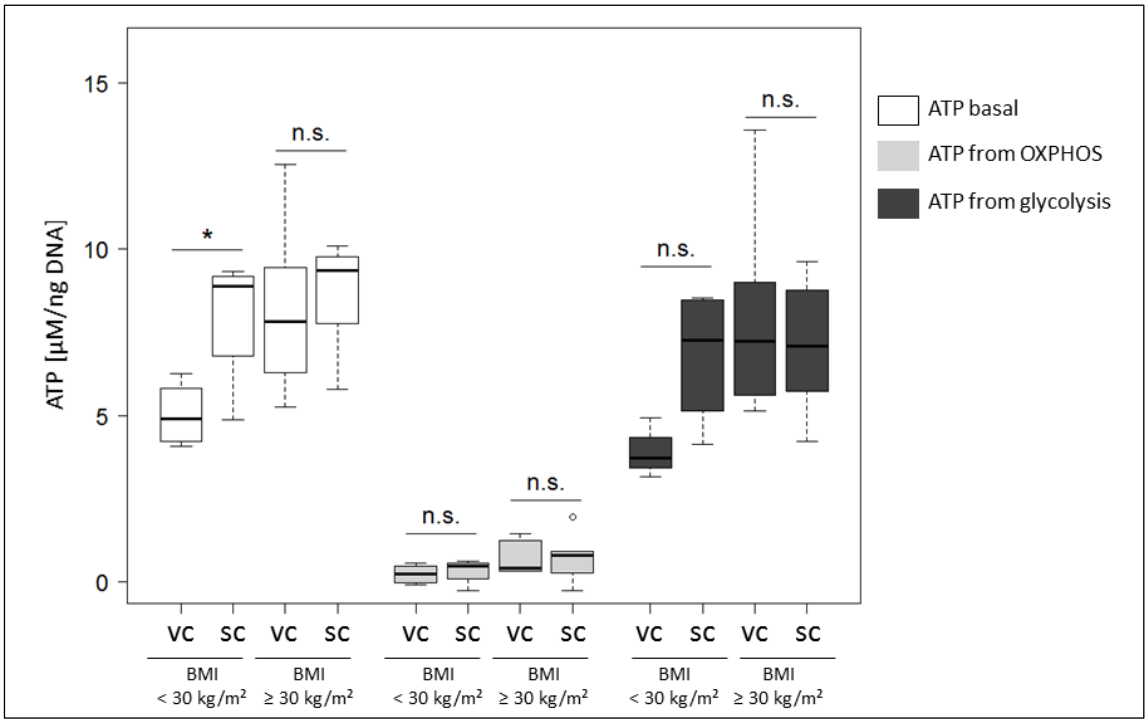

Figure 32: Comparison of visceral and subcutaneous adipocyte ATP production of different origin separated by donor's BMI values

Subjects were divided into two groups according to their BMI values (n = 4-8). Differences between visceral and subcutaneous lactate release were analyzed by Student's paired *t*-test. Asterisks indicate statistically significant differences between the two depots (vc vs. sc): Not significant (n.s.); *$p < 0.05$; **$p < 0.01$; ***$p < 0.001$.

Table 24: Comparison of visceral and subcutaneous adipocyte ATP production of different origin separated by donor's BMI

condition (n)	BMI < 30 kg/m²		*p*-value		BM ≥ 30 kg/m²		*p*-value	
	mean vc (±SD)	mean sc (±SD)			mean vc (±SD)	mean sc (±SD)		
ATP basal (4; 8)	5.04 (±0.99)	8.00 (±2.09)	*	**0.042**	8.12 (±2.34)	8.711 (±1.50)	n.s.	0.496
ATP from OXPHOS (4; 6)	0.24 (±0.30)	0.34 (±0.40)	n.s.	0.577	0.70 (±0.51)	0.75 (±0.74)	n.s.	0.811
ATP from glycolysis (4; 6)	3.89 (±0.75)	6.81 (±2.08)	n.s.	0.051	7.98 (±3.08)	7.09 (±2.06)	n.s.	0.534

Subjects were divided into two groups according to their BMI (n = 4-8). Differences between ATP levels of visceral and subcutaneous adipocytes were assessed using Student's paired *t*-test (n = 10-12). Values are expressed as means (±SD). Asterisks indicate statistically significant differences between the two depots (vc vs. sc): Not significant (n.s.); *p < 0.05; **p < 0.01; ***p < 0.001.

Furthermore, the association between ATP levels of the two depots within the same subject was determined, performing a Pearson's product-moment correlation. A significant correlation between ATP production of visceral and subcutaneous adipocytes was detected, when ATP levels derived from OXPHOS (r = 0.75; *p* = 0.01; Figure 33). Basal ATP levels and ATP levels from glycolysis did not show a statistically significant association between the subcutaneous and the visceral adipose tissue depot (Figure 33).

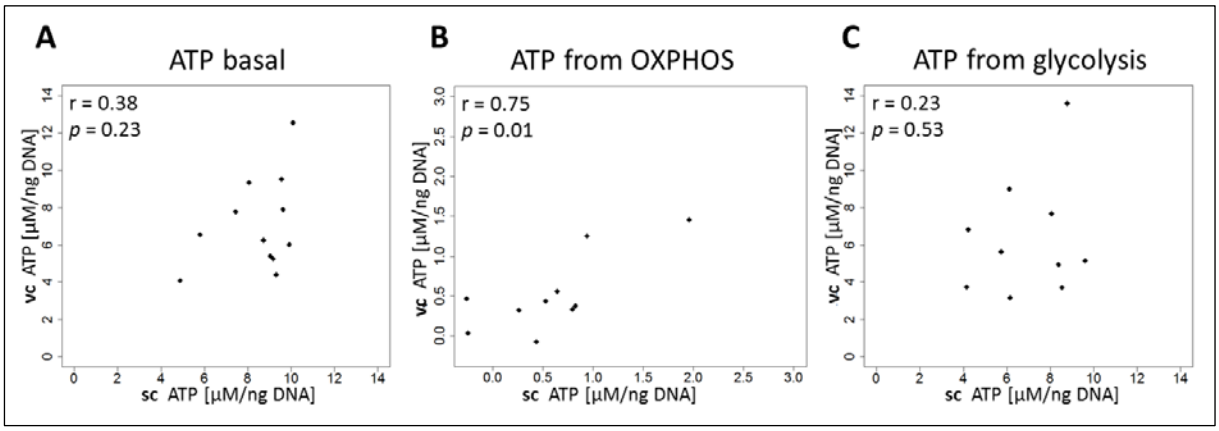

Figure 33: Association between visceral and subcutaneous ATP levels

Pearson's product-moment correlation was performed for analyzing the association between subcutaneous and visceral adipocyte ATP levels of different origins within the same subject. Only the association between visceral and subcutaneous adipocytes of ATP from OXPHOS was statistically significant (A: n = 12; B and C: n = 10).

It can be summed up that, even though there is no significant difference between ATP production independent of origin, between subcutaneous and visceral adipocytes, only ATP levels originated from OXPHOS correlate significantly between adipocytes from the two depots.

5 DISCUSSION

5.1 Adipocyte mitochondrial respiration in association to subject's BMI

Evidence from literature suggests that mitochondria are impaired in adipocytes of obese subjects. Some findings are based on gene expression analyses (Mustelin et al., 2008; Heinonen et al., 2015), but also functional investigations indicate that adipocyte mitochondria show lower respiratory rates when BMI is increasing (Yehuda-Shnaidman et al., 2010; Yin et al., 2014). In the present study, in isolated mitochondria, as well as isolated adipocytes, it was clearly showed that oxygen consumption of subcutaneous mitochondria is decreasing with increasing BMI. This was not due to changes in the mitochondrial membrane integrity, as LEAK respiration was not associated to the donor's BMI in both models. The results of the present work show for the first time an inverse association between BMI and oxygen consumption rates in subcutaneous adipocytes limited by OXPHOS, free OXPHOS, as well as ETS capacity, respiring on substrates for CI and CII. The measurement of mitochondrial oxygen consumption rates of adipocytes rather than isolated mitochondria is holding the chance to measure mitochondria within their cellular context including mitochondrial fusion and fission (Youle and van der Bliek, 2012; Brand and Nicholls, 2011).

The results from measuring adipocyte oxygen uptake represent mitochondrial capacity per cell and are therefore also dependent on mitochondrial abundance. In contrast to that, RCR is a measure for mitochondrial capacity independent from cellular mitochondrial abundance, as it is calculated by the ratio of OXPHOS capacity to LEAK respiration (Brand and Nicholls, 2011). As values of the cellular RCR were not significantly inverse associated with donor's BMI, the other respiratory states, which were decreased with increasing BMI, might be substantiated in a decreased mitochondrial content. Therefore, to further compare mitochondrial function, also normalized to mitochondrial content, and without a potential influence of different adipocyte sizes incorporating different numbers of mitochondria, measuring of isolated mitochondria is a suitable method. In contrast to measurements within isolated subcutaneous adipocytes, the RCR of isolated mitochondria was significantly reduced with increasing BMI. Whereas the other respiratory states determined in isolated subcutaneous mitochondria further confirmed the previous findings derived from subcutaneous adipocytes. LEAK respiration was also not found to be significantly associated with donor's BMI. Furthermore, also oxygen uptake during OXPHOS as well as free OXPHOS capacity was found to be reduced

with increasing BMI. Therefore, a reduced adipocyte mitochondrial respiration per cell is not only due to lower mitochondrial abundance, but might also be resulting from a reduced mitochondrial capacity per se. Differences of the obtained RCR in relation to donor's BMI could be due to the different approaches. Beside the difference of measuring mitochondrial respiration within their cellular context and isolated mitochondria, isolated mitochondria were only respiring on CII substrates and exclusively derived from female subjects. The substantiation for the deviating study protocol is firstly, that adipose tissue, where mitochondria were isolated from, derived from plastic surgery. As this surgery procedure is mainly recognized by women, it was only possible to include female subjects in this analysis. Secondly, the respiration rates of isolated adipocyte mitochondria are very low. Therefore, succinate was applied as a substrate, as hereby higher oxygen consumption rates can be achieved compared with NADH-based substrates, due to the prediction that with every pair of electrons of complex I driven respiration 10 protons are pumped into the inner membrane space whereas only 6 protons are pumped across the inner membrane with succinate as substrate. Thus, P/O ratio is lower with succinate as substrate than with NADH-based substrates (Nath, 2008; Brand and Nicholls, 2011). Higher oxygen consumption rates again allow to unravel even small differences in respiration. However, succinate as a substrate, measuring oxygen uptake of isolated mitochondria, is known to produce high levels of ROS by reverse electron transfer (Azzone et al., 1963). Therefore, rotenone was added, which prevents reverse electron transfer (Hinkle et al., 1967).

Reduced isoproterenol induced oxygen uptake rates has also been demonstrated in differentiated preadipocytes derived from obese compared with those from lean subjects (Yehuda-Shnaidman et al., 2010). Moreover, findings of the current study are in accordance with results of Yin and colleagues (Yin et al., 2014). Hereby, mitochondria were isolated from small and large subcutaneous adipocytes and oxygen consumption was expressed per cell or mitochondrial protein. Independent of the chosen normalization, as well as of adipocyte size, the authors found an inverse correlation between oxygen consumption and the donor's BMI in mitochondria from subcutaneous adipocytes. Divergent from the current study, no different respiratory states were assessed from Yin et al. (2014). Therefore, the distinctions of respiratory states, which give further implications on mitochondrial function, create unique value in addition to the study of Yin et al. (Yin et al., 2014).

Analog to the assessment of subcutaneous mitochondria, also oxygen uptake of isolated

omental adipocyte mitochondria was investigated in the study of Yin and colleagues (Yin et al., 2014). In contrast to the present study, also a significant inverse relation to the donor's BMI was found. This difference to our results might be founded within variations of the study design. As the present work did only measure oxygen uptake of visceral adipocytes rather than isolated mitochondria, this could possibly lead to deviating results. Furthermore, there are differences in the depot origin. Whereas Yin et al. (2014) investigated omental adipose tissue from the greater omentum; the adipose tissue samples of the current study originated from the proximity of the angel of His. It has been demonstrated before, that visceral adipose tissue is not homogenous, and gene expression is differently regulated between omental and mesenteric adipose tissue (Tchkonia et al., 2007). Moreover, although oxygen uptake is also expressed per cell in the publication of Yin and colleagues (2014), they determined cell number by cell counting whereas oxygen uptake in the current study is expressed per DNA amount (Yin et al., 2014). It is obvious that several metabolic processes may influence mitochondrial function. It is indeed suggested that physical activity is associated with impaired expression of adipose tissue OXPHOS genes (Mustelin et al., 2008). As the current study could not provide information concerning the subject's physical activity, this is a limitation of various studies dealing with mitochondrial function in adipose tissue and could, therefore, further explain differences within the study population and therefore varying results (Yin et al., 2014).

5.2 OXPHOS protein expression in obese and non-obese subjects

The results of the current study suggest that disturbances within the electron transport chain might be responsible for BMI-dependent impairments of the subcutaneous adipocyte mitochondrial respiratory capacity. To determine the molecular background for this diminished respiratory capacity, the amounts of defined single respiratory chain complex proteins were measured in subcutaneous adipocytes. To control for quantitative differences in the amounts of mitochondria in adipocyte proteins, CS protein was chosen for normalization. Significantly reduced amounts of NDUFB8 (subunit of complex I) and MT-CO2 (subunit of complex IV) were found in obese compared with non-obese subjects. These data were confirmed by a recently published study by Heinonen et al. (2016), investigating OXPHOS protein expression (NDUFB8 and MT-CO2) in subcutaneous adipocytes from lean and obese co-twins. They found significantly higher complex I levels and at least a trend ($p = 0.08$) towards higher complex IV levels per mitochondria in subcutaneous adipocytes from the

leaner co-twins (Heinonen et al., 2016). Results of the current study are further supported by an animal model, where caloric restriction lead to an increase in complex IV gene expression in white adipose tissue (WAT) of rats (Song et al., 2014). However, in the present study as well as in the study from Heinonen and colleagues (2016), protein amounts of selected subunits of the three other complexes were also demonstrated to be lower in obese compared with lean individuals, although these reductions were not statistically different (Heinonen et al., 2016). MT-CO2, which was found to be significantly reduced in obese subjects, is one of the three catalytic core subunits encoded for by mitochondrial DNA and is rate-limiting for electron transport (Capaldi, 1990). As at least in isolated mitochondria of subcutaneous adipocytes respiration was measured irrespective of complex I, only the reduced amounts of MT-CO2 might be able to partially explain the diminished mitochondrial respiratory capacity of adipocytes from obese subjects in the current study. Although all respiratory complexes were monitored, a limitation of the present study in this regard might be that only a small spectrum of subunits could be analyzed. Nevertheless, the data indicate that a qualitative change in complex composition and/or abundance could explain the differences in respiratory capacities. To further scrutinize the relevance of the lower complex IV levels in obese subjects, also complex IV activity was investigated, which is subsequently discussed in chapter 5.3.

5.3 Complex IV activity in association to subject's BMI

Results from OXPHOS protein expression (chapter 4.3) suggested impairments within complex I and complex IV in subcutaneous adipocytes in obesity. But in our hands a reduced protein expression of complex I cannot explain a reduced respiratory capacity with increasing BMI in the current study, due to the measurements of isolated mitochondria where complex I was inhibited by rotenone, only the activity of complex IV was further investigated. At complex IV, oxygen is the final acceptor for electrons that are transferred via the electron transport chain, and is finally reduced to water (Saraste, 1999). Therefore, a reduction of complex IV activity could be a limiting factor for mitochondrial oxygen consumption rates and hereby OXPHOS capacity.

Contrary to these expectations, the current study illustrated that mean as well as maximal complex IV activity normalized to protein is not related to donor's BMI. However, upon normalizing the determined activity levels to CS and therefore mitochondrial content, complex IV activity was increasing with increasing BMI. This implies that the observed

decrease in complex IV protein expression in obese subjects does not coincide with a decrease in complex IV activity. Furthermore, the statement of increased complex IV activity might compensate for reduced protein expression levels could not be confirmed, as complex IV activity and protein expression were not associated to each other. Therefore, it is more likely that the link, which was observed after normalizing to CS, can be reduced to a decrease of CS with increasing BMI.

So far, not much is known about the activity of adipocyte complex IV and its effect on mitochondrial respiration. Furthermore, also conflicting data exist. In a mice knockout model, created by Deepa et al. (2013), complex IV activity and complex IV assembly was impaired in WAT, which was associated with longevity, increased insulin sensitivity and lower body weight. These findings imply a beneficial rather than an unfavorable effect of reduced complex IV activity (Deepa et al., 2013). In contrast to that Soro-Arnaiz et al. (2016) suggested from mouse experiments that a reduced activity of complex IV in visceral WAT plays a role in age-dependent obesity and enables adipocyte expansion (Soro-Arnaiz et al., 2016). Besides the distinction that these are investigations in mice and not in humans, also the investigation of omental adipose tissue is in discrepancy to our study. In the current study only complex IV activity in subcutaneous adipose tissue was investigated. Therefore, it is unknown if there are differences in adipocytes derived from the visceral depot. However, the data of the present study clearly showed that a reduced protein expression, even of a rate-limiting subunit of complex IV, such as MTCO2 (Capaldi, 1990), it not necessarily accompanied by a reduced activity of the whole protein complex. Also a compensatory activity was not observed. Therefore, results of protein expression of single subunits must be interpreted cautiously and the mechanisms related to the decreased mitochondrial respiratory capacity in obese subjects remain elusive.

5.4 Mitochondrial content in subcutaneous adipocytes

Transmission electron microscopy is considered as the golden standard for measuring mitochondrial content. As access to electron microscopy is restricted, several more easily accessible markers were applied as a measure for mitochondrial content in the past (e.g. mtDNA copy number, VDAC, CS activity). For muscle tissue, some biomarkers for mitochondrial content have been evaluated. In detail, Larsen and colleagues (2012) determined the association of commonly used biochemical measures to the mitochondrial

abundance, defined by electron microscopy, in human skeletal muscle. Although mtDNA is a widely used marker for mitochondrial content, Larsen et al. could not find an association between mtDNA and the visible mitochondrial content, whereas cardiolipin and CS activity showed a strong association (Larsen et al., 2012). Although differences between skeletal muscle and adipose tissue are conceivable, in this thesis, CS protein expression was additionally used as a marker for mitochondrial content beside mtDNA copy numbers. Furthermore, within the protein determination of respiratory chain complex subunits (see chapter 4.3 and 4.4) CS protein abundance was also used as an indicator for the mitochondrial content. With regard to the results from Larsen and colleagues (2012), measured mtDNA copy numbers in adipocytes according to the donor's BMI values might be interpreted as reduced mtDNA content, rather than as reduced mitochondrial content, along with an increase in BMI. However, other studies have shown that mtDNA copy number is proportional to the transcription of mitochondrial genes (Malik and Czajka, 2013). As the present study provides combined results of a decreased mtDNA copy number as well as a reduced CS content with increasing donor's BMI, it can be considered that mitochondrial content per se is reduced in subcutaneous adipocytes of obese individuals. Studies from other groups, investigating omental adipose tissue, found similarities to findings in the subcutaneous depot (Christe et al., 2013; Lindinger et al., 2015). As in our study a decrease of visceral adipocyte respiratory capacity in obese subjects was not observed, it can be speculated that visceral mitochondria are capable of compensating these reduced amounts.

5.5 Adipocyte mitochondrial respiration in the context of T2DM

Adipocyte mitochondrial dysfunction accompanied by a decrease in mitochondrial OXPHOS has been repeatedly suggested to be involved the pathogenesis of T2DM. A link between mitochondrial dysfunction and T2DM is supported by studies with insulin sensitizing drugs. The treatment with pioglitazone leads to an increase in mtDNA in human subcutaneous adipose tissue (Bogacka et al., 2005). Furthermore, the treatment of obese mice with rosiglitazone was followed by an increase in adipocyte mitochondrial mass as well as an increase in adipocyte oxygen consumption rates (Wilson-Fritch et al., 2004). Impaired adipocyte mitochondrial function in T2DM independent of obesity was suggested by Dahlman and colleagues (2006), as they observed genes encoding for electron transport chain proteins to be downregulated in subcutaneous and even more pronounced in visceral adipose tissue

of diabetic women independent of obesity (Dahlman et al., 2006). Evidence from human studies, showing that mitochondrial OXPHOS capacity is reduced in T2DM is rare. Therefore, the current study investigated adipocyte mitochondrial respiration in diabetic and pre-diabetic subjects. The present study could not find an influence of the diabetic status on the relation between BMI and oxygen uptake during the different respiratory states in visceral or subcutaneous adipocytes. Moreover, also oxygen consumption rates of obese subjects with or without disturbances within their glucose homeostasis did not differ. To investigate the relationship between the diabetic status and oxygen consumption rates, probands were divided into groups referring to their glucose metabolism. Subjects were only referred to the control group (ND) when fasting blood glucose levels were < 110 mg/dl, HbA_{1c} < 5.7, and C-peptide < 4.4 mg/dl. Whereas fasting blood glucose levels as well as HbA_{1c} values are used as parameters for the diagnosis of T2DM or pre-diabetes, C-peptide is not recognized as a diagnostic tool (American Diabetes Association, 2013). However, C-peptide has been given attention as an early marker for T2DM (Saisho, 2016). Therefore, to avoid the inclusion of individuals with the onset of pre-diabetes, individuals with increased C-peptide levels were excluded from the control group. Although it was thoroughly differentiated between the two groups, there is still the possibility of subjects with disturbances within their glucose homeostasis being included in the control group, as there was no oral glucose tolerance test available for every subject. The possibility of errors in assigning subjects to the different groups could be one reason for the varying results found from Hansen and colleagues (2015). They showed that by measuring respiratory capacity of subcutaneous adipose tissue pieces, the respiratory flux, expressed per cell, was higher in obese compared with diabetic individuals (Hansen et al., 2015). In contrast to these observations, the present study could not find an influence of the diabetic status on respiratory outcomes per adipocyte. Measuring whole adipose tissue pieces involves the chance to bias the oxygen consumption rates by other cell types, present in the adipose tissue (Carswell et al., 2012). Therefore, it can be hypothesized that this might be also a reason for diverging results. Interestingly, another study also investigating lean subjects suffering from T2DM revealed that the activity of subcutaneous adipose tissue electron transport chains was not reduced in diabetic probands. However, the determined electron transport chain activities were found to be significantly lowered in obese compared with lean subjects and further decreased in obese subjects with T2DM (Chattopadhyay et al., 2011). In contrast to the current study where probands had BMI values

above 35 kg/m², mean BMI of overweight subjects in the study of Chattopadhyay et al. (2011) were between 28 and 29 kg/m². Consequently, it might be possible that differences between individuals with and without T2DM diminishe with the onset of obesity (BMI values above 30 kg/m²) (World Health Organization, 2000). This, in turn, is suggesting that obesity is the main determining factor for adipocyte mitochondrial respiration rather than the diabetic status.

To further investigate if adipocyte mitochondrial respiration is linked to T2DM independent from the group assignments, also characteristics of impairments within the glucose homeostasis and adipocyte mitochondrial respiration were analyzed. HbA_{1c} levels as well as fasting blood glucose levels of obese subjects (BMI ≥ 35 kg/m²) were not found to be associated with the determined mitochondrial respiratory states within a multiple regression analysis (Appendix: Table 33, Table 34). In summary, none of the results gained from the current study were indicating that mitochondrial respiration is particularly affected in adipocytes of obese diabetic or pre-diabetic compared with obese individuals without any disturbances in their glucose homeostasis.

In literature, it has been hypothesized that ATP depletion as a consequence of adipocyte mitochondrial dysfunction is an underlying mechanism of T2DM. In detail, it had been proposed that a decrease in adipocyte fatty acid oxidation as well as lipogenesis contribute to an increase in circulating FFA (Pauw et al., 2009). Furthermore, synthesizing and secreting the antidiabetic adipokine adiponectin require ATP, which is also supplied by mitochondrial OXPHOS (Szkudelski et al., 2011; Komai et al., 2014). In order to explore the hypothesis that disturbances of ATP levels might affect adipocytes in an unfavorable way and thus promote T2DM, also ATP levels were compared between the control group (ND) and the group including diabetic as well as pre-diabetic subjects (Appendix: Figure 35). No difference was observed between the two groups. Therefore, the current study is not indicating that adipocyte ATP levels are decreased in diabetic or pre-diabetic subjects. However, further insights into adipocyte energy homeostasis could be gained from investigating adenosine monophosphate (AMP) as well as levels of activated AMPK, a regulator of the cellular energy homeostasis. Therefore, a limitation of this study is that only ATP levels were determined.

Apart from ATP levels and mitochondrial respiration, other mitochondrial functions might be impaired within adipocytes of diabetic subject. For example, it was suggested that the dysregulation of calcium flux is associated with impaired mitochondrial biogenesis and this

could promote insulin resistance (Cedikova et al., 2016). This hypothesis is further supported by decreased mtDNA copy numbers in subcutaneous (Bogacka et al., 2005) and visceral adipose tissue (Lindinger et al., 2010) of diabetic subjects. If the impairment of other mitochondrial functions, apart from mitochondrial respiration, is linked with T2DM has therefore to be further investigated by future studies.

5.6 Adipocyte lactate release

In cell models it has been shown that inhibition of mitochondrial respiration is followed by an increase in lactate release (González-Barroso et al., 2012). Data of the current study are confirming these results also in human subcutaneous as well as visceral adipocytes. When adipocytes where treated with oligomycin in order to inhibit mitochondrial ATP production, the amount of the released lactate was doubled in both depots compared with basal lactate release. Hence, human adipocytes seem to compensate for impaired mitochondrial respiration with an increase in glycolysis.

Furthermore, we found a positive association for BMI and basal adipocyte lactate release normalized to DNA in both investigated depots. As, at least from animal models, it is also known that adipocyte size correlates with lactate release (reviewed in DiGirolamo et al., 1992), we also expressed lactate release per adipocyte volume instead of DNA. Contrary to what we found before, when expressing lactate release per cell, lactate release normalized to adipocyte volume did not reveal an association to donor's BMI (Appendix: Table 29). This finding is indicating that lactate release per cell is rising with increasing BMI which mainly can be explained by enlarged adipocytes. In total, the results are also in accordance with other studies, where it was already shown that obesity is accompanied by higher circulating blood lactate levels and, that those higher levels are referred to an increase of adipose tissue mass (Lovejoy et al., 1990; DiGirolamo et al., 1989; Jansson et al., 1994).

Increased lactate production from anaerobe glycolysis seen in large adipocytes, might be due to a lack of oxygen as the diffusion distance of oxygen in tissues amounts only to approximately 100-200 µM (Brahimi-Horn and Pouysségur, 2007). It is possible that hypoxic conditions may partially explain the increased lactate levels in our experiment, as we found adipocytes larger than 200 µM diameter. On the other hand, mitochondria in adipocytes are not centrally located, but rather surround the lipid droplet (Cinti, 2005). Hence, particularly in cultured isolated adipocytes, the distance for the diffusion of oxygen to reach mitochondria

are not equal to adipocyte diameters. However, with the increase of adipose tissue mass *in vivo*, vascularization is not growing in the same manner. Especially the capillary density was found to be decreased in subcutaneous adipose tissue of obese subjects (Pasarica et al., 2009; Spencer et al., 2011). Hence, a lack of vascularization and growing size of adipocytes could account for hypoxia in adipose tissue and therefore lead to an increased lactate production, as already suggested in literature (Pérez de Heredia et al., 2010; Lolmède et al., 2003). As vascularization is decreasing in subcutaneous adipose tissue of obese subjects but not in the visceral depot, that could contribute to the differences between visceral and subcutaneous adipocytes with regard to the link between the spare glycolytic capacity per cell and the donor's BMI (Gealekman et al., 2011).

The current work is the first report where it has been investigated if an impaired respiration is accompanied by a compensatory increase in glycolysis, and therefore, lactate release in human adipocytes. Although, except from basal lactate release in the visceral depot, all models showed a negative coefficient, and thus, implying that lactate release is increasing with decreased oxygen uptake, no statistically significant associations with mitochondrial respiration were observed. As this analysis was only performed in a smaller subpopulation, a rather small statistical power could be responsible for a missing link. Furthermore, it has to be noted that the conditions of respiratory measurements and lactate determination were not identical. To create best possible conditions for the oxygen uptake measurements, a respiration buffer (MIR05) was applied. For cell culture and lactate release, cell culture media (DMEM F12), which was approved to provide optimal conditions for isolated human mature adipocytes, was used. Furthermore, oxygen uptake was determined of permeabilized cells to gain better insights into different mitochondrial respiratory states. Moreover, adipocytes might behave differently when stored in an incubator or in a measuring chamber stirred at 750 rpm. Furthermore, there is the possibility that already released lactate is reabsorbed again by the adipocytes (Hajduch et al., 2000). This was not determined in our model and could therefore be a confounding variable. Nevertheless, especially in oligomycin treated cells the reabsorption of lactate might not be relevant, as pyruvate, which is supposed to be converted by the LDH from lactate, cannot be used as a substrate for mitochondrial respiration (Vergnes and Reue, 2014).

Although evidence for an inverse relation between mitochondrial respiration and lactate release was not provided, data of the current study indicate that adipocyte mitochondrial

respiration and lactate production is linked, especially when the marked effect of inhibiting mitochondrial ATP production on lactate release is taken into consideration. To what extent adipose tissue hypoxia in obese subjects is influencing mitochondrial respiration, therefore, has to be object of further investigations.

5.7 Adipocyte ATP levels

5.7.1 Assignment of ATP to mitochondrial OXPHOS or glycolysis

From literature it is known that under normal conditions 80 % of the mammalian cellular ATP demand is produced by the mitochondrial OXPHOS process, which is also substantiated, as this is the more efficient way of ATP production compared with glycolysis (Papa et al., 2012). Exploring the proportion of mitochondrial and glycolytic ATP production, the current study is, for the first time, providing results where adipocytes of two adipose tissue depots were investigated. Irrespective of adipocyte depot origin, the mitochondrial ATP production was not able to compensate the inhibition of glycolysis. Moreover, the data of the present study showed that inhibition of OXPHOS by oligomycin is only leading to a slight decrease of cellular ATP levels, indicating that glycolysis in adipocytes is, again irrespective of depot origin, more relevant for ATP production than mitochondrial OXPHOS. In detail, the study is suggesting that visceral adipocytes are more capable of compensating mitochondrial dysfunction by glycolysis, compared with subcutaneous adipocytes. In general, the data of the present study are in line with results from a mouse adipocyte model (3T3-L1 adipocytes), where it has been shown that ATP levels did not change after inhibiting mitochondrial biogenesis as glycolysis was compensating (Nie and Wong, 2009). Keuper et al. (2014) suggested from studying the human SGBS adipocytes that glycolysis is the preferred energy-producing pathway as mitochondrial ATP production was decreased after supplying glucose as a substrate. Furthermore, the authors observed that mitochondrial respiration was able to compensate a reduction of ATP production by glycolysis (Keuper et al., 2014). Although the current study is also highlighting the importance of glycolysis in adipocyte ATP production and the results are supporting the idea that glycolysis is the preferred source of ATP production, isolated human adipocytes were evidently not able to compensate glycolytic ATP output by mitochondrial ATP production. One reason for this divergent observation could be that 2-deoxy-D-glc is also indirectly inhibiting OXPHOS, as pyruvate converted from glucose cannot be used within the citrate cycle. Pyruvate, present in cell culture media (0.5 mM), might not be sufficient to fulfil

the substrate demand for mitochondrial ATP production, as in contrast, for mitochondrial respiration protocols a concentration of 5 mM has been established to enable a partially noncarrier-mediated pyruvate transport across the mitochondrial membrane (Gnaiger, 2014). Therefore, a limitation of our model is that to the applied media no additional pyruvate was added to ensure a pyruvate saturated environment.

5.7.2 ATP levels in in association to donor's BMI

Multiple regression analysis of the current study revealed a slight, but significantly positive relationship between donor's BMI and basal ATP levels in visceral adipocytes. In contrast to that, we did not find a link between ATP originated from OXPHOS or glycolysis and BMI in visceral adipocytes, which is in line with our previous findings that lactate release as well as OXPHOS capacity is not changed during obesity. Hence, the association of basal ATP levels and BMI in visceral adipocytes cannot be clearly deducted from deviations in ATP levels derived from OXPHOS or glycolysis in association to BMI. On the other hand, the determined ATP from OXPHOS and glycolysis might rather provide information concerning a compensatory capacity than being absolute values. Under this premise, our data are indicating that visceral adipocyte ATP levels are increasing with increasing BMI, but not the capacity of mitochondrial or glycolytic ATP production to take over if the other pathway is switched off. In a study from Christe et al. (2013), ATP production of isolated mitochondria from human omental adipocyte was measured and, hence, is comparable to our measurement of ATP from OXPHOS. In line with our results, the authors of this study did not find an association between mitochondrial ATP production and obesity (Christe et al., 2013).

In contrast to visceral adipocytes, no link between the amount of basal cellular ATP and donor's BMI in subcutaneous adipocytes was observed. With regard to our previous results this could be explained as in subcutaneous adipocytes an inverse relationship between BMI and OXPHOS capacity, as well as a positive association between lactate release and BMI was found. Consequently, it could be speculated that the two effects might annul each other. However, this would suggest that ATP levels separated in its origin would be associated to the donor's BMI, but this was not confirmed when investigating ATP levels, as no link in subcutaneous adipocytes between ATP from OXPHOS or glycolysis was observed. Equivalent to visceral, also for subcutaneous adipocytes the limitation of the study is that the measured levels of ATP from OXPHOS and glycolysis could be seen rather as capacities than the actual

contribution to cellular ATP levels. Furthermore, as stated before, the contribution of ATP from OXPHOS might be underestimated as the supplied pyruvate concentration of 0.5 mM might not be sufficient (Gnaiger, 2014).

Our study is not indicating that impairments within adipocyte mitochondrial respiration is leading to ATP depletion which could be followed by the inhibition of fatty acid re-esterification (Gaidhu and Ceddia, 2011) or a decrease of adiponectin secretion (Szkudelski et al., 2011; Komai et al., 2014). Nevertheless, ATP consuming processes might be shut down in order to keep cellular ATP levels to be stable. To test this assumption, further measurements targeting the ratio of AMP to ATP as well as the activation of AMPK are necessary to clarify adipocyte energy status in obese subjects.

5.7.3 ATP levels in association to mitochondrial OXPHOS capacities and lactate release

To the best of our knowledge, the present study analyzed for the first time if measurements of adipocyte mitochondrial respiration (OXPHOS and free OXPHOS capacity) as well as adipocyte glycolysis (lactate release), are associated to actual adipocyte ATP levels. The preceding hypothesis of this analysis was firstly that ATP levels and the corresponding measured pathway of origin is correlating directly with each other, and secondly that there exists an inverse relationship between the activity of one metabolic pathway of ATP production and actual ATP levels gained from the other metabolic pathway of ATP production, which would indicate a complementary regulation. This hypothesis was not confirmed by the current study, as no evidence for correlations between oxygen uptake rates during OXPHOS and free OXPHOS capacity and adipocyte ATP levels was observed. Although a significant inverse association between ATP from OXPHOS and OXPHOS as well as free OXPHOS capacity was determined, this was not significant as well as inverse anymore, when an outlier was excluded from the analysis. Analog to those results, no evidence was found for an association between any determined lactate release rates and the measured cellular ATP levels either. The divergence between the measurement of actual ATP levels and the corresponding measured metabolic pathway of ATP production might be due to unknown varying cellular ATP consuming processes in this model. To get better insights into the energy status of the cells, the ratio of AMP to ATP, as well as the activation of AMPK might be the objective of further studies. Apart from this biological aspect, also limitations of the applied model could

account for a missing link. Indeed, the conditions during ATP determination were different from those during the measurement of oxygen uptake, which was already discussed in 5.6. It is worth noting that also the applied substrates were differing such as pyruvate. Furthermore, also the conditions during lactate release differed from those during measuring cellular ATP concentrations, as the incubation time was for ATP determination 2.5 h and for lactate determination 24 h. These time points were chosen, as ATP measurement took place in a similar time frame as oxygen uptake measurements, but sensitivity of the lactate assay was best after the incubation of 24 h. As a consequence of the different time points of harvesting, the energy status of the analyzed adipocytes might be different, concnerning changes of media composition (secreted substances accumulate and substrates run short) (Carswell et al., 2012). Additionally, it has to be noted, that in the current study ATP from OXPHOS and ATP from glycolysis were determined during the complete inhibition of the other metabolic pathway of ATP production. Therefore, the gained ATP levels might rather represent the capacity to increase ATP production than the actual contribution to ATP levels under physiological conditions. In conclusion, this analysis has to be interpreted very cautiously, also due to the small number of included subjects (n = 5-10). Hence, further investigations are planned to follow, especially to increase the statistical power, as well as to exclude differences within the compared models.

5.8 Adipose tissue depot specific outcomes

5.8.1 Oxygen consumption rates of visceral and subcutaneous adipocytes

When analyzing the difference between oxygen uptake during different respiratory states of visceral and subcutaneous adipocytes, a first analysis only revealed significant lower oxygen consumption rates during LEAK respiration in subcutaneous adipocytes, whereas the remaining respiratory states did not differ between the two depots. After dividing the cohort in one group with BMI values less than 30 kg/m² and another group with BMI values greater or equal to 30 kg/m², deviating results were found. Hereby, the group, which included subjects with BMI values below 30 kg /m², inclined to have higher oxygen uptake rates in subcutaneous adipocytes during OXPHOS, free OXPHOS and ETS capacity, but not during LEAK respiration. Indeed, RCR was significantly higher in subcutaneous adipocytes. Although not all of these differences were statistically significant, they are opposite from findings within the group exclusively including subjects with BMI values greater or equal to 30 kg/m². In this group, no

significant difference was observed between RCR values of visceral and subcutaneous adipocytes. Moreover, all other oxygen consumption rates investigated were consistently and significantly lower in subcutaneous compared with visceral adipocytes. Therefore, although RCR was not statistically significantly related to donor's BMI values, an alteration with obesity limited to the subcutaneous depot is indicated. These findings are partially in accordance with results from Kraunsøe et al. (2010), where higher oxygen consumption rates during state 3 (OXPHOS capacity) as well as uncoupled respiration (ETS capacity) per mg visceral adipose tissue compared with subcutaneous adipose tissue were found in subjects with BMI values greater than 30 kg/m². However, when these oxygen uptake rates were expressed per cell, oxygen uptake of subcutaneous adipocytes was higher compared with visceral adipocytes. As hereby whole adipose tissue pieces instead of isolated adipocytes were measured, this could account for the observed difference (Kraunsøe et al., 2010). Yin and colleagues (2014), who studied isolated mitochondria from subcutaneous and omental adipose tissue, did not find a difference in oxygen uptake rates with regard to adipose tissue origin. Therefore, the results are in line with findings of the present study regarding subject with BMI values less than 30 kg/m². Interestingly, when oxygen consumption rates were divided into obese and lean subjects, as well as small and large adipocytes, the results revealed consistently higher oxygen uptake rates in subcutaneous adipocytes of lean individuals (irrespective of adipocyte size), but lower in subcutaneous adipocytes of obese individuals. Although these findings from Yin et al. (2010) were not statistically significant, the results are following the same trend as the results of the current study (Yin et al., 2014). Differences between respiratory measurements of the two adipose tissue depots might therefore be a matter of the subjects BMI and should be taken into consideration, when investigating differences between the two depots. Oxygen uptake during LEAK respiration was not assessed within the studies of Yin et al. (2014) and Kraunsøe et al. (2010). Surprisingly, LEAK respiration, which was not altered with increasing BMI in all other analysis of the current study, was found to be lower in subcutaneous compared with visceral adipocytes of obese subjects. LEAK respiration can be based on basal proton conductance and regulated inducible proton conductance by uncoupling proteins (Divakaruni and Brand, 2011). In our model, LEAK respiration due to uncoupling proteins might be insignificant, as uncoupling proteins were not induced. Nevertheless, there are physiological implications of LEAK respiration. One theory is that LEAK respiration is lowering mitochondrial superoxide production due to decreasing the proton motif force (Rolfe and

Brand, 1997; Divakaruni and Brand, 2011). Therefore, the current study is indicating that in obese subjects ROS production in subcutaneous adipocytes might be higher compared with visceral adipocytes. Again, this result is also supporting the main suggestion of the current study that impairments within adipocyte mitochondria in obese subjects are more relevant in the subcutaneous adipose tissue depot.

It is suggested that adipocytes of varying adipose tissue depots are genetically programmed in a different way (Gesta et al., 2006; Tchkonia et al., 2007). Therefore, physiological differences between adipocytes from distinct adipose tissue depots, as found in the current study in obese subjects, are likely to occur and have been reported frequently (Hube et al., 1996; Zierath et al., 1998; Dusserre et al., 2000). Nevertheless, despite differences of oxygen uptake rates between the two fat depots, oxygen uptake during every determined respiratory state significantly correlated between the two adipose tissue depots within the same subject. These observations are suggesting that although there are differences between visceral and subcutaneous adipocytes, especially in obese subjects, adipocyte mitochondrial respiration might be controlled similarly in the two adipose tissue depots.

5.8.2 Lactate release of visceral and subcutaneous adipocytes

The comparison of subcutaneous and visceral adipocyte lactate release, including all subjects, revealed consistently lower levels in the visceral depot. Whereas, if the cohort was divided in one group with lean and overweight individuals (BMI < 30 kg/m²) and another group with obese individuals (BMI ≥ 30 kg/m²), this finding remained only statistically significant for obese subjects. Nevertheless, also within the group incorporating subjects with BMI < 30 kg/m², there was a trend towards lower lactate levels within visceral adipocytes. As it is suggested that the sizes of adipocytes have significant influence on lactate release (DiGirolamo et al., 1992) also an analysis per volume rather than DNA was performed. Hereby, in the total cohort, including subjects with all BMI values, no significant differences were observed (Appendix:

Table 30). Also when only obese individuals were included (BMI ≥ 30 kg/m²), the statistically significant differences between the two depots were diminished. Only in lean and overweight subjects (BMI < 30 kg/m²) subcutaneous adipocyte lactate release after the addition of oligomycin was significantly higher compared with visceral adipocytes (Appendix: Table 31). This finding might indicate that subcutaneous adipocytes of these subjects are more capable to increase glycolysis, when mitochondrial OXPHOS is blocked. However, as delta lactate

release was not significantly different between the two depots, the observed difference might rather be substantiated in an additive effect of a greater basal lactate release of subcutaneous adipocytes, as in a greater capacity of subcutaneous adipocytes to increase glycolysis. In total, the results of the current study are suggesting that the difference between the lactate release of subcutaneous and visceral adipocytes per cell is due to smaller adipocytes of the visceral depot (Appendix: Figure 36). However, also in lean and overweight subjects, visceral adipocytes are smaller compared with subcutaneous adipocytes. That the difference between the two depots in these individuals was not statistically significant could be substantiated in a low statistical power due to a low number of subjects included in this group. Furthermore, also the potential of vascularization, which is only decreasing with obesity in the subcutaneous depot (Gealekman et al., 2011) could account for the finding that subcutaneous adipocyte lactate release and the capacity to increase lactate production after the inhibition of mitochondrial ATP production per cell was only significantly higher in obese subjects. In contrast to the present study, subcutaneous adipocytes from fasted rats showed lower levels of basal lactate production per cell compared with adipocytes from the mesenteric, epididymal, or retroperitoneal depot (Newby et al., 1988). These contrary findings could be substantiated in a different body fat distribution of subcutaneous and intra-abdominal adipose tissue in humans and rodents (Fried et al., 2015). Also, in mice an increase in vascularization of the subcutaneous depot with increasing BMI was found (Gealekman et al., 2008), which is contrary to what was observed in studying human adipose tissue (Gealekman et al., 2011).

Apart from differences between the two depots, especially lactate release per cell after the treatment with the complex V inhibitor oligomycin showed the strongest and most significant association between adipocytes of the visceral and the subcutaneous depot. The correlation between basal lactate release as well as the capacity to increase lactate release of subcutaneous and visceral adipocytes at least reached borderline significance. After expressing lactate release per volume, the correlation analysis between the two depots revealed varying results. In detail, the borderline significant association between basal lactate release of subcutaneous and visceral adipocytes disappeared, as well as the significant correlation of lactate levels between the two depots under the treatment with oligomycin. Only the link of the capacity to increase lactate release, was close to be significant (Appendix: Table 32). Therefore, it can be speculated that the correlation of lactate release between the

two depots might occur especially due to cell size, which is also correlating between the two depots within one subject (Appendix: Figure 37). Again, differences between lactate release and therefore a missing correlation between the two depots might be substantiated in different rates of vascularization of the two depots (Gealekman et al., 2011). However, the control of the capacity for increasing the rate of glycolysis, and thus, lactate release might be not only controlled locally, e.g. by the size of adipocyte, but also central regulatory mechanism might have an influence, as also found for mitochondrial respiration (5.8.1).

5.8.3 ATP levels in visceral and subcutaneous adipocytes

When comparing subcutaneous with visceral adipocyte ATP levels including all subjects irrespective of BMI, no difference was observed between the depots. After dividing the subjects into two groups referring to their BMI, the results differed. In the group including obese subjects there was still no difference in ATP levels between the two depots, which is also in line with previous findings from Vikman and colleagues (1995) (Vikman et al., 1995). Whereas subjects with BMI values below 30 kg/m² showed significantly lower visceral ATP levels compared with subcutaneous adipocytes. Furthermore, compared with subcutaneous adipocytes also visceral ATP levels derived from glycolysis were lower although this only reached borderline significance. Therefore, differences in basal ATP levels might occur rather due to higher glycolytic ATP levels in subcutaneous adipocytes, as there was no difference in ATP from OXPHOS. This is surprising as subjects with BMI values above 30 kg/m² showed a lower subcutaneous lactate release, whereas in subjects with BMI values below 30 kg/m² no difference between lactate release of subcutaneous and visceral adipocytes was observed in the present study. One reason for the deviating results could be that the uptake of lactate from subcutaneous and visceral adipocytes is differently. However, as discussed before, especially for oligomycin treated cells, this is not very likely (5.6). Additionally, the timeframe of incubations between adipocytes used for ATP determination and adipocytes used for measuring lactate release was not equal and could therefore bias the direct comparison of ATP levels and lactate release. Another reason for the discordant finding might be found in different energy demands of the two depots. In obese individuals, glycolytic rates are higher in visceral adipocytes. In lean and overweight individuals there is no difference between the two depots. Following the assumption of different energy requirements, the observed significantly lower ATP levels in subjects with BMI values below 30 kg/m² and the missing

difference between the two depots in adipocytes of obese subjects is leading to the speculation of higher energy requirements of visceral adipocytes irrespective of the subject's BMI. As subcutaneous adipocytes show lower adiponectin secretion rates compared with visceral adipocytes (Motoshima et al., 2002), and as the secretion of adiponectin requires ATP (Szkudelski et al., 2011; Komai et al., 2014), this could contribute to higher energy demands of visceral adipocytes. Energy requirements of visceral and subcutaneous adipocytes were not objective of published studies so far. However, further indications from the current study, supporting this hypothesis, were gained from correlation analysis of ATP levels between the subcutaneous and the visceral depot. Although the determined OXPHOS capacities as well as basal lactate release and lactate release following mitochondrial inhibition was correlated between the two depots, investigating cellular ATP levels a correlation was only found for ATP levels derived from OXPHOS. ATP derived from glycolysis as well as basal ATP levels, though, did not correlate between adipocytes of the two depots. Therefore, the results are suggesting that the required ATP might be different between the two depots. To prove this hypothesis, also AMP as well as the activation of AMPK should be determined in future studies. Hereby, more insights about energy requirements and consumption rates of visceral and subcutaneous adipocytes could be gained.

6 CONCLUSION AND OUTLOOK

The current study showed that mitochondrial respiratory capacity of human subcutaneous adipocytes is decreasing with increasing BMI. Moreover, mtDNA and CS protein expression, as indicators for mitochondrial abundance, were decreasing in subcutaneous adipocytes with increasing subject's BMI. As also isolated mitochondria of subcutaneous adipocytes showed lower respiratory rates with increasing obesity, it can be concluded that impairments within subcutaneous adipocyte mitochondrial respiration occurs independently of mitochondrial content.

Although several studies emphasize the negative impact particularly of visceral adipose tissue on metabolic comorbidities in obeity, the present work did not find a significantly inverse relation of visceral adipocyte mitochondrial respiration and subject's BMI value. Still, for the first time it was shown that mitochondrial oxygen uptake of neither isolated subcutaneous nor visceral adipocytes is particularly impaired in obese subjects showing deteriorations within their glucose homeostasis. Therefore, impaired subcutaneous adipocyte mitochondrial respiration seems to be rather linked to obesity itself than to T2DM, and thus, might not contribute to the pathogenesis of T2DM. As previous publications found adipocyte mitochondria to be altered in individuals suffering from T2DM, other mitochondrial functions, rather than mitochondrial respiration, might be impaired in adipocytes of diabetic subjects and have to be further investigated.

Protein expression analyses of subcutaneous adipocytes suggested that a reduced amount of the electron transport chain complex IV could be responsible for the BMI dependent decline in mitochondrial respiration. However, this was not confirmed by activity measurements of complex IV. Therefore, further efforts should be made to unravel the molecular background of an impaired mitochondrial function in subcutaneous adipocytes of obese subjects.

Particularly respiratory capacity linked to ATP production (free OXPHOS capacity) was found to be reduced in subcutaneous adipocytes with increasing BMI. However, this finding was not accompanied by a parallel decrease of adipocyte ATP levels. Nevertheless, an impaired mitochondrial respiration could lead to an altered ratio of AMP to ATP followed by the activation of AMPK. As a consequence, ATP consuming pathways might be downregulated in order to keep cellular ATP levels to be stable. Therefore, the activation of AMPK as well as the

ratio of AMP to ATP should be investigated in future studies to gain further knowledge about consequences of mitochondrial respiration for the energy status of adipocytes. Additionally, the results of the study implied that glycolysis is the main source of ATP in human adipocytes and that adipocyte lactate release is increasing with increasing BMI due to the parallel enlargement of adipocytes. Hence, ATP levels are not altered, as glycolysis is able to compensate for an impaired mitochondrial ATP production. Due to these results, and to the fact that several studies suggest a hypoxic state in adipose tissue of obese individuals, future investigations should also focus on hypoxia as a potential underlying cause of impaired mitochondrial respiration in subcutaneous adipocytes of obese individuals.

7 APPENDIX

7.1 Applied chemicals

Table 25: List of applied chemicals

Chemicals	Supplier, Country
2-deoxy-D-glucose	Sigma-Aldrich, Germany
ADP	Sigma-Aldrich, Germany
Antimycin A	Sigma-Aldrich, Germany
Ascorbic acid	Sigma-Aldrich, Germany
Bromophenol blue	VWR, Germany
BSA	Sigma-Aldrich, Germany
BSA faf	Carl Roth, Germany
$CaCl_2$	Carl Roth, Germany
Carbonyl cyanide 4-(trifluoromethoxy)phenylhydrazone	Sigma-Aldrich, Germany
Collagenase	Biochrom, Germany
cOmplete	Roche, Switzerland
Cytochrome c from equine heart	Sigma-Aldrich, Germany
Deoxycholate	Sigma-Aldrich, Germany
Digitonin	Sigma-Aldrich, Germany
DMEM/F12	ThermoFisher Scientific, USA
DTT	Omnilab, Germany
EDTA	Merck, Germany
EGTA	Sigma-Aldrich, Germany
Glycerin	Merck, Germany
Glycin	Merck, Germany
HCl	Carl Roth, Germany
Hepes	Sigma-Aldrich, Germany
Hydrazine hydrate	Sigma-Aldrich, Germany
Hydrazine sulphate	Sigma-Aldrich, Germany
KCl	Carl Roth, Germany
KH_2PO_4	Carl Roth, Germany
Lactatedehydrogenase	Sigma-Aldrich, Germany
Malate	Sigma-Aldrich, Germany
Methanol	Sigma-Aldrich, Germany
$MgCl_2*6H_2O$	Carl Roth, Germany
$MgSO_4x7\ H_2O$	Merck, Germany
NaCl	Carl Roth, Germany
NAD+	Sigma-Aldrich, Germany
NADH	Sigma-Aldrich, Germany
$NaH_2PO_4xH_2O$	Merck, Germany
NaOH	J.T.Baker, Netherlands
Nonidet P-40	Sigma-Aldrich, Germany

Chemicals	Supplier, Country
Nylon mesh 2,000 µM	VWR, USA
Nylon mesh 200 µM	VWR, USA
Object slide	VWR, USA
Odyssey® blocking buffer	LI-COR, USA
Oligomycin	Sigma-Aldrich, Germany
PBS	Biochrom, Germany
Pen-Strep	Sigma-Aldrich, Germany
Phenol:chloroform:isoamyl alcohol	Carl Roth, Germany
Phenylmethanesulfonylfluoride (PMSF)	Sigma-Aldrich, Germany
PhosSTOP	Roche, Switzerland
Potassium lactobionate	Sigma-Aldrich, Germany
Proteinase K	Qiagen, Germany
Pyruvate	Sigma-Aldrich, Germany
SDS	AppliChem, Germany
Succinate	Sigma-Aldrich, Germany
Sucrose	Carl Roth, Germany
Taurin	Sigma-Aldrich, Germany
Tris	Sigma-Aldrich, Germany
Tween® 20	Sigma-Aldrich, Germany
Zirconium/glass-Beads® (ø 0.5 mm)	Carl Roth, Germany

7.2 Subject's details

Table 26: Subject's details

	Isolated mitochondrial respiration	Isolated mitochondrial respiration based on cell size	Western blot analysis and CIV activity	mtDNA/ nDNA	sc adipocyte respiration	vc adipocyte respiration	sc ATP levels	vc ATP levels	sc lactate secrection	vc lactate release
	n = 16	n = 5	n = 20	n = 17	n = 40	n = 47	n = 32	n = 29	n = 17	n = 18
BMI [kg/m²]	25 ± 5 [18; 36]	28 ± 6 [22; 36]	27 ± 6 [19; 41]	28 ± 6 [19; 41]	44 ± 14 [21;70]	42 ± 14 [21;70]	41 ± 14 [19; 66]	41 ± 13 [21;61]	41 ± 15 [19; 66]	42 ± 14 [21; 66]
age	41 ± 13 [27; 68] (n = 13)	41 ±10 [31; 56]	43 ± 13 [23; 65]	44 ± 13 [23; 65]	46 ± 13 [18;70]	49 ± 13 [18;74]	48 ± 13 [18; 73]	48 ± 14 [18;73]	48 ± 15 [19; 77]	49 ± 15 [19; 77]
female	16	5	20	17	27	27	23	21	13	13
male	-	-	-	-	13	20	9	8	4	5
T2DM	-	-	-	-	10	10	5	3	2	2
pre-diabetes	-	-	-	-	4	4	4	5	4	4

Values for BMI and age are expressed as means ±SD [minimum, maximum]. Subject's age of respiratory measurements of isolated mitochondria was only available for 13 subjects.

7.3 Additional results

Table 27: LDH activity and donor's BMI

time point of measurement (n)	coefficient LDH	R^2	*p*-value	
Before permeabilization (77)	0.060	0.009	n.s.	0.41
After permeabilization (72)	0.018	0.032	n.s.	0.13

LDH activity was determined indirectly by measuring NAD^+, which is originating from the conversion of pyruvate to L-lactate with NADH as a cofactor. LDH activity before permeabilization was measured in the media where adipocytes were diluted 1:2. LDH activity after permeabilization was determined in MIR05 buffer after permeabilization with digitonin and the determination of oxygen consumption rates by high-resolution respirometry. Hereby adipocytes were diluted 1:10. Therefore, LDH activity after permeabilization was multiplied by five in order to gain the same proportion of LDH activity before and after permeabilization. A multiple regression analysis with donor's BMI and LDH activity was performed. Estimated coefficient for donor's LDH activity and multiple R^2 of the model are given. Asterisks indicate if the corresponding coefficient is not equal to zero. Not significant (n.s.); *p < 0.05; **p < 0.01; ***p < 0.001.

Table 28: LDH activity in subjects with different diabetic status

time point of measurement (n)	mean ND (±SD)	mean DiGH (±SD)	*p*-value	
Before permeabilization (16; 14)	28.4 (±27.6)	22.8 (±14.5)	n.s.	0.44
After permeabilization (16; 14)	212.8 (±191.8)	164.6 (±152.1)	n.s.	0.41

LDH activity was determined indirectly by measuring NAD^+, which is originating from the conversion of pyruvate to L-lactate with NADH as a cofactor. LDH activity before permeabilization was measured in the media where adipocytes were diluted 1:2. LDH activity after permeabilization was determined in MIR05 buffer after permeabilization with digitonin and the determination of oxygen consumption rates by high-resolution respirometry. Hereby adipocytes were diluted 1:10. Therefore, LDH activity after permeabilization was multiplied by five in order to gain the same proportion of LDH activity before and after permeabilization. Differences between the LDH activity of subjects with different diabetic status (ND vs. DiGH were assessed using Student's paired *t*-test (n = 14-16). Values are expressed as means (±SD). Asterisks indicate statistically significant differences between the two depots (vc vs. sc): Not significant (n.s.); *p < 0.05; **p < 0.01; ***p < 0.001.

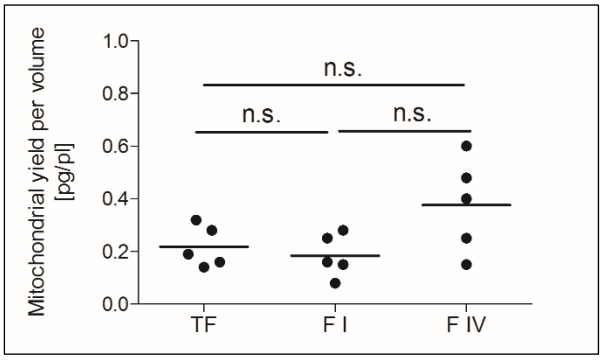

Figure 34: Mitochondrial yield per volume in fractionated adipocytes

Mitochondria were isolated from adipocytes of the TF, FI and FIV. Differences between TF, FI, and FIV were analyzed using a one-way ANOVA. No significant difference was detected between the mitochondrial yield per volume (pl) of the TF, FI, and FIV. Asterisks indicate statistically significant differences between the two conditions: Not significant (n.s.); *p < 0.05; **p < 0.01; ***p < 0.001.

Table 29: Multiple regression analysis: lactate release per volume adipocytes and donor's BMI adjusted for age

condition	fat depot (n)	coefficient BMI	R^2	*p*-value	
vc basal lactate	vc (18)	0.001	0.05	n.s.	0.43
sc basal lactate	sc (17)	-0.0004	0.03	n.s.	0.72
vc lactate +oligomycin	vc (9)	0.002	0.19	n.s.	0.47
sc lactate +oligomycin	sc (10)	-0.0005	0.28	n.s.	0.84
vc delta lactate	vc (9)	0.0003	0.08	n.s.	0.92
sc delta lactate	sc (10	-0.0009	0.44	n.s.	0.58

A multiple regression analysis with donor's BMI and adipocyte lactate release per volume, adjusted for age and separated in accordance to the adipose tissue depot of origin was performed. Estimated coefficient for donor's BMI and multiple R^2 of the model are given. Asterisks indicate if the corresponding coefficient is not equal to zero. Not significant (n.s.); *p < 0.05; **p < 0.01; ***p < 0.001.

Table 30: Comparison of visceral and subcutaneous lactate release per volume

condition (n)	mean vc (±SD)	mean sc (±SD)	*p*-value	
Lactate basal (16)	0.22 (±0.07)	0.22 (±0.07)	n.s.	0.80
Lactate with oligomycin (9)	0.42 (±0.14)	0.50 (±0.15)	n.s	0.15
delta lactate (9)	0.22 (±0.13)	0.28 (±0.10)	n.s	0.14

Differences between lactate release of visceral and subcutaneous adipocytes per volume were assessed using Student's paired *t*-test (n = 9-16). Values are expressed as means (±SD). Asterisks indicate statistically significant differences between the two depots (vc vs. sc): Not significant (n.s.); *p < 0.05; **p < 0.01; ***p < 0.001.

Table 31: Comparison of visceral and subcutaneous lactate release per volume adipocytes separated by donor's BMI

condition (n)	BMI < 30 kg/m²		*p*-value		BM ≥ 30 kg/m²		*p*-value	
	mean vc (±SD)	mean sc (±SD)			mean vc (±SD)	mean sc (±SD)		
lactate basal (5; 11)	0.19 (±0.08)	0.24 (±0.10)	n.s.	0.09	0.24 (±0.07)	0.21 (±0.05)	n.s.	0.23
lactate with oligomycin (4; 5)	0.43 (±0.20)	0.54(±0.14)	*	0.0498	0.42 (±0.09)	0.46 (±0.15)	n.s.	0.63
Delta lactate (4; 5)	0.27 (±0.16)	0.32 (±0.08)	n.s.	0.39	0.18 (±0.10)	0.24 (±0.12)	n.s.	0.31

Subjects were divided into two groups according to their BMI. Differences of visceral and subcutaneous lactate release per volume adipocytes were analyzed by the Student's paired *t*-test. Only in lean subjects, statistically significant higher lactate concentrations after the addition of oligomycin were observed compared with visceral adipocytes. Asterisks indicate statistically significant differences between the two depots (vc vs. sc): Not significant (n.s.); *p < 0.05; **p < 0.01; ***p < 0.001.

Table 32: Correlation between visceral and subcutaneous adipocyte lactate release per volume

condition	r	*p*-value		n
basal lactate	0.17	n.s.	0.52	17
lactate+oligomycin	0.54	n.s.	0.13	9
delta lactate	0.65	n.s.	0.057	9

Pearson's product-moment correlation was performed for analyzing the association between subcutaneous and visceral adipocyte basal lactate release, lactate release with the addition of oligomycin, and delta lactate release (basal lactate release - lactate release under oligomycin) within the same subject. Asterisks indicate if the lactate releases of visceral and subcutaneous adipocytes significantly correlate with each other. Not significant (n.s.); *p < 0.05; **p < 0.01; ***p < 0.001.

Table 33: Adipocyte oxygen consumption and donor's HbA_{1c} (%) levels adjusted for age

respiratory state	fat depot (n)	coefficient HbA_{1c}	R^2	*p*-value	
OXPHOS capacity	vc (23)	-0.38	0.93	n.s.	0.93
	sc (20)	-2.75	0.13	n.s.	0.64
LEAK respiration	vc (23)	-0.12	0.01	n.s.	0.94
	sc (20)	-1.30	0.04	n.s.	0.56
free OXPHOS capacity	vc (23)	-0.26	0.02	n.s.	0.94
	sc (20)	-1.44	0.19	n.s.	0.72
ETS capacity	vc (23)	-1.08	0.01	n.s.	0.78
	sc (20)	-1.00	0.11	n.s.	0.84

A multiple regression analysis with donor's HbA_{1c} (%) levels and respiratory states of adipocytes adjusted for age and separated in accordance to the adipose tissue depot of origin was performed. Estimated coefficient for donor's HbA_{1c} (%) values and multiple R^2 of the model are given. Asterisks indicate if the corresponding coefficient is not equal to zero. Not significant (n.s.); *p < 0.05; **p < 0.01; ***p < 0.001.

Table 34: Adipocyte oxygen consumption and donor's fasting plasma glucose concentrations adjusted for age

respiratory state	fat depot (n)	coefficient blood glucose	R^2	*p*-value	
OXPHOS capacity	vc (22)	0.04	0.01	n.s.	0.72
	sc (20)	-0.03	0.12	n.s.	0.92
LEAK respiration	vc (22)	0.01	0.01	n.s.	0.90
	sc (20)	0.01	0.02	n.s.	0.84
free OXPHOS capacity	vc (22)	0.03	0.02	n.s.	0.70
	sc (20)	-0.04	0.20	n.s.	0.64
ETS capacity	vc (22)	0.01	0.003	n.s.	0.94
	sc (20)	0.03	0.11	n.s.	0.78

A multiple regression analysis with donor's fasting plasma glucose concentrations and respiratory states of adipocytes adjusted for age and separated in accordance to the adipose tissue depot of origin was performed. Estimated coefficient for donor's fasting plasma glucose concentrations and multiple R^2 of the model are given. Asterisks indicate if the corresponding coefficient is not equal to zero. Not significant (n.s.); *p <0.05; **p < 0.01; ***p <0.001

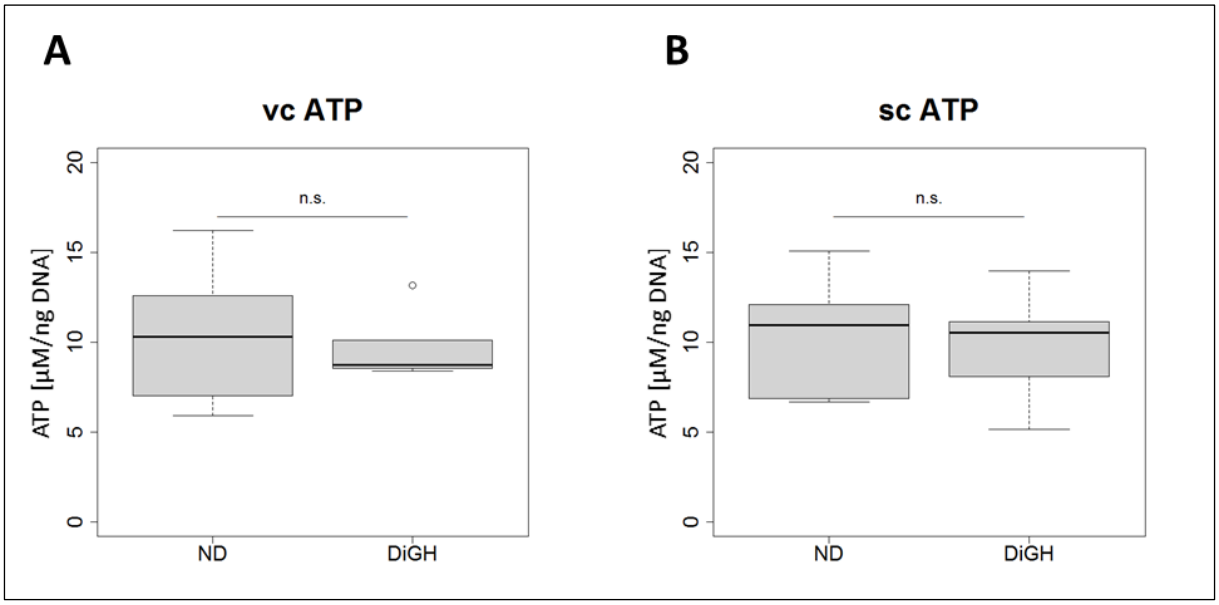

Figure 35: Comparison of ATP levels of subjects with BMI values ≥ 35 kg/m² and different diabetic status

A multiple regression analysis for ATP, adjusted for age, and the diabetic state (ND or DiGH) was performed for adipocytes of subjects with BMI > 35 kg/m². The results are separated according to the corresponding adipose tissue depot. Vc ND: n =14; vc DiGH: n = 16; sc ND: n =14; sc DiGH: n = 15. Asterisks indicate statistically significant differences between the two groups (ND vs. DiGH): Not significant (n.s.); *p <0.05; **p < 0.01; ***p <0.001

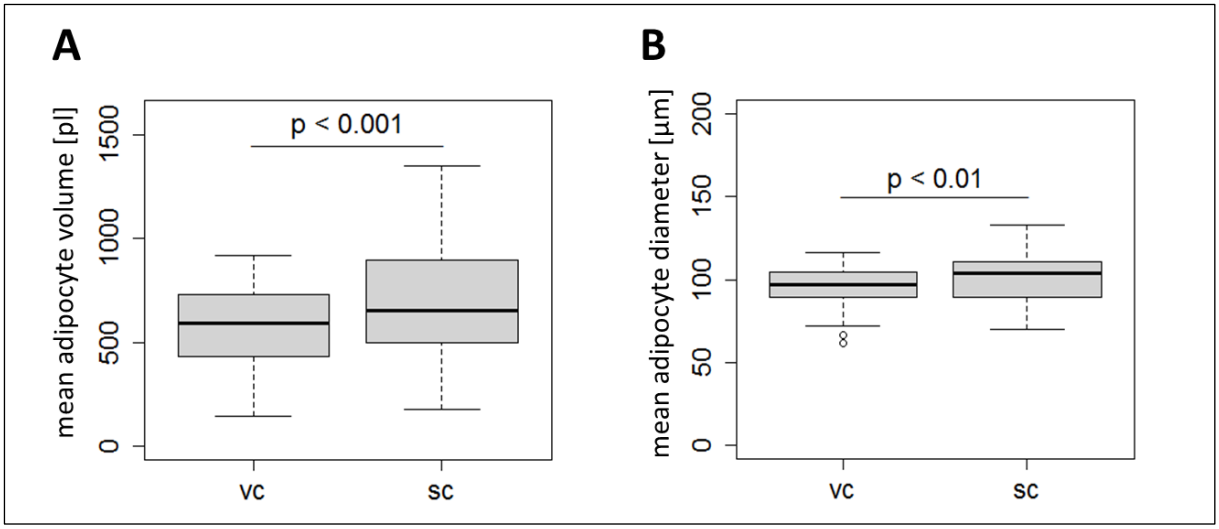

Figure 36: Comparison of visceral and subcutaneous adipocyte volume and diameter

Differences between the mean volume and mean diameter of visceral and subcutaneous adipocytes were assessed using Student's paired *t*-test (n = 49).

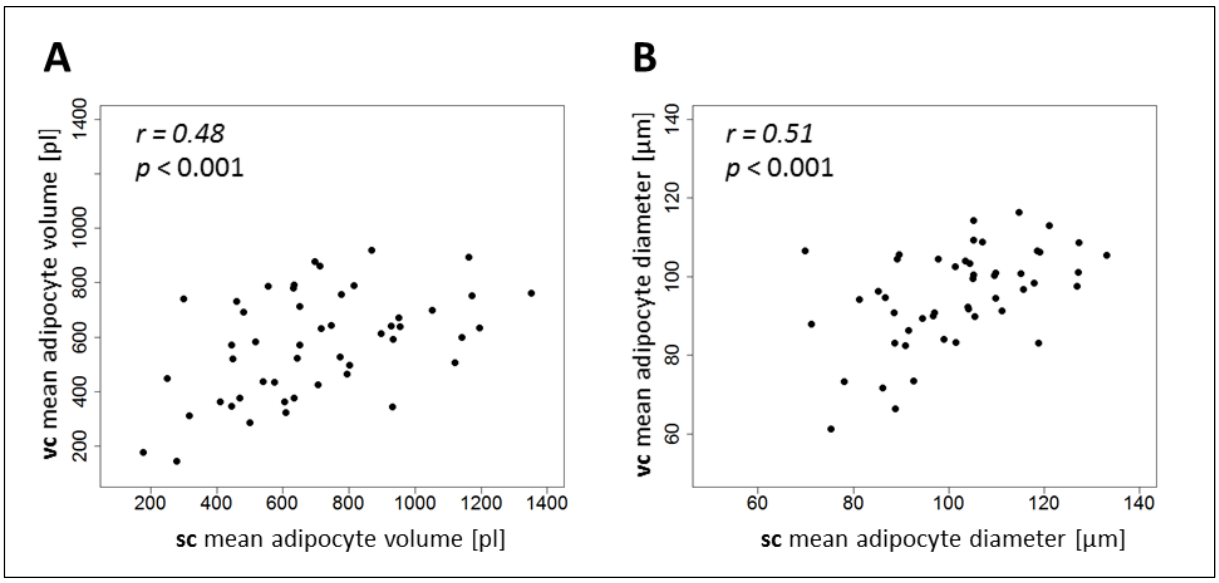

Figure 37: Correlation of visceral and subcutaneous adipocytes volume and diameter

Pearson's product-moment correlation was performed for analyzing the association between subcutaneous and visceral adipocytes volume (A) and diameter (B) within the same subject. Both cell size indicators correlated statistically significant between the two depots (n = 49).

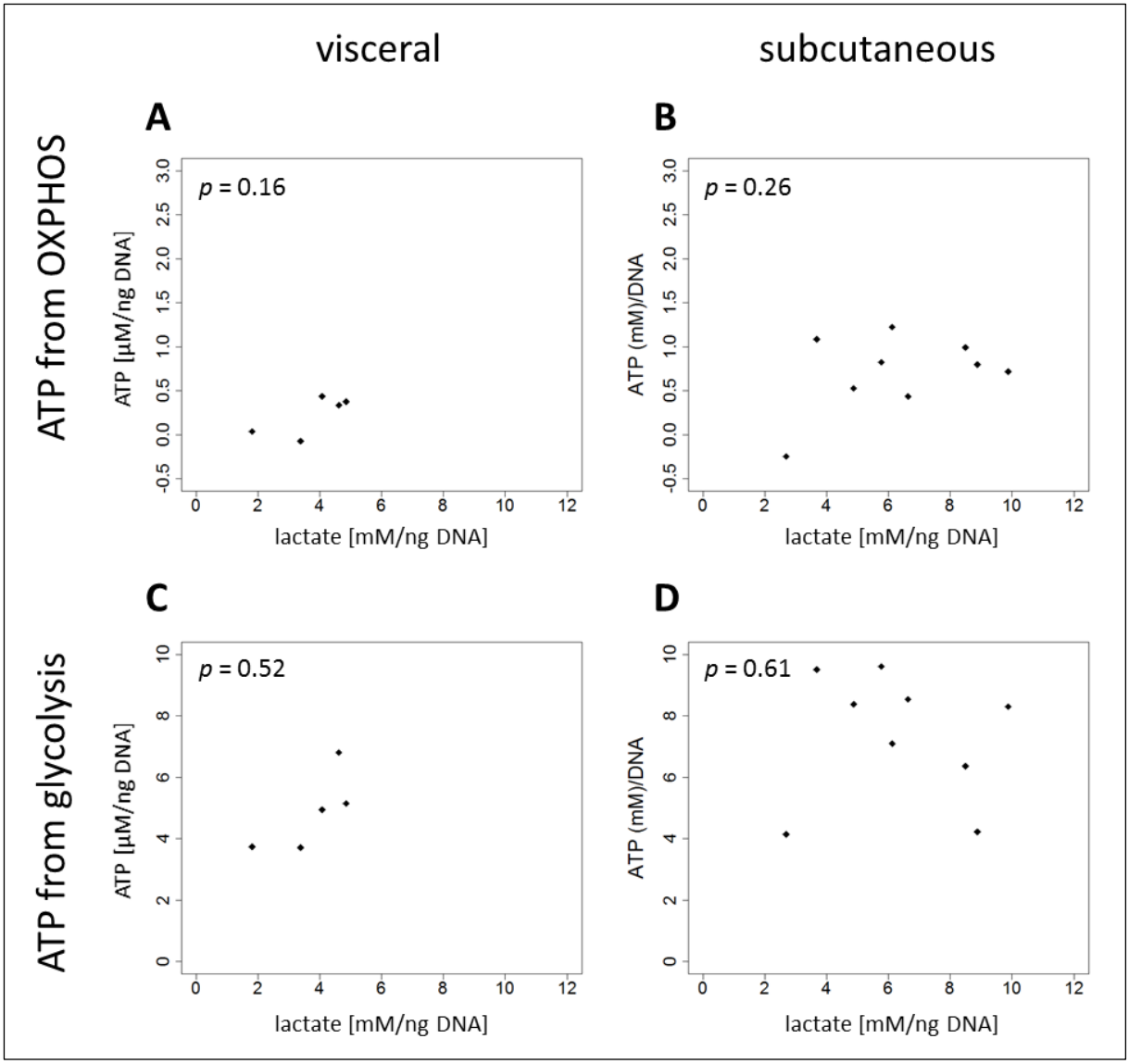

Figure 38: ATP of different origin and lactate release after the inhibition of mitochondrial ATP production

Luminometrically determined ATP levels per DNA from OXPHOS (+ 2-deoxy-D-glc (100 mM) A: n = 5and B: n = 9) and from glycolysis (+ oligomycin (1 µg/ml) C: n = 5 and D: n = 9) were plotted against lactate release after the incubation with oligomycin. *p* values originate from multiple regression analysis and are adjusted for donor's age.

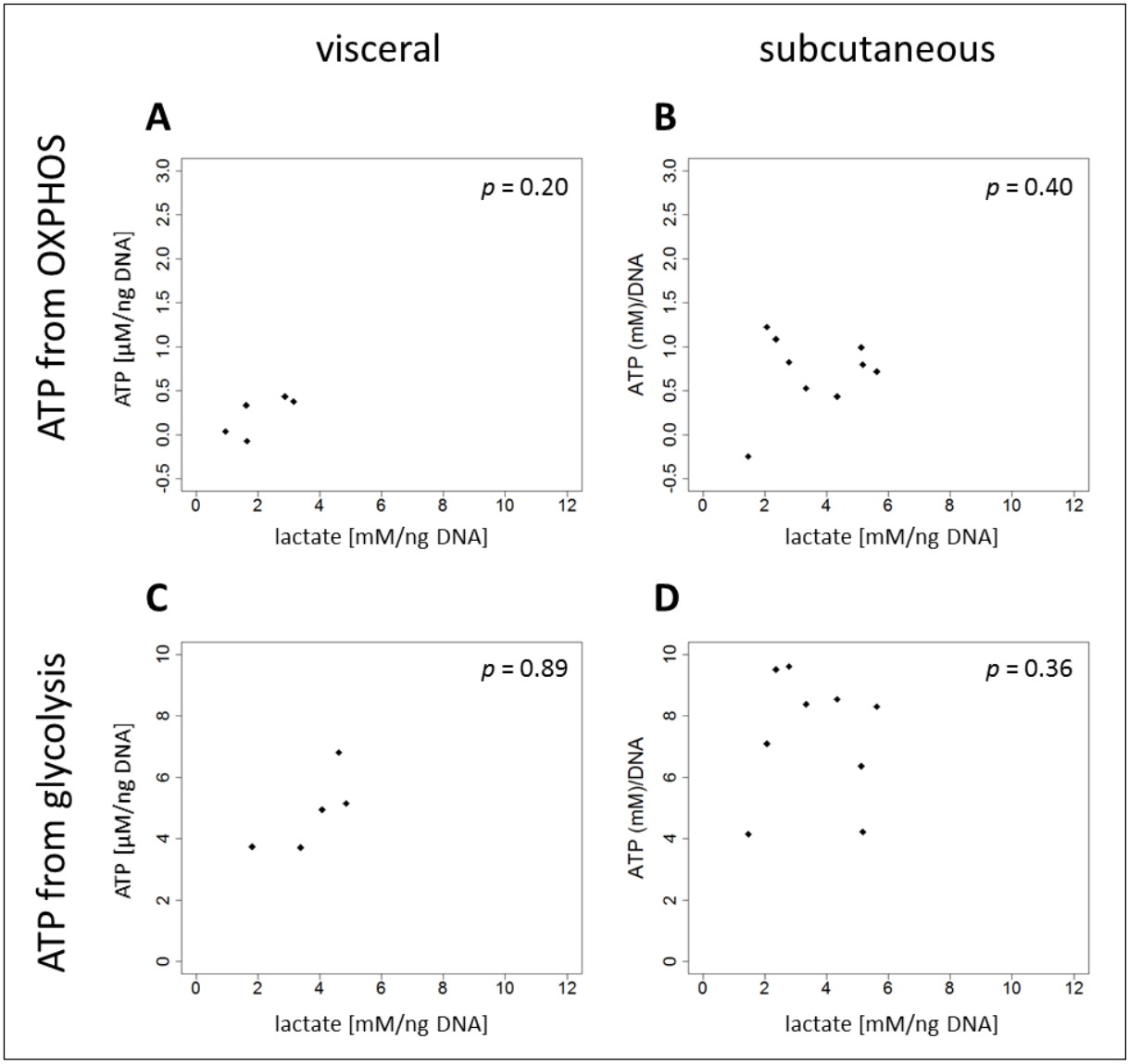

Figure 39: ATP of different origin and capacity of increasing lactate release when mitochondrial ATP production is inhibited

Luminometrically determined ATP levels per DNA from OXPHOS (+ 2-deoxy-D-glc (100 mM) A: n = 5 and B: n = 9) and from glycolysis (+ oligomycin (1 µg/ml) C: n = 5 and D: n = 9) were plotted against delta lactate release after the incubation with oligomycin. p values originate from multiple regression analysis and are adjusted for subject's age.

7.4 Applied R codes

Name of dataset: dat

F Test for equality of variances:

```
var.test(dat$vc.variable,dat$sc.variable)
```

Student's t-test:

```
t.test(dat$vc.variable,dat$sc.variable,
alternative = "two.sided",
paired = T,
var.equal = TRUE)
```

Wilcoxon signed rank test:

```
wilcox.test(dat$vc.variable,dat$sc.variable,
alternative = "two.sided",
paired = T)
```

Pearson's product-moment correlation:

```
cor.test(dat$vc.variable,dat$sc.variable)
```

Mean and standard deviation:

```
mean(dat$vc.variable[!is.na(dat$sc.variable)&is.na(dat$vc.variable)==F])
sd(dat$vc.variable[!is.na(dat$sc.variable)&is.na(dat$vc.variable)==F])
```

Multiple regression analyses:

```
model.name=lm(variable.A~variable.B+age, data=dat)
summary(model.name)
```

Exclusion of subjects with BMI values ≤ 35 kg/m²

```
dat_subpopulation=dat[is.na(dat$BMI)==FALSE&dat$BMI>35,]
```

Division in healthstatus:

```
healthstatus=factor(,levels=c("ND","DiGH"))
healthstatus[dat$ND=="x"]="ND"
healthstatus[dat$DiGH=="x"]="DiGH"
```

Interaction term analysis:

```
model.name=lm(variable~BMI*healthstatus,data=dat)
summary(model.name)
```

Figures:

```
boxplot((dat$vc.variable[!is.na(dat$sc.variable)&is.na(dat$vc.variable)==F]),(dat$sc.variable[!is.na(dat
$vc.variable)&is.na(dat$sc.variable)==F]),
        col ="lightgrey",
        ylim=c(from,to),
        ylab=(“name"),
        border = "black",
        cex.main=2.75,
        cex.axis=1.9,
        cex.lab=2.25,
        cex=1.5,
        names=c("vc","sc"),
        main="Title")


plot(   dat$variable.B,
        dat$ variable.A,
        xlab=("variable.A"),
        ylab=("variable.B"),
        ylim=c(from,to),
        xlim=c((from,to),
        pch=(17),
        col=("black"),
        main="Title",
        font.main=("20"),
        cex.main=2.75,
        cex.axis=1.9,
        cex.lab=2.25,
        cex=1.5,
        box(lwd=1.5, col="black"))
```

8 REFERENCES

Alberts, B.; Bray, D.; Lewis, J.; Raff, M.; Roberts, K.; Watson, J.D. (Eds.) (1994): Molecular biology of the cell. 3rd. New York: Garland Science.

American Diabetes Association (2013): Diagnosis and Classification of Diabetes Mellitus. *Diabetes care* 37 (Supplement 1), 81–90.

Anderson, S.; Bankier, A.T.; Barrell, B.G.; de Bruijn, M.H.; Coulson, A.R.; Drouin, J. et al. (1981): Sequence and organization of the human mitochondrial genome. *Nature* 290 (5806), 457–465.

Archibald, J.M. (2015): Endosymbiosis and Eukaryotic Cell Evolution. *Current Biology* 25 (19), R911–921.

Arita, Y.; Kihara, S.; Ouchi, N.; Takahashi, M.; Maeda, K.; Miyagawa, J. et al. (1999): Paradoxical decrease of an adipose-specific protein, adiponectin, in obesity. *Biochemical and biophysical research communications* 257 (1), 79–83.

Azzone, G.F.; Ernster, L.; Weinbach, E.C. (1963): Succinate-linked acetoacetate reduction. I. Endergonic reduction of acetoacetate by succinate in liver mitochondria. *The Journal of biological chemistry* 238, 1825–1833.

Baranova, A.; Collantes, R.; Gowder, S.J.; Elariny, H.; Schlauch, K.; Younoszai, A. et al. (2005): Obesity-related differential gene expression in the visceral adipose tissue. *Obesity surgery* 15 (6), 758–765.

Basat, O.; Ucak, S.; Ozkurt, H.; Basak, M.; Seber, S.; Altuntas, Y. (2006): Visceral adipose tissue as an indicator of insulin resistance in nonobese patients with new onset type 2 diabetes mellitus. *Experimental and clinical endocrinology & diabetes* 114 (2), 58–62.

Bereiter-Hahn, J.; Vöth, M. (1994): Dynamics of mitochondria in living cells: shape changes, dislocations, fusion, and fission of mitochondria. *Microscopy research and technique* 27 (3), 198–219.

Berg, A.H.; Combs, T.P.; Du, X.; Brownlee, M.; Scherer, P.E. (2001): The adipocyte-secreted protein Acrp30 enhances hepatic insulin action. *Nature medicine* 7 (8), 947–953.

Björntorp, P.; Sjöström, L. (1971): Number and size of adipose tissue fat cells in relation to metabolism in human obesity. *Metabolism* 20 (7), 703–713.

Blaak, E.E.; van Baak, M.A.; Kemerink, G.J.; Pakbiers, M.T.; Heidendal, G.A.; Saris, W.H. (1995): Beta-adrenergic stimulation and abdominal subcutaneous fat blood flow in lean, obese, and reduced-obese subjects. *Metabolism* 44 (2), 183–187.

Blüher, M.; Wilson-Fritch, L.; Leszyk, J.; Laustsen, P.G.; Corvera, S.; Kahn, C.R. (2004): Role of insulin action and cell size on protein expression patterns in adipocytes. *The Journal of biological chemistry* 279 (30), 31902–31909.

Boden, G.; Chen, X. (1995): Effects of fat on glucose uptake and utilization in patients with non-insulin-dependent diabetes. *The Journal of clinical investigation* 96 (3), 1261–1268.

Bogacka, I.; Xie, H.; Bray, G.A.; Smith, S.R. (2005): Pioglitazone induces mitochondrial biogenesis in human subcutaneous adipose tissue in vivo. *Diabetes* 54 (5), 1392–1399.

Boon, M.R.; Zammit, V.A. (1988): Use of a selectively permeabilized isolated rat hepatocyte preparation to study changes in the properties of overt carnitine palmitoyltransferase activity in situ. *The Biochemical journal* 249 (3), 645–652.

Brahimi-Horn, M.C.; Pouysségur, J. (2007): Oxygen, a source of life and stress. *FEBS Letters* 581 (19), 3582–3591.

Brand, M.D.; Nicholls, D.G. (2011): Assessing mitochondrial dysfunction in cells. *Biochemical Journal* 435 (2), 297–312.

Bruun, J.M.; Lihn, A.S.; Pedersen, S.B.; Richelsen, B. (2005): Monocyte chemoattractant protein-1 release is higher in visceral than subcutaneous human adipose tissue (AT): implication of macrophages resident in the AT. *The Journal of Clinical Endocrinology & Metabolism* 90 (4), 2282–2289.

Cancello, R.; Tordjman, J.; Poitou, C.; Guilhem, G.; Bouillot, J.L.; Hugol, D. et al. (2006): Increased infiltration of macrophages in omental adipose tissue is associated with marked hepatic lesions in morbid human obesity. *Diabetes* 55 (6), 1554–1561.

Capaldi, R.A. (1990): Structure and function of cytochrome c oxidase. *Annual review of biochemistry* 59, 569–596.

Carswell, K.A.; Lee, M.J.; Fried, S.K. (2012): Culture of isolated human adipocytes and isolated adipose tissue. *Methods in molecular biology* 806, 203–214.

Cedikova, M.; Kripnerová, M.; Dvorakova, J.; Pitule, P.; Grundmanova, M.; Babuska, V. et al. (2016): Mitochondria in White, Brown, and Beige Adipocytes. *Stem Cells International* 2016 (4, part 1), 6067349.

Chan, D.C. (2006): Mitochondrial Fusion and Fission in Mammals. *Annual Review of Cell and Developmental Biology* 22 (1), 79–99.

Chance, B.; Williams, G.R. (1955): Respiratory enzymes in oxidative phosphorylation. III. The steady state. *The Journal of biological chemistry* 217 (1), 409–427.

Chattopadhyay, M.; GuhaThakurta, I.; Behera, P.; Ranjan, K.R.; Khanna, M.; Mukhopadhyay, S.; Chakrabarti, S. (2011): Mitochondrial bioenergetics is not impaired in nonobese subjects with type 2 diabetes mellitus. *Metabolism* 60 (12), 1702–1710.

Chevillotte, E.; Giralt, M.; Miroux, B.; Ricquier, D.; Villarroya, F. (2007): Uncoupling protein-2 controls adiponectin gene expression in adipose tissue through the modulation of reactive oxygen species production. *Diabetes* 56 (4), 1042–1050.

Chistiakov, D.A.; Sobenin, I.A.; Revin, V.V.; Orekhov, A.N.; Bobryshev, Y.V. (2014): Mitochondrial aging and age-related dysfunction of mitochondria. *BioMed Research International* 2014 (4), 238463.

Choi, K.; Kim, Y.B. (2010): Molecular mechanism of insulin resistance in obesity and type 2 diabetes. *The Korean journal of internal medicine* 25 (2), 119–129.

Christe, M.; Hirzel, E.; Lindinger, A.; Kern, B.; Flüe, M. von; Peterli, R. et al. (2013): Obesity affects mitochondrial citrate synthase in human omental adipose tissue. *ISRN Obesity* 2013 (3, part 2), 826027.

Cinti, S. (2005): The adipose organ. *Prostaglandins, Leukotrienes and Essential Fatty Acids* 73 (1), 9–15.

Cnop, M.; Havel, P.J.; Utzschneider, K.M.; Carr, D.B.; Sinha, M.K.; Boyko, E.J. et al. (2003): Relationship of adiponectin to body fat distribution, insulin sensitivity and plasma lipoproteins: evidence for independent roles of age and sex. *Diabetologia* 46 (4), 459–469.

Cotillard, A.; Poitou, C.; Torcivia, A.; Bouillot, J.L.; Dietrich, A.; Klöting, N. et al. (2014): Adipocyte size threshold matters: link with risk of type 2 diabetes and improved insulin resistance after gastric bypass. *The Journal of Clinical Endocrinology & Metabolism* 99 (8), E1466-70.

Cryer, A.; Van, R.L.R. (1985): New perspectives in adipose tissue. Structure, function, and development. London, Boston: Butterworths.

Dahlman, I.; Forsgren, M.; Sjögren, A.; Nordström, E.A; Kaaman, M.; Näslund, E. et al. (2006): Downregulation of electron transport chain genes in visceral adipose tissue in type 2 diabetes independent of obesity and possibly involving tumor necrosis factor-alpha. *Diabetes* 55 (6), 1792–1799.

Deepa, S.S.; Pulliam, D.; Hill, S.; Shi, Y.; Walsh, M.E.; Salmon, A. et al. (2013): Improved insulin sensitivity associated with reduced mitochondrial complex IV assembly and activity. *The FASEB Journal* 27 (4), 1371–1380.

D'Erchia, A.M.; Atlante, A.; Gadaleta, G.; Pavesi, G.; Chiara, M.; Virgilio, C. de et al. (2015): Tissue-specific mtDNA abundance from exome data and its correlation with mitochondrial transcription, mass and respiratory activity. *Mitochondrion* 20, 13–21.

DiGirolamo, M.; Newby, F. D.; Hill J.O. (1989): Blood lactate levels in human obesity. *International journal of obesity* (13), 394.

DiGirolamo, M.; Newby, F. D.; Lovejoy, J. (1992): Lactate production in adipose tissue: a regulated function with extra-adipose implications. *The FASEB Journal* 6 (7), 2405–2412.

Dillard, T.H.; Purnell, J.Q.; Smith, M.D.; Raum, W.; Hong, D.; Laut, J.; Patterson, E.J. (2013): Omentectomy added to Roux-en-Y gastric bypass surgery: a randomized, controlled trial. *Surgery for obesity and related diseases* 9 (2), 269–275.

Divakaruni, A.S.; Brand, M.D. (2011): The regulation and physiology of mitochondrial proton leak. *Physiology* 26 (3), 192–205.

Dresner, A.; Laurent, D.; Marcucci, M.; Griffin, M.E.; Dufour, S.; Cline, G.W. et al. (1999): Effects of free fatty acids on glucose transport and IRS-1-associated phosphatidylinositol 3-kinase activity. *The Journal of clinical investigation* 103 (2), 253–259.

Dubois, S.G.; Heilbronn, L.K.; Smith, S.R.; Albu, J.B.; Kelley, D.E.; Ravussin, E. (2006): Decreased expression of adipogenic genes in obese subjects with type 2 diabetes. *Obesity* 14 (9), 1543–1552.

Dupont, G. (2014): Modeling the intracellular organization of calcium signaling. Wiley interdisciplinary reviews. *Systems biology and medicine* 6 (3), 227–237.

Dusserre, E.; Moulin, P.; Vidal, H. (2000): Differences in mRNA expression of the proteins secreted by the adipocytes in human subcutaneous and visceral adipose tissues. *Biochimica et biophysica acta* 1500 (1), 88–96.

Elmore, S. (2007): Apoptosis: a review of programmed cell death. *Toxicologic pathology* 35 (4), 495–516.

Fried, S.K.; Bunkin, D.A.; Greenberg, A.S. (1998): Omental and subcutaneous adipose tissues of obese subjects release interleukin-6: depot difference and regulation by glucocorticoid. *The Journal of Clinical Endocrinology & Metabolism* 83 (3), 847–850.

Fried, S.K.; Lee, M.J.; Karastergiou, K. (2015): Shaping fat distribution: New insights into the molecular determinants of depot- and sex-dependent adipose biology. *Obesity* 23 (7), 1345–1352.

Gahan, M.E.; Miller, F.; Lewin, S.R.; Cherry, C.L.; Hoy, J.F.; Mijch, A. et al. (2001): Quantification of mitochondrial DNA in peripheral blood mononuclear cells and subcutaneous fat using real-time polymerase chain reaction. *Journal of clinical virology* 22 (3), 241–247.

Gaidhu, M.P. Pinky; Ceddia, R.B. Bacis (2011): The role of adenosine monophosphate kinase in remodeling white adipose tissue metabolism. *Exercise and sport sciences reviews* 39 (2), 102–108.

Gealekman, O.; Burkart, A.; Chouinard, M.; Nicoloro, S.M.; Straubhaar, J.; Corvera, S. (2008): Enhanced angiogenesis in obesity and in response to PPARgamma activators through adipocyte VEGF and ANGPTL4 production. *American journal of physiology. Endocrinology & Metabolism* 295 (5), E1056-64.

Gealekman, O.; Guseva, N.; Hartigan, C.; Apotheker, S.; Gorgoglione, M.; Gurav, K. et al. (2011): Depot-specific differences and insufficient subcutaneous adipose tissue angiogenesis in human obesity. *Circulation* 123 (2), 186–194.

Genome Bioinformatics Group (2017): UCSC Genome Browser. Version. Available online at http://genome.ucsc.edu/.

Gesta, S.; Blüher, M.; Yamamoto, Y.; Norris, A.W.; Berndt, J.; Kralisch, S. et al. (2006): Evidence for a role of developmental genes in the origin of obesity and body fat distribution. *Proceedings of the National Academy of Sciences of the United States of America* 103 (17), 6676–6681.

Giaccia, A.J.; Simon, M.C.; Johnson, R. (2004): The biology of hypoxia: the role of oxygen sensing in development, normal function, and disease. *Genes & development* 18 (18), 2183–2194.

Gnaiger, E. (2008): Polarographic Oxygen Sensors, the Oxygraph, and High-Resolution Respirometry to Assess Mitochondrial Function. Published in: James A. Dykens und Yvonne Will (Eds.): Drug-Induced Mitochondrial Dysfunction. Hoboken, USA: John Wiley & Sons, Inc, 325–352, zuletzt geprüft am 2/11/2016.

Gnaiger, E. (2009): Capacity of oxidative phosphorylation in human skeletal muscle. *The International Journal of Biochemistry & Cell Biology* 41 (10), 1837–1845.

Gnaiger, E. (2014): Mitochondrial Pathways and Respiratory Control. An Introduction to OXPHOS Analysis. Available online at http://wiki.oroboros.at/images/f/fc/Gnaiger_2014_Mitochondr_Physiol_Network_MitoPathways.pdf.

Gnaiger, E.; Forstner, H. (1983): Polarographic Oxygen Sensors. Aquatic and Physiological Applications. Berlin, Heidelberg, New York: Springer Verlag.

Gnaiger, E.; Kuznetsov, A.V.; Schneeberger, S.; Seiler, R.; Brandacher, G.; Steurer, W.; Margreiter, R.: Mitochondria in the Cold. Published in: Heldmaier, Klingenspor (Ed.) 2000 – Life in the Cold, 431–442.

Goldrick, R.B.; McLoughlin, G.M. (1970): Lipolysis and lipogenesis from glucose in human fat cells of different sizes. Effects of insulin, epinephrine, and theophylline. *The Journal of clinical investigation* 49 (6), 1213–1223.

González-Barroso, M.M.; Anedda, A.; Gallardo-Vara, E.; Redondo-Horcajo, M.; Rodríguez-Sánchez, L.; Rial, E. (2012): Fatty acids revert the inhibition of respiration caused by the antidiabetic drug metformin to facilitate their mitochondrial β-oxidation. *Biochimica et biophysica acta* 1817 (10), 1768–1775.

Goodpaster, B.H.; Thaete, F.L.; Simoneau, J.A.; Kelley, D.E. (1997): Subcutaneous abdominal fat and thigh muscle composition predict insulin sensitivity independently of visceral fat. *Diabetes* 46 (10), 1579–1585.

Goossens, G.H.; Bizzarri, A.; Venteclef, N.; Essers, Y.; Cleutjens, J.P.; Konings, E. et al. (2011): Increased adipose tissue oxygen tension in obese compared with lean men is accompanied by insulin resistance, impaired adipose tissue capillarization, and inflammation. *Circulation* 124 (1), 67–76.

Griffin, M.E.; Marcucci, M.J.; Cline, G.W.; Bell, K.; Barucci, N.; Lee, D. et al. (1999): Free fatty acid-induced insulin resistance is associated with activation of protein kinase C theta and alterations in the insulin signaling cascade. *Diabetes* 48 (6), 1270–1274.

Hajduch, E.; Heyes, R.R.; Watt, P.W.; Hundal, H.S. (2000): Lactate transport in rat adipocytes: identification of monocarboxylate transporter 1 (MCT1) and its modulation during streptozotocin-induced diabetes. *FEBS Letters* 479 (3), 89–92.

Halberg, N.; Khan, T.; Trujillo, M.E.; Wernstedt-Asterholm, I.; Attie, A.D.; Sherwani, S. et al. (2009): Hypoxia-inducible factor 1alpha induces fibrosis and insulin resistance in white adipose tissue. *Molecular and cellular biology* 29 (16), 4467–4483.

Hallgren, P.; Sjöström, L.; Hedlund, H.; Lundell, L.; Olbe, L. (1989): Influence of age, fat cell weight, and obesity on O2 consumption of human adipose tissue. *The American journal of physiology* 256 (4 Pt 1), E467-74.

Hansen, M.; Lund, M.T.; Gregers, E.; Kraunsøe, R.; van Hall, G.; Helge, J.W.; Dela, F. (2015): Adipose tissue mitochondrial respiration and lipolysis before and after a weight loss by diet and RYGB. *Obesity* 23 (10), 2022–2029.

Harford, K.A.; Reynolds, C.M.; McGillicuddy, F.C.; Roche, H.M. (2011): Fats, inflammation and insulin resistance: insights to the role of macrophage and T-cell accumulation in adipose tissue. *The Proceedings of the Nutrition Society* 70 (4), 408–417.

Harman-Boehm, I.; Blüher, M.; Redel, H.; Sion-Vardy, N.; Ovadia, S.; Avinoach, E. et al. (2007): Macrophage infiltration into omental versus subcutaneous fat across different populations: effect of regional adiposity and the comorbidities of obesity. *The Journal of Clinical Endocrinology & Metabolism* 92 (6), 2240–2247.

Hauner, H. (2005): Secretory factors from human adipose tissue and their functional role. *The Proceedings of the Nutrition Society* 64 (2), 163–169.

Hayashi, J.; Takemitsu, M.; Goto, Y.; Nonaka, I. (1994): Human mitochondria and mitochondrial genome function as a single dynamic cellular unit. *The Journal of cell biology* 125 (1), 43–50.

Heinonen, S.; Buzkova, J.; Muniandy, M.; Kaksonen, R.; Ollikainen, M.; Ismail, K. et al. (2015): Impaired Mitochondrial Biogenesis in Adipose Tissue in Acquired Obesity. *Diabetes* 64 (9), 3135–3145.

Heinonen, S.; Muniandy, M.; Buzkova, J.; Mardinoglu, A.; Rodríguez, A.; Frühbeck, G. et al. (2016): Mitochondria-related transcriptional signature is downregulated in adipocytes in obesity: a study of young healthy MZ twins. *Diabetologia* 60 (1), 169–181.

Hinkle, P. C.; Butow, R.A.; Racker, E.; Chance, B. (1967): Partial resolution of the enzymes catalyzing oxidative phosphorylation. XV. Reverse electron transfer in the flavin-cytochrome beta region of the respiratory chain of beef heart submitochondrial particles. *The Journal of biological chemistry* 242 (22), 5169–5173.

Hirsch, J.; Batchelor, B. (1976): Adipose tissue cellularity in human obesity. *Clinics in endocrinology and metabolism* 5 (2), 299–311.

Hodson, L.; Humphreys, S.M.; Karpe, F.; Frayn, K.N. (2013): Metabolic signatures of human adipose tissue hypoxia in obesity. *Diabetes* 62 (5), 1417–1425.

Hoffstedt, J.; Arner, E.; Wahrenberg, H.; Andersson, D. P.; Qvisth, V.; Löfgren, P. et al. (2010): Regional impact of adipose tissue morphology on the metabolic profile in morbid obesity. *Diabetologia* 53 (12), 2496–2503.

Hosogai, N.; Fukuhara, A.; Oshima, K.; Miyata, Y.; Tanaka, S.; Segawa, K. et al. (2007): Adipose tissue hypoxia in obesity and its impact on adipocytokine dysregulation. *Diabetes* 56 (4), 901–911.

Hotta, K.; Funahashi, T.; Arita, Y.; Takahashi, M.; Matsuda, M.; Okamoto, Y. et al. (2000): Plasma concentrations of a novel, adipose-specific protein, adiponectin, in type 2 diabetic patients. *Arteriosclerosis, thrombosis, and vascular biology* 20 (6), 1595–1599.

Houten, S.M.; Wanders, R.J.A. (2010): A general introduction to the biochemistry of mitochondrial fatty acid β-oxidation. *Journal of Inherited Metabolic Disease* 33 (5), 469–477.

Hube, F.; Lietz, U.; Igel, M.; Jensen, P.B.; Tornqvist, H.; Joost, H.G.; Hauner, H. (1996): Difference in leptin mRNA levels between omental and subcutaneous abdominal adipose tissue from obese humans. *Hormone and metabolic research* 28 (12), 690–693.

Jansson, P.A.; Larsson, A.; Smith, U.; Lönnroth, P. (1994): Lactate release from the subcutaneous tissue in lean and obese men. *The Journal of clinical investigation* 93 (1), 240–246.

Kaaman, M.; Sparks, L.M.; van Harmelen, V.; Smith, S.R.; Sjölin, E.; Dahlman, I.; Arner, P. (2007): Strong association between mitochondrial DNA copy number and lipogenesis in human white adipose tissue. *Diabetologia* 50 (12), 2526–2533.

Kajimoto, K.; Terada, H.; Baba, Y.; Shinohara, Y. (2005): Essential role of citrate export from mitochondria at early differentiation stage of 3T3-L1 cells for their effective differentiation into fat cells, as revealed by studies using specific inhibitors of mitochondrial di- and tricarboxylate carriers. *Molecular Genetics and Metabolism* 85 (1), 46–53.

Kanehisa, M.; Sato, Y.; Kawashima, M.; Furumichi, M.; Tanabe, M. (2016): KEGG as a reference resource for gene and protein annotation. *Nucleic acids research* 44 (D1), D457-62.

Kern, P.A.; Di Gregorio, G.B.; Lu, T.; Rassouli, N.; Ranganathan, G. (2003): Adiponectin expression from human adipose tissue: relation to obesity, insulin resistance, and tumor necrosis factor-alpha expression. *Diabetes* 52 (7), 1779–1785.

Keuper, M.; Jastroch, M.; Yi, C.X.; Fischer-Posovszky, P.; Wabitsch, M.; Tschöp, M.H.; Hofmann, S.M. (2014): Spare mitochondrial respiratory capacity permits human adipocytes to maintain ATP homeostasis under hypoglycemic conditions. *The FASEB Journal* 28 (2), 761–770.

Khosla, T.; Lowe, C.R. (1967): Indices of obesity derived from body weight and height. *British journal of preventive & social medicine* 21 (3), 122–128.

King, J. L.; DiGirolamo, M. (1998): Lactate production from glucose and response to insulin in perifused adipocytes from mesenteric and epididymal regions of lean and obese rats. *Obesity research* 6 (1), 69–75.

Klein, S.; Fontana, L.; Young, V.L.; Coggan, A.R.; Kilo, C.; Patterson, B.W.; Mohammed, B.S. (2004): Absence of an effect of liposuction on insulin action and risk factors for coronary heart disease. *The New England journal of medicine* 350 (25), 2549–2557.

Klöting, N.; Fasshauer, M.; Dietrich, A.; Kovacs, P.; Schön, M.R.; Kern, M. et al. (2010): Insulin-sensitive obesity. American journal of physiology. *Endocrinology & Metabolism* 299 (3), E506-15.

Koh, E.H.; Park, J.Y.; Park, H.S.; Jeon, M.J.; Ryu, J.W.; Kim, M. (2007): Essential Role of Mitochondrial Function in Adiponectin Synthesis in Adipocytes. *Diabetes* 2007 (56), 2973–2981.

Komai, A.M.; Brännmark, C.; Musovic, S.; Olofsson, C.S. (2014): PKA-independent cAMP stimulation of white adipocyte exocytosis and adipokine secretion: modulations by Ca2+ and ATP. *The Journal of physiology* 592 (23), 5169–5186.

Kraunsøe, R.; Boushel, R.; Hansen, C.N.; Schjerling, P.; Qvortrup, K.; Støckel, M. et al. (2010): Mitochondrial respiration in subcutaneous and visceral adipose tissue from patients with morbid obesity. *The Journal of physiology* 588 (Pt 12), 2023–2032.

Larsen, C.M.; Faulenbach, M.; Vaag, A.; Vølund, A.; Ehses, J.A.; Seifert, B. et al. (2007): Interleukin-1-receptor antagonist in type 2 diabetes mellitus. *The New England journal of medicine* 356 (15), 1517–1526.

Larsen, S.; Nielsen, J.; Hansen, C.N.; Nielsen, L.B.; Wibrand, F.; Stride, N. et al. (2012): Biomarkers of mitochondrial content in skeletal muscle of healthy young human subjects. *The Journal of physiology* 590 (14), 3349–3360.

Lecoultre, V,; Peterson, C.M.; Covington, J.D.; Ebenezer, P.J.; Frost, E.A.; Schwarz, J.M.; Ravussin, E. (2013): Ten nights of moderate hypoxia improves insulin sensitivity in obese humans. *Diabetes care* 36 (12), e197-8.

Lee, K.Y.; Gesta, S.; Boucher, J.; Wang, X.L.; Kahn, C.R. (2011): The differential role of Hif1β/Arnt and the hypoxic response in adipose function, fibrosis, and inflammation. *Cell metabolism* 14 (4), 491–503.

Lee, W. J.; Chong, K.; Aung, L.; Chen, S.C.; Ser, K.H.; Lee, Y.C. (2017): Metabolic Surgery for Diabetes Treatment: Sleeve Gastrectomy or Gastric Bypass? *World journal of surgery* 41 (1), 216–223.

Li, M.X.; Dewson, G. (2015): Mitochondria and apoptosis: emerging concepts. *F1000prime reports* 7, 42.

Lindinger, A.; Peterli, R.; Peters, T.; Kern, B.; von Flüe, M.; Calame, M. et al. (2010): Mitochondrial DNA Content in Human Omental Adipose Tissue. *Obesity surgery* 20 (1), 84–92.

Lindinger, P.W.; Christe, M.; Eberle, A.N.; Kern, B.; Peterli, R.; Peters, T. et al. (2015): Important mitochondrial proteins in human omental adipose tissue show reduced expression in obesity. *Journal of Proteomics* 124, 79–87.

Lionetti, L.; Mollica, M.P.; Lombardi, A.; Cavaliere, G.; Gifuni, G.; Barletta, A. (2009): From chronic overnutrition to insulin resistance: the role of fat-storing capacity and inflammation. *Nutrition, metabolism, and cardiovascular* diseases 19 (2), 146–152.

Lolmède, K.; Durand de Saint Front, V; Galitzky, J.; Lafontan, M.; Bouloumié, A. (2003): Effects of hypoxia on the expression of proangiogenic factors in differentiated 3T3-F442A adipocytes. *International journal of obesity* 27 (10), 1187–1195.

Lovejoy, J.; Mellen, B.; DiGirolamo, M. (1990): Lactate generation following glucose ingestion: relation to obesity, carbohydrate tolerance and insulin sensitivity. *International journal of obesity* 14 (10), 843–855.

Lovejoy, J.; Newby, F.D.; Gebhart, S.S.; DiGirolamo, M. (1992): Insulin resistance in obesity is associated with elevated basal lactate levels and diminished lactate appearance following intravenous glucose and insulin. *Metabolism* 41 (1), 22–27.

Lu, R.H.; Ji, H.; Chang, Z.G.; Su, S.S.; Yang, G.S. (2010): Mitochondrial development and the influence of its dysfunction during rat adipocyte differentiation. *Molecular biology reports* 37 (5), 2173–2182.

Malik, A.N.; Czajka, A. (2013): Is mitochondrial DNA content a potential biomarker of mitochondrial dysfunction? *Mitochondrion* 13 (5), 481–492.

Max Rubner-Institut (2008): Nationale Verzehrsstudie II. Ergebnisbericht, Teil 1. Bundesforschungsinstitut für Ernährung und Lebensmittel. Available online at http://www.bmel.de/SharedDocs/Downloads/Ernaehrung/NVS_Ergebnisbericht.pdf?__blob=publicationFile.

McBride, H.M.; Neuspiel, M.; Wasiak, S. (2006): Mitochondria: More Than Just a Powerhouse. *Current Biology* 16 (14), R551–R560.

Motoshima, H.; Wu, X.; Sinha, M.K.; Hardy, V.E.; Rosato, E.L.; Barbot, D.L. et al. (2002): Differential Regulation of Adiponectin Secretion from Cultured Human Omental and Subcutaneous Adipocytes: Effects of Insulin and Rosiglitazone. *The Journal of Clinical Endocrinology & Metabolism* 87 (12), 5662–5667.

Mustelin, L.; Pietiläinen, K.H.; Rissanen, A.; Sovijärvi, A.R.; Piirilä, P.; Naukkarinen, J. et al. (2008): Acquired obesity and poor physical fitness impair expression of genes of mitochondrial oxidative phosphorylation in monozygotic twins discordant for obesity. *American journal of physiology. Endocrinology & Metabolism* 295 (1), E148-54.

Nath, S. (2008): The new unified theory of ATP synthesis/hydrolysis and muscle contraction, its manifold fundamental consequences and mechanistic implications and its applications in health and disease. *International journal of molecular sciences* 9 (9), 1784–1840.

Newby, F.D.; Sykes, M.N.; DiGirolamo, M. (1988): Regional differences in adipocyte lactate production from glucose. *The American journal of physiology* 255 (5 Pt 1), E716-22.

Newby, F.D.; Wilson, L.K.; Thacker, S.V.; DiGirolamo, M. (1990): Adipocyte lactate production remains elevated during refeeding after fasting. *The American journal of physiology* 259 (6 Pt 1), E865-71.

Nie, Y.; Wong, C. (2009): Suppressing the activity of ERRα in 3T3-L1 adipocytes reduces mitochondrial biogenesis but enhances glycolysis and basal glucose uptake. *Journal of Cellular and Molecular Medicine* 13 (9b), 3051–3060.

Ouchi, N.; Walsh, K. (2007): Adiponectin as an anti-inflammatory factor. *Clinica chimica acta* 380 (1-2), 24–30.

Paolisso, G.; Tataranni, P.A.; Foley, J.E.; Bogardus, C.; Howard, B.V.; Ravussin, E. (1995): A high concentration of fasting plasma non-esterified fatty acids is a risk factor for the development of NIDDM. *Diabetologia* 38 (10), 1213–1217.

Papa, S.; Martino, P.L.; Capitanio, G.; Gaballo, A.; Rasmo, D. de; Signorile, A.; Petruzzella, V. (2012): The oxidative phosphorylation system in mammalian mitochondria. Published in: Roberto Scatena, Patrizia Bottoni und B. Giardina (Eds.): Advances in mitochondrial medicine, Bd. 942. Dordrecht, New York: Springer, 3–37.

Park, A.; Kim, W.K.; Bae, K.H. (2014): Distinction of white, beige and brown adipocytes derived from mesenchymal stem cells. *World journal of stem cells* 6 (1), 33–42.

Pasarica, M.; Sereda, O.R.; Redman, L.M.; Albarado, D.C.; Hymel, D.T.; Roan, L.E. et al. (2009): Reduced adipose tissue oxygenation in human obesity: evidence for rarefaction, macrophage chemotaxis, and inflammation without an angiogenic response. *Diabetes* 58 (3), 718–725.

Pauw, A. de; Tejerina, S.; Raes, M.; Keijer, J.; Arnould, T. (2009): Mitochondrial (dys)function in adipocyte (de)differentiation and systemic metabolic alterations. *The American journal of pathology* 175 (3), 927–939.

Peirce, V.; Carobbio, S.; Vidal-Puig, A. (2014): The different shades of fat. *Nature* 510 (7503), 76–83.

Pérez de Heredia, F.; Wood, I.S.; Trayhurn, P. (2010): Hypoxia stimulates lactate release and modulates monocarboxylate transporter (MCT1, MCT2, and MCT4) expression in human adipocytes. *European Journal of Physiology* 459 (3), 509–518.

Poissonnet, C.M.; Burdi, A.R.; Bookstein, F.L. (1983): Growth and development of human adipose tissue during early gestation. *Early human development* 8 (1), 1–11.

Prentki, M.; Nolan, C.J. (2006): Islet beta cell failure in type 2 diabetes. *The Journal of clinical investigation* 116 (7), 1802–1812.

Priyanka, A.; Anusree, S.S.; Nisha, V.M.; Raghu, K.G. (2014): Curcumin improves hypoxia induced dysfunctions in 3T3-L1 adipocytes by protecting mitochondria and down regulating inflammation. *BioFactors* 40 (5), 513–523.

Rank Brothers Ltd (2002): The Rank Brothers Oxygen Electrode. Operating Manual.

Rausch, M.E.; Weisberg, S.; Vardhana, P.; Tortoriello, D.V. (2008): Obesity in C57BL/6J mice is characterized by adipose tissue hypoxia and cytotoxic T-cell infiltration. *International journal of obesity* 32 (3), 451–463.

Regazzetti, C.; Peraldi, P.; Grémeaux, T.; Najem-Lendom, R.; Ben-Sahra, I.; Cormont, M. et al. (2009): Hypoxia decreases insulin signaling pathways in adipocytes. *Diabetes* 58 (1), 95–103.

Robin, E. D.; Wong, R. (1988): Mitochondrial DNA molecules and virtual number of mitochondria per cell in mammalian cells. *Journal of cellular physiology* 136 (3), 507–513.

Roden, M.; Price, T. B.; Perseghin, G.; Petersen, K. F.; Rothman, D. L.; Cline, G. W.; Shulman, G. I. (1996): Mechanism of free fatty acid-induced insulin resistance in humans. *The Journal of clinical investigation* 97 (12), 2859–2865.

Rolfe, D.F.; Brand, M.D. (1997): The physiological significance of mitochondrial proton leak in animal cells and tissues. *Bioscience reports* 17 (1), 9–16.

Saisho, Y. (2016): Postprandial C-Peptide to Glucose Ratio as a Marker of β Cell Function: Implication for the Management of Type 2 Diabetes. *International journal of molecular sciences* 17 (5), 744.

Saraste, M. (1999): Oxidative phosphorylation at the fin de siècle. *Science* 283 (5407), 1488–1493.

Scheffler, I.E. (2001): A century of mitochondrial research: achievements and perspectives. *Mitochondrion* 1 (1), 3–31.

Scheffler, I.E. (2008): Mitochondria. 2nd ed. Hoboken, N.J: Wiley-Liss.

Schuster, D.P. (2009): Changes in physiology with increasing fat mass. *Seminars in pediatric surgery* 18 (3), 126–135.

Semenza, G.L. (2011): Oxygen sensing, homeostasis, and disease. *The New England journal of medicine* 365 (6), 537–547.

Skurk, T.; Alberti-Huber, C.; Herder, C.; Hauner, H. (2007a): Relationship between Adipocyte Size and Adipokine Expression and Secretion. *The Journal of Clinical Endocrinology & Metabolism* 92 (3), 1023–1033.

Skurk, T.; Ecklebe, S.; Hauner, H. (2007b): A novel technique to propagate primary human preadipocytes without loss of differentiation capacity. *Obesity* 15 (12), 2925–2931.

Smolen, J.E.; Stoehr, S.J.; Boxer, L.A. (1986): Human neutrophils permeabilized with digitonin respond with lysosomal enzyme release when exposed to micromolar levels of free calcium. *Biochimica et biophysica acta* 886 (1), 1–17.

Song, J.; Ke, S.F.; Zhou, C.C.; Zhang, S.L.; Guan, Y.F.; Xu, T.Y. et al. (2014): Nicotinamide phosphoribosyltransferase is required for the calorie restriction-mediated improvements in oxidative stress, mitochondrial biogenesis, and metabolic adaptation. *The Journals of Gerontology: Biological Sciences* 69 (1), 44–57.

Soro-Arnaiz, I.; Li, Q.O.Y.; Torres-Capelli, M.; Meléndez-Rodríguez, F.; Veiga, S.; Veys, K. et al. (2016): Role of Mitochondrial Complex IV in Age-Dependent Obesity. *Cell Reports* 16 (11), 2991–3002.

Spalding, K.L.; Arner, E.; Westermark, P.O.; Bernard, S.; Buchholz, B.A.; Bergmann, O. et al. (2008): Dynamics of fat cell turnover in humans. *Nature* 453 (7196), 783–787.

Spencer, M.; Unal, R.; Zhu, B.; Rasouli, N.; McGehee, R.E.; Peterson, C.A.; Kern, P.A. (2011): Adipose tissue extracellular matrix and vascular abnormalities in obesity and insulin resistance. *The Journal of Clinical Endocrinology & Metabolism* 96 (12), E1990-8.

Szkudelski, T.; Nogowski, L.; Szkudelska, K. (2011): Short-term regulation of adiponectin secretion in rat adipocytes. *Physiological research* 60 (3), 521–530.

Tchkonia, T.; Lenburg, M.; Thomou, T.; Giorgadze, N.; Frampton, G.; Pirtskhalava, T. et al. (2007): Identification of depot-specific human fat cell progenitors through distinct expression profiles and developmental gene patterns. *American journal of physiology. Endocrinology & Metabolism* 292 (1), E298-307.

Thörne, A.; Lönnqvist, F.; Apelman, J.; Hellers, G.; Arner, P. (2002): A pilot study of long-term effects of a novel obesity treatment: omentectomy in connection with adjustable gastric banding. *International journal of obesity* 26 (2), 193–199.

Trayhurn, P. (2013): Hypoxia and Adipose Tissue Function and Dysfunction in Obesity. *Physiological Reviews* 93 (1), 1–21.

van den Borst, B.; Schols, A.M.W.J.; Theije, C. de; Boots, A.W.; Köhler, S.E.; Goossens, G.H.; Gosker, H.R. (2013): Characterization of the inflammatory and metabolic profile of adipose tissue in a mouse model of chronic hypoxia. *Journal of Applied Physiology* 114 (11), 1619–1628.

van Harmelen, V.; Reynisdottir, S.; Eriksson, P.; Thörne, A.; Hoffstedt, J.; Lönnqvist, F.; Arner, P. (1998): Leptin secretion from subcutaneous and visceral adipose tissue in women. *Diabetes* 47 (6), 913–917.

Vergnes, L.; Reue, K. (2014): Adaptive Thermogenesis in White Adipose Tissue: Is Lactate the New Brown(ing)? *Diabetes* 63 (10), 3175–3176.

Vikman, H.L.; Hreniuk, S.P.; Kauffman, G.F.; LaNoue, K.F.; Martin, L.F.; Ohisalo, J.J. (1995): Cyclic AMP and glycerol concentrations in freeze-clamped human omental and subcutaneous adipose tissues. *International journal of obesity* 19 (6), 388–391.

Wang, B.; Wood, I.S.; Trayhurn, P. (2007): Dysregulation of the expression and secretion of inflammation-related adipokines by hypoxia in human adipocytes. *European Journal of Physiology* 455 (3), 479–492.

Wang, P.; Mariman, E.; Renes, J.; Keijer, J. (2008): The secretory function of adipocytes in the physiology of white adipose tissue. *Journal of cellular physiology* 216 (1), 3–13.

Weyer, C.; Foley, J.E.; Bogardus, C.; Tataranni, P.A.; Pratley, R.E. (2000): Enlarged subcutaneous abdominal adipocyte size, but not obesity itself, predicts type II diabetes independent of insulin resistance. *Diabetologia* 43 (12), 1498–1506.

Weyer, C.; Funahashi, T.; Tanaka, S.; Hotta, K.; Matsuzawa, Y.; Pratley, R.E.; Tataranni, P.A. (2001): Hypoadiponectinemia in obesity and type 2 diabetes: close association with insulin resistance and hyperinsulinemia. *The Journal of Clinical Endocrinology & Metabolism* 86 (5), 1930–1935.

Wiesner, R.J.; Rüegg, J.C.; Morano, I. (1992): Counting target molecules by exponential polymerase chain reaction: copy number of mitochondrial DNA in rat tissues. *Biochemical and biophysical research communications* 183 (2), 553–559.

Wilson-Fritch, L.; Nicoloro, S.; Chouinard, M.; Lazar, M.A.; Chui, P.C.; Leszyk, J. et al. (2004): Mitochondrial remodeling in adipose tissue associated with obesity and treatment with rosiglitazone. *The Journal of clinical investigation* 114 (9), 1281–1289.

Wood, I.S.; Stezhka, T.; Trayhurn, P. (2011): Modulation of adipokine production, glucose uptake and lactate release in human adipocytes by small changes in oxygen tension. *European Journal of Physiology* 462 (3), 469–477.

World Health Organization (2000): Obesity. Preventing and managing the global epidemic. Published in: World Health Organization (Ed.): WHO Technical Report Series, Bd. 894.

World Health Organization (2015): Obesity and overweigth. Fact sheet N°311. Updated January 2015.

World Health Organization (2016): Global report on diabetes. Ed.World Health Organization. Geneva, Switzerland.

Yamauchi, T.; Kamon, J.; Waki, H.; Terauchi, Y.; Kubota, N.; Hara, K. et al. (2001): The fat-derived hormone adiponectin reverses insulin resistance associated with both lipoatrophy and obesity. *Nature medicine* 7 (8), 941–946.

Ye, J.; Gao, Z.; Yin, J.; He, Q. (2007): Hypoxia is a potential risk factor for chronic inflammation and adiponectin reduction in adipose tissue of ob/ob and dietary obese mice. *American journal of physiology. Endocrinology & Metabolism* 293 (4), E1118-28.

Yehuda-Shnaidman, E.; Buehrer, B.; Pi, J.; Kumar, N.; Collins, S. (2010): Acute stimulation of white adipocyte respiration by PKA-induced lipolysis. *Diabetes* 59 (10), 2474–2483.

Yin, X.; Lanza, I.R.; Swain, J.M.; Sarr, M.G.; Nair, K.S.; Jensen, M.D. (2014): Adipocyte Mitochondrial Function Is Reduced in Human Obesity Independent of Fat Cell Size. *The Journal of Clinical Endocrinology & Metabolism* 99 (2), E209–E216.

Youle, R.J.; van der Bliek, A.M. (2012): Mitochondrial fission, fusion, and stress. *Science* 337 (6098), 1062–1065.

Yu, C.; Chen, Y.; Cline, G.W.; Zhang, D.; Zong, H.; Wang, Y. et al. (2002): Mechanism by which fatty acids inhibit insulin activation of insulin receptor substrate-1 (IRS-1)-associated phosphatidylinositol 3-kinase activity in muscle. *The Journal of biological chemistry* 277 (52), 50230–50236.

Zachariah, P.J.; Chen, C.Y.; Lee, W.j.; Chen, S.C.; Ser, K.H.; Chen, J.C.; Lee, Y.C. (2016): Compared to Sleeve Gastrectomy, Duodenal-Jejunal Bypass with Sleeve Gastrectomy Gives Better Glycemic Control in T2DM Patients, with a Lower β-Cell Response and Similar Appetite Sensations: Mixed-Meal Study. *Obesity surgery* 26 (12), 2862–2872.

Zhang, Y.; Proenca, R.; Maffei, M.; Barone, M.; Leopold, L.; Friedman, J.M. (1994): Positional cloning of the mouse obese gene and its human homologue. *Nature* 372 (6505), 425–432.

Zierath, J.R.; Livingston, J.N.; Thorne, A.; Bolinder, J.; Reynisdottir, S.; Lonnqvist, F.; Arner, P. (1998): Regional difference in insulin inhibition of non-esterified fatty acid release from human adipocytes: relation to insulin receptor phosphorylation and intracellular signalling through the insulin receptor substrate-1 pathway. *Diabetologia* 41 (11), 1343–1354.

LIST OF FIGURES

LIST OF TABLES

ACKNOWLEDGEMENTS

Mein besonderer Dank gilt Herrn Prof. Dr. Hauner, für die herausragende Möglichkeit an seinem Lehrstuhl meine Dissertation erstellen zu können, für die kontinuierliche Unterstützung, die Diskussionsbereitschaft und den wissenschaftlichen Input während der Erstellung dieser Arbeit sowie für die Übernahme des Erstgutachtens. Herrn PD Dr. Skurk möchte ich herzlich danken für die Betreuung, angefangen am ersten Tag bis hin zur Fertigstellung dieser Arbeit. Herzlichen Dank für die ständige Unterstützung, die Gesprächs- und Diskussionsbereitschaft, den wissenschaftlichen Input sowie für diverse Cappuccinos während Besprechungen. Herrn Prof. Dr. Klingenspor möchte ich nicht nur für die Übernahme des Zweitgutachtens danken, sondern auch für die Zeit die er sich nahm, Ergebnisse zu diskutieren, kritisch nachzufragen und neue wertvolle Impulse für den weiteren Projektverlauf zu geben. Frau Prof. Dr. Daniel danke ich recht herzlich für die Übernahme des Vorsitzes während der Promotionsprüfung. Mein herzlicher Dank gilt außerdem Dr. Theresa Schöttl, die jederzeit bereit war ihr exzellentes technisches Wissen rund um Oroboros, Clarke Elektrode & Co. mit mir zu teilen sowie wissenschaftliche Fragen zu diskutieren und stets wertvolle Impulse zu geben. Herzlichen Dank auch an Herrn Prof. Dr. Hüttl, Dr. Kramer, Frau Koller und das restliche Team der Chirurgischen Klinik München Bogenhausen sowie Herrn Dr. Limberger und Team des Kreisklinikums Schrobenhausen für die hervorragende Kooperation in den letzten Jahren. Manuela Hubersberger möchte ich für die Vermittlung von Unmengen an Labor-Knowhow sowie ihr überdurchschnittliches und nicht selbstverständliches Engagement zu jeglicher Tages- und Nachtzeit danken. Mein bester Dank gilt außerdem Dr. Lynne Stecher, die gerne bereit war jede statistische Herausforderung ausführlich zu erklären und zu diskutieren. Sylvia Heinrich möchte ich für all ihre Unterstützung während meiner Zeit am Lehrstuhl meinen herzlichen Dank aussprechen. Überdies möchte ich allen Kolleginnen und Kollegen für das gute Arbeitsklima, ihre Unterstützung sowie den wissenschaftlichen Austausch danken. Insbesondere Julia Kunath, Dr. Therese Halvorsen Røst, Dr. Tina Brennauer, Dr. Heekyoung Lee und Kun Qian. Dr. Katrin Stücher möchte ich für den fortwährenden wissenschaftlichen Austausch danken, der bereits in Gießen seinen Ursprung hatte. Meinen Eltern möchte ich dafür danken, dass sie mir die Freiheit gelassen haben, ohne Leistungsdruck die Freude am Lernen selbst zu entdecken, für den fortwährenden Glauben an mich und meine Leistungen und für die Unterstützung während meines gesamten Studiums.

Ebenfalls möchte ich mich bei meiner Schwester und meinem Schwager bedanken, für ihre Unterstützung sowie aufmunternden und motivierenden Worte in den letzten Jahren. Mein ganz besonderer Dank gilt Malte, der mich während der gesamten Promotionszeit unterstützt hat und durch dessen Zuspruch ich sowohl die Herausforderungen einer Promotion überhaupt erst angenommen als auch zum Abschluss gebracht habe.